University of Basilicata
Department of Sciences

PhD SCHOOL IN EARTH SCIENCE

XXVIII Cycle (2012-2015)

Coordinator: Prof. G. Spilotro

MULTIDISCIPLINARY APPROACH TO THE ENVIRONMENTAL QUALITY ASSESSMENT OF THE PIETRA DEL PERTUSILLO FRESH-WATER RESERVOIR (BASILICATA, ITALY)

PhD thesis

Tutor:
Dr. Michele Paternoster

Co-tutors:
Prof. Giacomo Prosser
Prof. Albina Colella
Dr. Rosa Sinisi

PhD student
Elisabetta Fortunato

This PhD project was funded by Fondazione Eni Enrico Mattei (FEEM) according to a research agreement with the Department of Sciences of the University of Basilicata.

The scientific project coordinators have been Prof. G. Prosser, full professor in Structural Geology and Dr. M. Paternoster, researcher in Geochemistry and Vulcanology at the Department of Sciences of the University of Basilicata.

The project is in accordance with the FEEM's mission to create a multidisciplinary network of researchers working on several innovative projects in order to improve the quality of decision-making in public and private spheres.

“Without data

you’re just another person

with an opinion”

(W. Edwards Deming)

Index

Abstract 008

Riassunto 012

1. Introduction 016

    References

2. The study area 024

    2.1 The Pietra del Pertusillo catchment

        2.1.1 Geography

        2.1.2 Geology

            Short description of Meso-Cenozoic units

        2.1.3 Structural features

        2.1.4 Geomorphology

    2.2 The Pietra del Pertusillo fresh-water reservoir

        2.2.1 Geography

        2.2.2 Limnology

        2.2.3 Previous monitoring programs of lake sediments

    References

3. Materials and methods……………………………………………………………………..065

3.1 Sampling

3.1.1 The bedrock

Meso-Cenozoic Formations

Quaternary deposits

3.1.2 The fluvio-lacustrine sediments

3.13 The lacustrine core sediments

3.2 Analytical techniques

3.2.1 Grain size

3.2.2 XRPD (X-Ray Powder Diffraction)

3.2.3 Chemical analyses (ICP-MS)

Bedrock samples

Quaternary and fluvio-lacustrine sediments

Lacustrine core sediments

Stratigraphic description

(TOC) Total Organic Carbon

References

4. Results ………………………………………………………………………………………..087

4.1 The fluvio-lacustrine sediments

4.2 The lacustrine sediments

4.3 Grain size distribution, XRPD and TOC

4.4 Chemical composition of sediments and rocks

4.5 Enrichment factors

4.5.1 Vertical profiles

Bulk fraction

Clay fraction

4.5.2 The areal distribution of the enrichment factors

References

5. Discussion……………………………………………………………………………………………140

5.1 The methodological approach to the environmental quality assessment of the fresh-water reservoir sediments.

5.2 Facies interpretation and assessment of the depositional environment

5.3 Mineralogical composition of the deep lacustrine sediments

5.4 Distribution of the elements of environmental interest in the Pertusillo system

5.5 Comparison of the lacustrine sediment values with the regulatory levels

References

6. Conclusions………………………………………………………………………………………164

Acknowledgments……………………………………………………………………………………168

Appendices……………………………………………………………………………………………172

Appendix 1: The regulatory framework for sediments of inland waters

1.1 Extra-European guidelines

1.2 European guidelines

1.3 Italian guidelines

Appendix 2: Geological map of the high Agri Valley

Appendix 3: Schedules of Meso-Cenozoic rocks and Quaternary deposits

Appendix 4: Details about the core drilling and splitting

Appendix 5: The granulometric curves of fluvio-lacustrine samples

Appendix 6: The diffractograms of fluvio-lacustrine and lacustrine samples

Appendix 7: Stratigraphic logs

Appendix 8: Certificates of chemical analyses

ABSTRACT/ RIASSUNTO

Abstract

The Pietra del Pertusillo fresh-water reservoir is an artificial lake located in the high Agri River Valley (Basilicata); its dam wall was completed in 1963 for producing hydroelectric energy and providing water for human use to Puglia and Basilicata Southern Italian regions (approximately 2 million people). Pertusillo lake lies within a national park because of the presence of many special protected areas.

This reservoir is a natural laboratory for assessing the sediment pollution from human activities, including: plastics and other industrial activities, agricultural activities, waste-water treatment plants, landfills, farms. In addition, the Pertusillo reservoir is located in the area of the largest oil field in the onshore of western Europe, including: 27 oil wells, a deep-water reinjection well and a first treatment oil plant. This anthropogenic pressure may thus represent an impact factor on the environmental equilibrium and consequently the knowledge and control on its quality represents a relevant environmental challenge.

The lacustrine sediments represent the natural sink for nutrients and possible pollutants, which tend to accumulate in relation to the nature and composition of the solid matrix but also the concentration and characteristics of the substances themselves. Moreover the deeper sediments, deposited under undisturbed condition, represent the "historical memory" of the ecosystem.

Sub-aqueous lake sediments were investigated in May 2014, sampled using a small platform and a gravity corer (UWITEC, Austria) of 90 mm diameter which allowed to drill 19 cores up to 2 m long from the sediment/water interface. Of these, 15 cores were collected in order to evaluate the stratigraphy, mineralogy and chemistry of its sediments; the other four ones for hydrocarbon analysis (not included in this study).

Further, in order to assess the provenance effects on the composition of lake sediments, the bedrock (Meso-Cenozoic rocks and Quaternary fluvio-lacustrine deposits) and the fluvio-

lacustrine sediments of the main "Pietra del Pertusillo" tributaries, close to the detrital supply entry points of Pietra del Pertusillo lake (peri-lacual zone) were also sampled.

A bed-by-bed stratigraphic-sedimentological description of each core was performed on the basis of various macroscopic features (e.g. grain-size, textures, primary structures, colors, etc.) by using facies analysis techniques; consequently a large number of core samples (147) belonging to the muddy facies were collected from the working half of each core for subsequent x-ray powder diffraction analyses (XRPD). 24 samples were selected to perform grain size, TOC and chemical analysis: in particular those that showed the highest peaks of interstratified clay minerals together with illite peaks opened at low 2ϑ angles, indicating a degradation of the illite for the benefit of the interstratified clay minerals.
Chemistry (major, minor and trace elements) was performed on powdered samples by ICP-MS technique after lithium metaborate/tetraborate fusion to facilitate the destruction of possible resistate minerals.

Eleven lithofacies lead us to recognize three different depositional sub-environments: the delta areas, strongly affected by dramatic water-level fluctuations with prevalent coarse sediments sourced by the main Agri River and by the other lateral tributaries; the transitional areas, testifying the progressive deepening of the lacustrine water; the lacustrine zone s.s., constantly submerged, characterized by muddy sediments with locally thin dark grey to black anoxic beds, that become more frequent towards the distal and deeper areas.

The mineralogical composition of the lacustrine samples is essentially clastic and reflects the mineralogical composition of the parent rocks: quartz (Qz), calcite (C), feldspar (Feld.), muscovite/illite (M/Ill.), chlorite (Ch) and minor amount of mixed-layered clay minerals are the main identified mineralogical phases; dolomite (D) was found only at the confluence of the Agri River.

The trace elements of environmental interest (V, Ba, Cr, Co, Ni, Cu, Zn, Pb and As) mostly derived from the weathering and erosion of the surrounding source rocks; in particular the

mafic component and the quaternary deposits could play an important role. The EF values, frequently <2, confirm their geogenic origin.

The anthropogenic contribution is spatially limited to two single spots: the core R for Cu, Cr, Zn and Pb and the core I for Pb. In particular the core R was closest to the State Road 598 and basinwards of the Spetrizzone-Scazzero months, in whose catchment a waste water treatment plant and several dumpings are located. The core I was collected in the Maglia arm, in whose catchment different anthropogenic activities are located: intense agricultural activities, a landfill, a waste water treatment plant and a local airfield.

All the elements are below the upper threshold values for canadian sediments guidelines and except for V, below the national threshold values; however the $EF_{(bedrock)}$ values of vanadium, constantly < 2, prove its geogenic origin.

Riassunto

Il lago di Pietra del Pertusillo, oggetto del presente studio, è un invaso artificiale completato nel 1963 mediante la costruzione di uno sbarramento sul fiume Agri, nella parte alta della valle omonima (Basilicata). Le acque invasate sono utilizzate, oltre che per la produzione di energia elettrica, anche per soddisfare le esigenze idropotabili della Regione Puglia e quelle irrigue della Regione Basilicata. L'invaso è incluso nel territorio del Parco dell'Appennino Lucano Val d'Agri Lagonegrese, e fa parte del sistema di aree protette Natura 2000 della Regione Basilicata, costituito da aree SIC (Siti di Interesse Comunitario) e ZPS (Zone a Protezione Speciale) che hanno lo scopo di tutelare habitat e specie di particolare pregio ed interesse, individuati nelle direttive comunitarie.

L'invaso è un laboratorio naturale per lo studio di possibili impatti ambientali dovuti a varie attività antropiche presenti nel suo bacino di drenaggio, tra cui: industrie plastiche ed altre attività industriali, attività agricole, impianti di depurazione urbani e industriali, discariche, fattorie. Inoltre il Pertusillo è situato in prossimità del più grande giacimento petrolifero dell'Europa continentale occidentale, comprendente 27 pozzi di sviluppo, un pozzo di reiniezione delle acque di processo e un centro di primo trattamento degli idrocarburi estratti. Questa pressione antropica può avere un impatto sul suo equilibrio ambientale e di conseguenza la conoscenza e il controllo della qualità ambientale rappresenta una sfida rilevante.

I sedimenti di laghi naturali e artificiali sono considerati una matrice interessante nella quale sostanze nutrienti e possibili inquinanti tendono ad accumularsi in relazione alla natura e alla composizione della matrice solida ma anche alla concentrazione e alle caratteristiche delle sostanze stesse. I sedimenti più profondi, inoltre, sono indisturbati e rappresentano la "memoria storica" dell'attività dell'ecosistema.

Nel maggio 2014 è stato effettuato il carotaggio dei sedimenti lacustri con il supporto logistico della ditta austriaca UWITEC, che ha fornito anche tutta l'attrezzatura per il

campionamento, tra cui una piattaforma a motore e un carotiere a gravità; in tutto sono state prelevate 19 carote di lunghezza variabile fino a 2 m all'interfaccia acqua/sedimento, di cui 15 da destinare alle analisi stratigrafiche, chimiche e mineralogiche; le altre 4 sono state utilizzate per l'analisi degli idrocarburi, che comunque non sono oggetto del presente studio.

Per quantificare la concentrazione di background dei vari elementi sono stati prelevati 46 campioni appartenenti alle formazioni Meso-Cenozoiche a frazione pelitico-silico-clastica dominante e ai depositi Quaternari affioranti nel bacino di drenaggio dell'invaso. Sono stati altresì campionati 18 campioni di sedimenti fluvio-lacustri lungo la fascia perilacuale in prossimità delle confluenze dei principali affluenti nell'invaso per valutare l'apporto proveniente dai vari sottobacini.

Su ciascuna carota è stata eseguita una dettagliata analisi sedimentologico-stratigrafica basata sulle caratteristiche macroscopiche (granulometria, tessitura, strutture primarie, colore, ecc.), usando le tecniche dell'analisi di facies. Sono stati, quindi, campionati tutti i livelli appartenenti alle facies più fangose per un totale di 147 campioni da destinare alle analisi diffrattometriche. Un'ulteriore selezione fra i campioni aventi i maggiori picchi di minerali argillosi interstratificati insieme a picchi dell'illite aperti verso i bassi angoli, indice di una degradazione in atto dell'illite a vantaggio dei minerali argillosi interstratificati ha consentito di ottenere 24 campioni da destinare ad analisi granulometriche, per la misura del carbonio organico totale e chimiche.

I campioni litoidi sono stati polverizzati in giara di agata, mentre i depositi inconsolidati e i sedimenti fluvio-lacustri sono stati setacciati in umido; la frazione < 63 µm, così ottenuta, è stata sottoposta ad analisi granulometriche, mineralogiche e chimiche.

Le analisi chimiche sugli elementi maggiori, minori e in traccia sono state eseguite con ICP-MS in seguito a fusione con metaborato/tetraborato di litio per la distruzione delle fasi più resistenti.

Sulla base dei caratteri sedimentologici macroscopici sono state identificate 11 lithofacies a partire dalle quali l'invaso è stato suddiviso in 3 sub-ambienti deposizionali: le aree di delta che corrispondono alle foci dell'Agri e degli altri affluenti secondari, fortemente influenzate dalle fluttuazioni del livello del lago; le aree di transizione, le cui facies caratteristiche *testimoniano un progressivo approfondimento del livello del lago; il bacino lacustre s.s.; qui i sedimenti, costantemente sommersi, assumono un colore prevalementemente grigiastro, indice di un ambiente poco ossigenato e diventano completamente neri in corrispondenza di livelli centimetrici che aumentano verso lo sbarramento in spessore, quantità e intensità di colore.*

La composizione mineralogica dei sedimenti dell'invaso è prevalentemente clastica e riflette la composizione mineralogica delle rocce affioranti: quarzo, carbonati, feldspati, muscovite/illite, clorite e in misura minore minerali argillosi interstratificati. La dolomite è presente solo alla confluenza dell'Agri.

Gli elementi in traccia di interesse ambientale considerati (V, Ba, Cr, Co, Ni, Cu, Zn, Pb and As) derivano prevalentemente dall'alterazione delle rocce affioranti, tra cui le rocce a componente mafica e i depositi quaternari potrebbero giocare un ruolo importante. Per valutare la presenza di un eventuale contributo antropico nei sedimenti lacustri, sono stati anche calcolati i fattori di arricchimento per gli elementi suddetti.

Essi risultano quasi sempre inferiori di 2 per tutti gli elementi, confermandone l'origine geogenica.

Il contributo antropogenico è puntuale ed è limitato alla carota R per Cu, Cr, Zn e Pb e ad un campione della carota I per il solo Pb. La carota R è stata campionata in un punto del lago situato in prossimità della Strada Statale 598 e a valle della foce dei fiumi Scazzero-Spetrizzone, nel cui bacino di drenaggio sono presenti un depuratore urbano e vari scarichi domestici. La carota I è localizzata a valle della confluenza del fiume Maglia, nel cui bacino sono presenti: un'intensa attività agricola, una discarica, un impianto di depurazione urbano, e un'aviosuperficie di piccole dimensioni.

I sedimenti lacustri sono stati, altresì, confrontati con dei valori normativi di riferimento nazionali (i Livelli Chimici di Riferimento suggeriti da ISPRA per i sedimenti fluviali e le Concentrazioni Soglia di Contaminazione per i suoli ad uso verde pubblico e industriale contenuti D. lgs. 152/2006 e s.m.i.) e internazionali (i valori soglia inferiore e superiore dettati dalla giurisdizione canadese per i sedimenti lacustri). Dal confronto è risultato che tutti gli elementi sono compresi entro i valori soglia canadesi e, ad eccezione del vanadio,

risultano inferiori ai valori di riferimento nazionali. Tuttavia i fattori di arricchimento del vanadio, sempre inferiori a 2, confermano la sua origine geogenica.

INTRODUCTION

1. Introduction

The Pietra del Pertusillo fresh-water reservoir is an artificial lake located in the high Agri Valley (Basilicata), in the municipalities of Grumento Nova, Montemurro and Spinoso, in the southwestern part of Basilicata region. Its dam wall was built during the period 1957-1963 to store approximately 155 million m^3 of water for both providing water supply for irrigation (32.3 %) and drinking in Puglia and Basilicata Southern Italian regions (67.7% to satisfy approximately 2 million people), and producing hydroelectric energy. Therefore, for its storage capacity and its watershed area, the Pertusillo dam is one of the strengths of regional water supply.

Pertusillo lake lies within the National Park “Appennino Lucano Val d’Agri Lagonegrese” and it is part of Natura 2000, the ecological network of protected areas in the territory of the European Union, aimed to assure the long-term survival of Europe’s most endangered species and habitats. It consists of Sites of Community Importance (SCI IT9210143) declared under the Habitats Directive (92/43/EEC) and Special Protected Area for Birds (SPA IT9210270), designed under the Birds Directive (2009/147/EC).

This reservoir is also a natural laboratory for assessing the sediment pollution from human activities. In fact, in the last decades, in the high Agri Valley, a significant economic change took place, moving from a primitive economy to new industrial activities, among which the exploitation of the largest oil field in the onshore of western Europe. There, the Eni-Shell joint-venture performs hydrocarbon extractions from 40 oil-wells, 27 of which actually produce about 83.000 barrels/day of oil and 3.030.000 Sm^3/day of natural gas. In addition a first treatment oil plant with an oil production capacity of 104.000 barrels/day and a deep-water reinjection well are present. Other human activities developed across the marginal areas of the Pietra del Pertusillo lake, including: waste-water treatment plants, landfills, farms, plastics and other industrial activities.

This anthropogenic pressure may thus represent an impact factor on the environmental equilibrium of the Pietra del Pertusillo fresh-water reservoir and consequently the knowledge and control of the quality of its water and sediments represents a relevant environmental challenge.

Heavy metals are among the most common environmental pollutants stressing the biotic community and are released into the environment by the weathering of rocks or by many human activities, such as the mining activities, the industrial and domestic effluents, the combustion of fossil fuels, etc. They are transported by rivers or in general by channelized flows or by the atmospheric dust and tend to accumulate in natural depressed areas (lakes, seas, oceans). In aquatic systems, heavy metals can be dissolved into solutions as free-ions for short time; however they are mainly suspended as colloids or adsorbed onto organic and inorganic compounds, such as iron-manganese oxides and hydroxides, clay minerals and organic matter, the most reactive phases in aquatic environments (Ammar et al., 2015; Yao et al., 2007; De Vivo et al., 2004)

The surface layer of a sediment is in a continuous hydrochemical evolution, and this implies the possibility of heavy metals releases, from sediment into the aqueous matrix in the form of compounds or free-ions. Generally, free-ions are more relevant in environmental pollution studies since they are readily bioavailable and highly persistent; as metals do not undergo any metabolic change or degradation, they move up the trophic levels, undergoing processes of bioaccumulation and biomagnification critical for the health (Stankovic et al., 2014; Christophoridis et al., 2009; De Vivo et al., 2004).

However, there is a regulatory gap about dangerous substances in sediments of internal waters. In fact the Directive on Environmental Quality Standards (Directive 2008/105/EC), on the basis of the Water Framework Directive (2000/60/EC), sets environmental quality standards (EQS) for the substances in surface (fluvial, lacustrine, transitional and coastal) waters but not in its sediments. To overcome this gap, Member States may decide what approach to use for defining the maximum threshold values for dangerous substances in sediments. Commonly, the threshold values for dangerous elements in soils are used.

Italy implemented the Water Framework Directive by a Legislative Decree 152/2006 “Norms Concerning the Environment”, commonly called “Single Environmental Text”, which shows a great interest in aquatic systems, but does not contain specific quality standards for river or lake sediments. Therefore, even in Italy, the threshold concentration values ('*CSC*') for soils, laid down in the Single Environmental Text and subsequent amendments (Column A, Table 1, Annex 5, Title V, Part IV of Legislative Decree 152/06), are used as standards for sediments quality.

In 2009 and 2011, ISPRA (*Istituto Superiore per la Protezione e la Ricerca Ambientale*) implemented a methodological approach for assessing environmental quality applied to Saline and Alento stream sediments (Abruzzo Region) but to date no studies about lacustrine sediments are available (see Appendix 1).

Unlike the surficial sediments, the deep lacustrine sediments represent the historical memory of an ecosystem, recording the past environmental changes caused by both natural and artificial events; the lacustrine sediments therefore allow us to reconstruct the history of the depositional events and define their possible origin.

Although the use of lake sediments as environmental archives is well established, reservoir sediments have less frequently been used as temporal records and there is a lack of information concerning this topic. *Abraham et al. (1999)*, *Shotbolt et al. (2001, 2005), Van Metre et al. (2001)* provided useful knowledge on the processes and consequently on factors affecting the distribution of sediments in reservoirs. Reservoirs are of great interest because they are generally located close to urban centers and industrial plants where contamination events can frequently occur.

With this in mind, the present work represents the first systematic and comprehensive study of Pietra del Pertusillo fresh-water reservoir for the understanding of sedimentological and minero-chemical processes occurring in the reservoir. To achieve these goals, a detailed study of stratigraphic and sedimentological features of nineteen sediment cores was carried out.

Further, the fluvio-lacustrine sediments of the main Pietra del Pertusillo tributaries were analyzed in order to assess the inputs coming from each upstream drainage basins.
Chemical (ICP-MS) and mineralogical (XRPD) analyses were performed on selected sediment samples. Element concentrations have been compared to upper continental crust standards and local bedrock composition in order to evaluate possible geochemical anomalies. The chemical composition of bedrock was retrieved by Meso-Cenozoic and Quaternary deposits outcropping in the investigated area.

The proposed multidisciplinary (sedimentological, mineralogical, geochemical) study focuses on: the reconstruction of the depositional settings; the type and distribution of minerals; the major, minor and trace elements contents and distribution in sediment cores. This study provides a methodological approach to assess the environmental quality of the reservoir sediments compensating for the lack of the European and Italian current laws.

References

- Abraham et al., 1999. *Sediment type distribution in reservoirs: sediment source versus morphometry*. Environmental Geology 38 (2).

- Ammar et al., 2015. *Reservoir sediments: a sink or source of chemicals at the surface water-groundwater interface*. Environ Monit Assess (2015) 187:579 DOI 10.1007/s10661-015-4791-0.

- Anselmi et al., 1996. *La sedimentazione nell'invaso artificiale del Pertusillo (fiume Agri, Basilicata)*. Geologia Tecnica & Ambientale, 4.

- Australian and New Zealand Environment and Conservation Council, Agriculture and Resource Management Council of Australia and New Zealand, 2001. *Australian and New Zealand guidelines for fresh and marine water quality. The Guidelines.* Volume 1. ISBN 09578245 0 5 (set) ISSN 1038 7072.

- Bianchini et al., 2002. *Chemical–mineralogical characterisation of clay sediments around Ferrara (Italy): a tool for an environmental analysis*. Applied Clay Science 21, 165– 176.

- Canadian Council of Ministers of the Environment, 2001. *Canadian Environmental Quality Guidelines*.

- CRA-ABP (Firenze) 2007. *Invaso Pertusillo (PZ) Rilievi batimetrici e sedimentometrici al 29 settembre 2007*. Nell'ambito del progetto REL: Attività tecnico-scientifiche nell'ambito del Progetto Operativo "Attività di assistenza tecnica e supporto agli enti concessionari nel settore dell'uso irriguo delle risorse idriche".

- Christophoridis et al., 2009. *Occurrence and distribution of selected heavy metals in the surface sediments of Thermaikos Gulf, N. Greece. Assessment using pollution indicators*. J. Hazard Mater. 168, 1082–1091.

- De Bartolomeo et al., 2010. *Il problema dei sedimenti lacuali*. Nell'ambito del progetto: Conoscenze, valutazioni, proposte per il futuro del lago Trasimeno. Dipartimento Specialità Medico-Chirurgiche e sanità Pubblica, Università degli studi di Perugia.

- De Vivo et al., 2004. *Geochimica ambientale*. *Metalli potenzialmente tossici*. Liguore Editore.

- *Decreto legislativo 3 aprile 2006, n. 152*. Norme in materia ambientale.

- *Directive 2000/60/EC of the European Parliament and of the Council of 23 October 2000*. Official Journal of the European Communities, L 327/1, 22.12.2000.

- Directive 2008/105/EC of the European Parliament and of the Council of 16 December 2008. Official Journal of the European Union. L 348/84, 24.12.2008.

- ISPRA, 2009. *Proposta per la valutazione dello stato qualitativo dei sedimenti fluviali nel sito di interesse nazionale Fiumi Saline ed Alento*.

- ISPRA, 2011. *Standard di qualità di sedimenti fluviali e lacuali*. Criteri e Proposta. Rapporto 154/2011.

- Liaghati et al., 2003. *Heavy metal distribution and controlling factors within coastal plain sediments, Bells Creek catchment, southeast Queensland, Australia.* Environment International, 29: 935-948.

- Shotbolt et al., 2001. *Establishing the sediment stratigraphy of reservoirs in the Southern Pennines, Uk*. Hydrological Sciences-Journal des sciences hydrologiques, 46(5).

- Shotbolt et al., 2005. *The use of reservoir sediments as environmental archives of catchment inputs and atmospheric pollution*. Progress in Physical Geography 29, 3 pp. 337–361.

- Stankovic et al., 2014. *Biota as toxic metal indicators*. Environ Chem Lett (2014) 12:63–84 DOI 10.1007/s10311-013-0430-6.

- Van Metre et al., 2001. *Differences in lake and reservoir sedimentation – implications for sediment coring studies.* Proceedings of the Seventh Federal Interagency Sedimentation Conference, March 25 to 29, Reno, Nevada.

- Yao and Gao, 2007. *Heavy metal research in lacustrine sediments*. Chinese Journal of Oceanology and Limnology Vol. 25 No. 3, P. 444-454, 2007. DOI: 10.1007/s00343-007-0444-7.

THE STUDY AREA

2. The study area

2.1 The Pietra del Pertusillo catchment

2.1.1 Geography

The Pietra del Pertusillo watershed matches with a geographical and socio-economic homogeneous sub-region, called High Agri Valley (HAV), which extends over a length of about 30 km and a maximum width of about 12 km; its average altitude is 600 m a.s.l. The HAV covers an area of about 530 km^2, in which the Agri, the main river of the homonymous valley, receives the waters of its main tributaries: Caolo, Sciaura (during the low-standing of the Pertusillo lake) on the right side of the valley; Molinara, Alli, Casale-Grumentino (during the low-standing of the Pertusillo lake) on the left side. The river takes origin from the water sources of Piana del Lago, between Maruggio and Lama mountains, at an elevation of about 1300 m a.s.l., and flows into the Ionian Sea, near Policoro, after a total distance of about 127 km.

The area includes 10 municipalities (Grumento Nova, Marsicovetere, Marsico Nuovo, Moliterno, Montemurro, Paterno, Sarconi, Spinoso, Tramutola, Viggiano) for a total population of about 30,000 inhabitants, with a population density of 53,1 inhabitants per square kilometer, except for Spinoso and Montemurro, having a population density of 31,8 inhabitants per square kilometer. The population is clustered in the polycentric nucleus of Villa d'Agri (Marsicovetere), which represents the main service center, with a higher resident population of 5,000 unit.

The HAV is characterized by a consistent presence of intensive agricultural activities in predominantly hilly environments thanks to the occurrence of waters and rich soils and by a unique forest heritage with a rich biodiversity that have stimulated tourism growth.

In recent decades, together with an ancient rural economy based on agriculture, wood and dairy production, new industrial activities have been undertaken, mainly located in the HAV industrial district (about 190 ha), in the towns of Viggiano and Grumento Nova. Hydrocarbon extraction, related to the largest oil field in the onshore of western Europe, is the most important industrial activity; here, the join-venture Eni (with a majority stake of 60,77%) - Shell performs hydrocarbon extraction through 27 oil wells, actually producing about 83.000 barrels/day of oil and 3.030.000 Sm^3/day of natural gas, almost the 10% of the national demand. A first treatment oil plant became operational in 1996 with the Monte Alpi production line, whereas COVA (Val d'Agri Oil Centre) started its production in 2001 and has actually an oil production capacity of 104.000 barrels/day. It collects the hydrocarbon extracted from each well and through five production lines separates it into three phases: the crude oil is sent, through an about 136 km long underground pipeline, to the ENI's refinery of Taranto, in the nearby Puglia region; the natural gas, pre-treated at COVA, is delivered into the SNAM's transportation network; the process wastewater is re-injected into the deep-water injection well of Costa Molina 2.

In the HAV industrial district, other micro-manufacturing firms are also present; the most relevant sectors in terms of employees are manufacturing (small industries), construction and related industries (stone processing, production of lime and concrete, metal and wood carpentry), as well as professional, scientific and technical activities. The transport of materials and finished goods inside and outside the industrial area represents one of the critical aspects with a significant impact on the environment. In fact, due to the absence of a railway, road transport is carried by trucks along the SS 598 *Fondo Valle dell'Agri,* which connects the industrial area to the motorway (Loperte and Cosmi, 2015).

According to the data provided by the Provincia of Potenza's Chambers of Commerce (December 2012), in the above-mentioned 10 municipality of the HAV, 3061 anthropic activities among which 1513 belonging to the primary and the secondary sectors, are located.

Strictly connected to these anthropic activities, a number of domestic, domestic-like, meteoric dumpings, 4 urban and 2 industrial wastewater treatment plants, 2 landfill and a local airfield are also present.

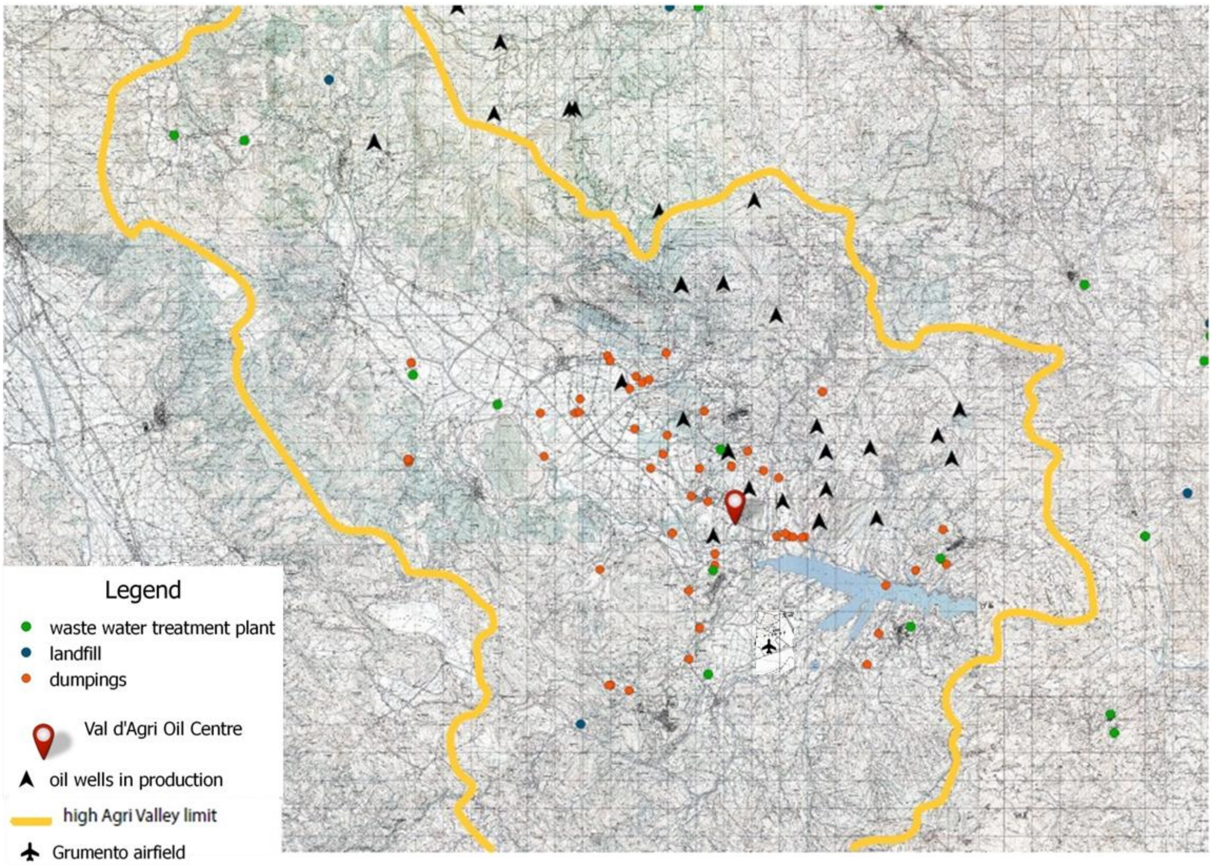

Figure 1. The location of the main anthropic activities in the high Agri Valley (Data provided by Provincia of Potenza in February 2013).

The growth of the industrial activities together with the abandonment of less-favored agricultural areas located at high elevation and the enlargement of riparian vegetation that benefited from ad hoc regulations concerning habitat protection and conservation produced the abandonment of most of the grass and pasture areas to the advantage of all the forest covers, which increased of 11% (about 5000 ha) during the 1985–2009 time period, which coincides largely with the discovery and exploitation of the oil resources in the area (Simoniello et al., 2015).

2.1.2 Geology

The (HAV) is a Quaternary NW–SE intermontane basin located in the axial zone of the Southern Apennines mountain belt, an east-verging fold-and-thrust belt developed as an accretionary wedge from the late Oligocene to the early Pleistocene, due to the eastward migration of the Apenninic arc (fig. 2) (Prosser, 1996; Cello et al., 2000; Giano et al., 2000; Giocoli et al., 2015; Gueguen et al., 2015).

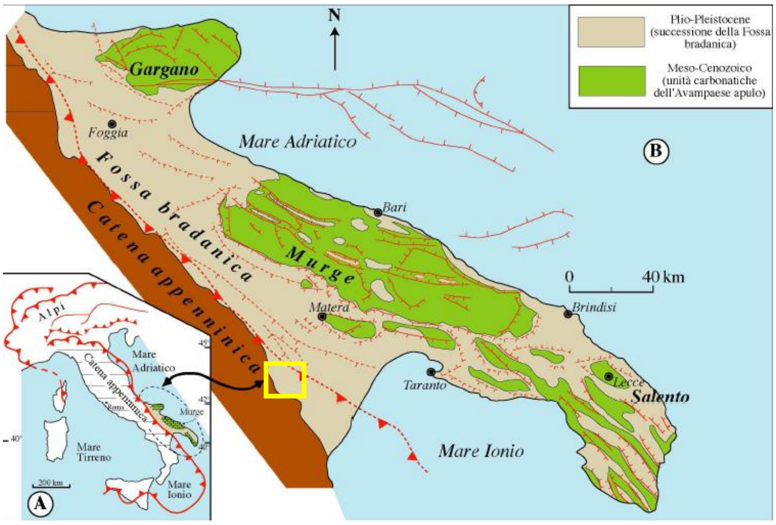

Figure 2. The three main paleogeographic domains through the Southern Apennines. The yellow rectangle shows the location of the study area (Prosser, 1996).

Paleogeographic restorations of the tectonic units cropping out in the HAV have been proposed by several authors with different models and interpretations (Selli, 1962; Scandone, 1967; 1972; Ogniben, 1969; D'Argenio et al., 1972; Sgrosso, 1986; Pescatore et al., 1988; 1999; Ben Avraham et al., 1990; Patacca et al., 1990; 1992b; Marsella et al., 1995; Monaco et al., 1998; Menardi Noguera & Rea, 2000). In Southern Apennine tectonic units derived from deformation of the Afro-Adriatic paleomargin; from west to east these are represented by: the Liguride and Sicilide complexes, of Cretaceous to Eocene age, derived from the Liguria-Piedmont Ocean; the Apennine Platform carbonates, of Late Triassic to Tertiary age and the units of the Lagonegro Basin, from late Paleozoic/Triassic to Tertiary age (Zembo, 2010; Prosser, 2012; Gueguen et al., 2015). These units, representing the substratum of the HAV, were tectonically emplaced over Plio-Pleistocene foredeep basins located on top of the Apulian Carbonate Platform, which represents the autochthonous foreland of the Southern Apennines (fig. 3). In HAV this latter unit has been detected only in the subsurface during the oil exploration.

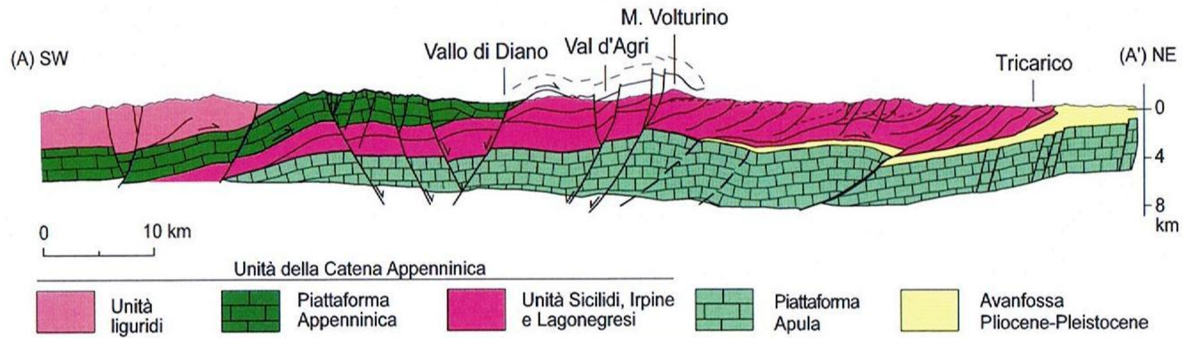

Figure 3. The relationships between the different tectonic units in the Southern Apennines. (Prosser, 1996).

In the southeastern part of the valley, bedrock consists of Tertiary siliciclastic sediments, namely the Albidona Formation (Flysch) and the Gorgoglione Flysch (Carbone et al., 1991). These outcrops separate the HAV from the middle to lower Agri Valley, mostly characterized by the Pliocene-Pleistocene deposits of the S. Arcangelo basin. The HAV probably emerged during Pliocene, since outcropping units of this age are absent, as indicated in the review by Carbone et al. (1991). Pliocene units are present further east, in the middle and lower valley, within the S. Arcangelo basin.

Youngest units are represented by Pleistocene and Holocene deposits, of continental origin (Anselmi et al., 1996).

Short description of Meso-Cenozoic units

This paragraph contains a short description of each tectonic unit outcropping in the HAV. The following description starts from the most internal units, which occupy the highest position in the tectonic edifice.

<u>Ligurian Complex</u>

The term is used to indicate allochthonous sheets of Cretaceous - Eocene age derived from basinal internal domains floored by the Tethyan oceanic crust. In the HAV an ophiolite-bearing succession of black shales, identified as Crete Nere, outcrops between the Raparo and the Sirino mountains and is overlaid by mixed calcareous-siliciclastic turbidites belonging to Saraceno Formation. This Formation consists of thin layers of grey- brown calcilutites and calcarenites with interbedded black cherty grey shales. Several sandstone levels, more frequent upwards, are also present. Near the Tramutola and Viggiano villages, the *Valle del Cavolo* Formation, similar to the Saraceno Formation, outcrops.

<u>The Campania - Lucania Platform units</u>

The tectonic units derived from the Campania-Lucania Platform (which is also indicated in the geological literature as Inner Platform or Western Platform) form the bulk of the carbonate massifs in the Campania-Lucania Apennines. The carbonate rocks belonging to this unit are not very widespread in the HAV basin and mainly make up the mountain ranges located on the right margin of the basin and, in addition, isolated peaks on the right (Monticello and Grumento) and on the left side (Viggiano), which is the most advanced outcrop of the Campania-Lucania Platform units along the thrust front. On the right side of the basin, the stratigraphic succession of the Campania-Lucania carbonates begins with the upper Triassic dolomites. These rocks show frequently a cataclastic deformation, appearing as incoherent coarse sands; for this reason, only few outcrops of the dolomite sequence show well preserved primary features. This interval is very thick in the south-western area and tends to progressively close northward and eastward, disappearing completely north of the Agri River. Above the cataclastic interval, shallow-water limestones (Jurassic - lower Cretaceous) of the Campania - Lucania Platform and a calciclastic slope succession (the *Monti della Maddalena* succession) in the northern-western part of the valley crop out. On the left side (Viggiano mountain), the paleontological features of the Mesozoic carbonates (widespread presence of dasyclads, benthic foraminifera and mudstones with fenestral structures) probably suggest a deposition within a subtropical inner shallow platform. Because of the absence of features related to a slope environment, this carbonate succession cropping out in the area of the Viggiano mountain is referred to the tectonic unit of Alburno Cervati Unit, that represent the internal realm of the Apennine platform (Lechler M. et al., 2012).

The Lagonegro basin Units

They are the most widespread units, outcropping in the northern and in the southwestern sectors of the basin. These units derived from the deformation of a basin of Mesozoic age originally located between the Apennine Platform to the west and the Apulia Platform to the east. The sedimentary succession, deposited inside the basin from the lower Triassic to the Paleogene, recorded a progressive deepening of the sea level.

The oldest unit is represented by the Facito Mt. Formation (middle Triassic), a chaotic complex made up by gray, green and red silty shales and pebbly mudstones including huge slides of different lithologies (Patacca E. & Sandone P., 2008). The stratigraphic intervals above are represented by:

- the Calcari con Selce Formation (Upper Triassic): a close alternance of thin-bedded nodular calcilutites and red clays grading upwards into gray cherty limestones with shaly interbeds;
- the Scisti Silicei Formation: (Rhaetian-Jurassic): predominantly siliceous, radiolarian-rich deposits accumulated below the CCD;
- The Galestri Formation (Neocomian-Aptian *p.p.*): gray-brown siliceous shales associated with gray siliceous calcilutites and with gray-whitish marls. The calcilutites, represented by thick layers from few centimeters to meters, show the typical fractures of the landscape stone.

The Lagonegro Units are organized into two major thrust sheets: i) the lower thrust sheet (Lagonegro I), with more distal depositional characters in the Scisti Silicei and Galestri Formations, in which the Monte Facito Formation is lacking together with dolomitization in the Calcari con Selce Formation; ii) the upper thrust sheet (Lagonegro II) with abundant carbonate turbidites made up of shallow-water derived clasts.

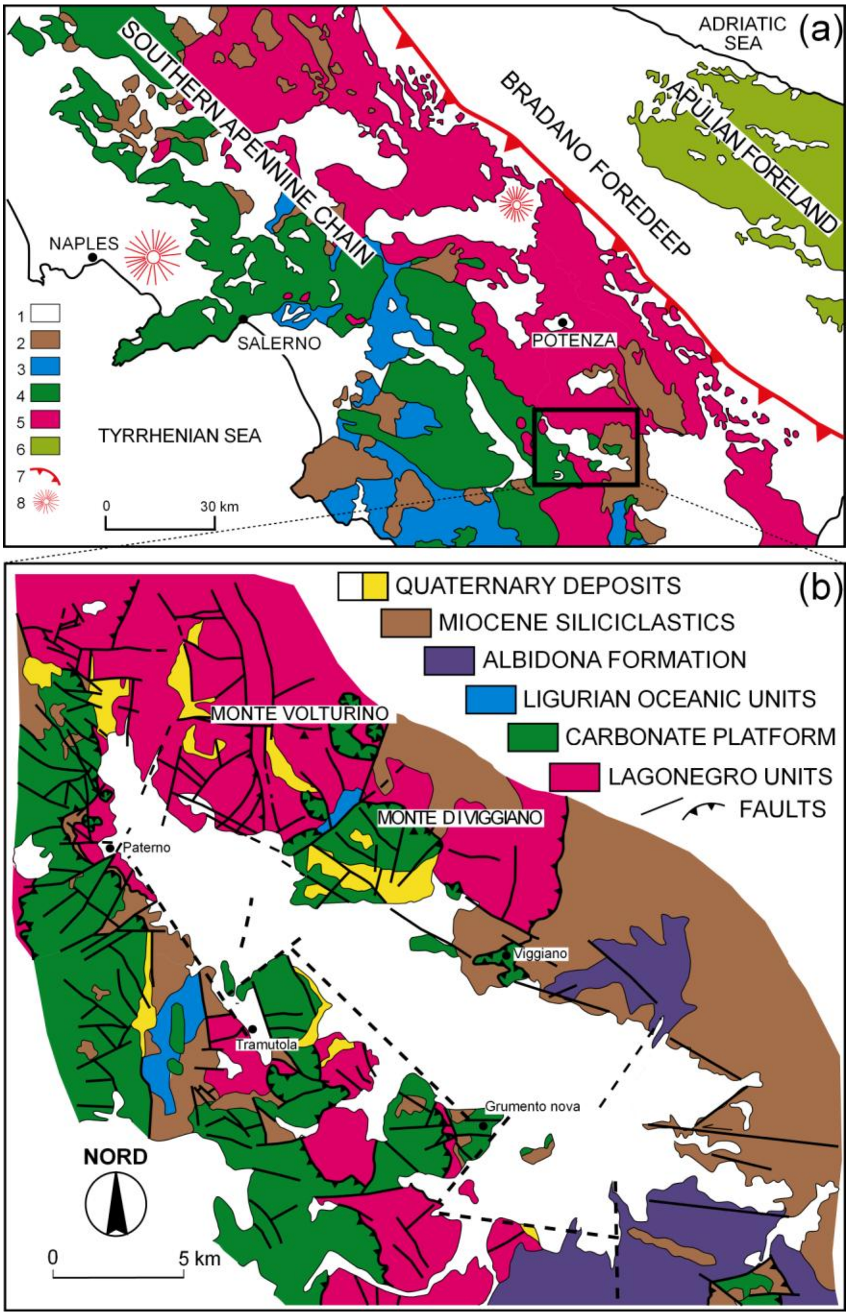

Figure 4. a) Geological sketch map of the Southern Apennines (the study area is reported in the frame). b) Schematic geological map of the High Agri River valley (Source: Giano, 2011).

<u>The Albidona Flysch</u>

The Albidona Flysch consists of alternating gray-yellowish sandstone, marl and silty clays with intercalations of whitish carbonate megaturbidites. It outcrops in the eastern portion of the HAV basin mainly on the right side of the valley and even in Caolo stream valley

(Tramutola). The age of these deposits is controversial together with their paleogeographic position within the tectonic evolution of the chain. Some authors believe that it is a flysch originally deposited in the Liguride domain and then translated as a nappe (Mostardini et al., 1966; Ogniben,1969; Pavan & Pirini, 1963 and Vezzani, 1970); others consider it as a piggy-back deposit, or a meso- autochthonous formation, lying unconformably on the nappes (Selli, 1962; Lentini et al., 1987; Bonardi, et al.,1985; Catalano & Monaco, 1990).

The Gorgoglione Flysch

The Gorgoglione Flysch (middle Langhian - lower Tortonian) formed in a piggy-back trough during the Apennine orogenic compressional phase and consists of three sequences of terrigenous sediments, (arenaceous and arenaceous – conglomeratic sequence; arenaceous – marly sequence; silty - arenaceous – marly sequence), interbedded and repeated several times at different stratigraphic heights, marking several pulsating turbiditic events. It outcrops in the eastern portion of the HAV basin mainly on the left side of the valley, close to the Pertusillo lake, and even in the Caolo stream valley (Tramutola). In the left-side sector the pelitic-arenaceous sequence prevails (Gueguen et al., 2015).

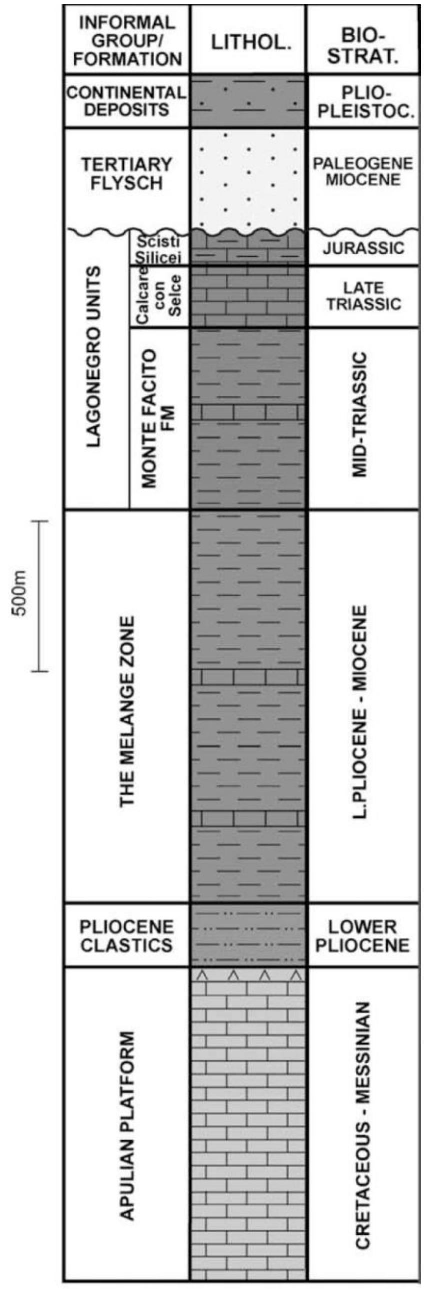

Figure 5. Synthetic well log deduced for the HAV oil field area (Source: Shiner et al., 2004).

Quaternary deposits

Continental clastic Quaternary units crop out close to the Pertusillo lake, on both the right and the left side of the valley, where about 100 m of thickness are exposed. The exposed part of the syntectonic basin infill is represented by: "Brecce di Galaino e Marsicovetere" and "Brecce di Serra Mare", (Di Niro & Giano, 1995; Giano et al., 1997a; Boenzi et al., 2004), Lower – Middle Pleistocene slope breccia bodies, exposed only along the north-eastern and the south-western basin flank; the “Complesso Val d’Agri” (Di Niro et al., 1992; Di Niro & Giano, 1995), a group of clastic units of Mid - Upper Pleistocene age, deposited in alluvial and lacustrine environment.

Zembo (2010) reconstructed the stratigraphic architecture of the Quaternary HAV deposits and proposed a new allostratigraphic model for the basin’s deposits (fig. 6). The Agri Valley allogroup, up to 100m thick, consists of four unconformity-bounded units, representing distinct depositional intervals related to regional tectonic and environmental changes, overlying the lower Pleistocene deposits of the Spinoso Conglomerate Formation (Zembo 2006; 2010). Bottom up the Agri Valley allogroup is composed of four alloformations: Pietra del Pertusillo, Valle del Nasillo, Vallone dell’Aspro and Torrente Casale. This sequence reflects a progradation of fan systems in a lacustrine-palustrine setting, followed by expansion of a new alluvial-fluvial system (Zembo, 2010) and matches the Complesso Val d’Agri (Di Niro et al.,1992; Di Niro & Giano, 1995; Boenzi et al., 2004).

Carbone et al. (2010) recognized a Pietra del Pertusillo supersynthem as an unconformity-bounded stratigraphic unit, including the Brecce di Galaino, corresponding to the Spinoso Conglomerate Formation of Zembo (2010). The Pietra del Pertusillo supersynthem, instead, matches the Agri Valley allogroup and the Complesso Val d’Agri.

I have chosen to take into consideration in my work the reconstruction of Zembo (2010) because it it based on the Quaternary deposit outcropping close to the Pertusillo fresh-water reservoir. A short description of the Quaternary deposits will follow below.

Spinoso Conglomerates Formation

It consists of well cemented, stratified and locally weathered, coarse and very coarse conglomerates. If altered, they are interspersed in a sandy - clay matrix with brown to reddish streaks. The deposits are uplifted at various elevations only along the south - eastern basin flank (Spinoso village), where they outcrop and have been interpreted by Zembo (2010) as bedload - dominated braided channel deposits within coarse -grained alluvial fans.

Agri Valley Allogroup

Pietra del Pertusillo Alloformation

The Pietra del Pertusillo Alloformation (PPA) is the lowermost unit of the Agri Valley allogroup, and consists of silty clays and clays, with gravel, sand and pebbly mudstone lenses. Coarsening - upward cycles become dominant towards the top where a paleosol, characterized by calcrete horizons marked by pale yellow hue of the matrix and a high frequency of dense calcareous nodules, yellowish in colour, with hardpan and mottles of carbonate. Petrocalcic layers, root traces and vertebrate remains locally occur. The environmental significance of (PPA) is interpreted by Zembo (2010) in terms of low-gradient, low-energy, unstratified lake and marginal lake environment, in which water level fluctuated. The more coarse deposits can be interpreted as small fan - delta bodies and sandsheet bars at the confluences between the lake and its tributaries.

Valle del Nasillo Alloformation

The Valle del Nasillo Alloformation (VNA) is a wedge made up of poorly sorted, coarse-grained conglomerates and gravels with subordinate silty and fine sands and totally differs from the underlying Pietra del Pertusillo Alloformation. It reaches 40 m in thickness adjacent to the south-eastern margin of the basin and thins to the north-west. Zembo (2006, 2010) recognized facies related to the mass-transport mechanisms of a proximal alluvial fan environment. In general the alloformation shows the typical features of coalescent alluvial fan deposits, derived from a rapid deposition by hyperconcentrated flow during catastrophic flood events. On top of the VNA there is a buried paleosol, corresponding to a mature fersiallitic weathering profile (5–10 m thick), bright brown to reddish brown in colour (high iron impregnation in groundmass), with frequent clay coatings (illuviation processes) and Fe–Mn nodules.

The Vallone dell’Aspro Alloformation

The Vallone dell’Aspro Alloformation (VAA) includes the most widespread sediments in the HAV basin and forms the bulk of the Agri Valley allogroup in the outcropping area. It represents the largest volume portion of the Quaternary clastic succession, reaching a maximum thickness of 70 m in outcrop along the northern side and 30-40 m in the south-central portion.

The VAA is a composite sedimentary body represented by three main facies associations: two gravely sand depositional elements, which intercalate a sandy-silt one. Zembo (2010) interpreted it as the axial braided alluvial system intercalated with the transverse alluvial fans deposits. Silty and clayey levels contain associations of typical continental mollusks, probably related to large vegetated areas interconnected to river channels, also testified by the roots of fingerprints and plant fragments that indicate the incipient formation of paleosols. Organic-rich layers suggest the deposition in the distal areas of the plain, in ponds or otherwise in poorly drained environments; red and purplish ferruginous concretions and abundant orange and red veins and, locally, concretions of freshwater limestones (travertines) are also present.

In the basal part of the VAA a thin (15 cm) and weathered volcanic ash layer occurs.

In the Montemurro area the top of the VAA shows the presence of a thick reddish-brown pedocomplex formed by two fairly similar paleosols, showing a moderate accumulation of Fe–Mn oxides/hydroxides.

<u>Torrente del Casale Alloformation</u>

The Torrente del Casale Alloformation (TCA) crops out close to the marginal slopes of the basin and is represented by poorly sorted coarse deposits (gravels/conglomerates, gravelly sands and subordinately sands), prograding–aggrading from both the opposite borders of the basin. Two depositional elements, a northern and a southern one, are present and characterized by the same facies association. The abundant sandy-silty fraction gives deposits a typical yellow-ocher colour.

The facies associations belonging to this alloformation are typical of massive hyperconcentrated flows, with high density and energy, producing badly organized gravel deposits in a proximal to middle alluvial fan environment. The coarser and massive facies are located in the foothill areas; the finest and best-organized associations are located in the areas connecting with the terraced deposits of the alluvial plain.

The growth of the alluvial fans belonging to TCA is the last depositional step, followed by the incision of the Agri tributaries, which cut their recent and present riverbeds of Holocene age, inside the Agri Valley allogroup.

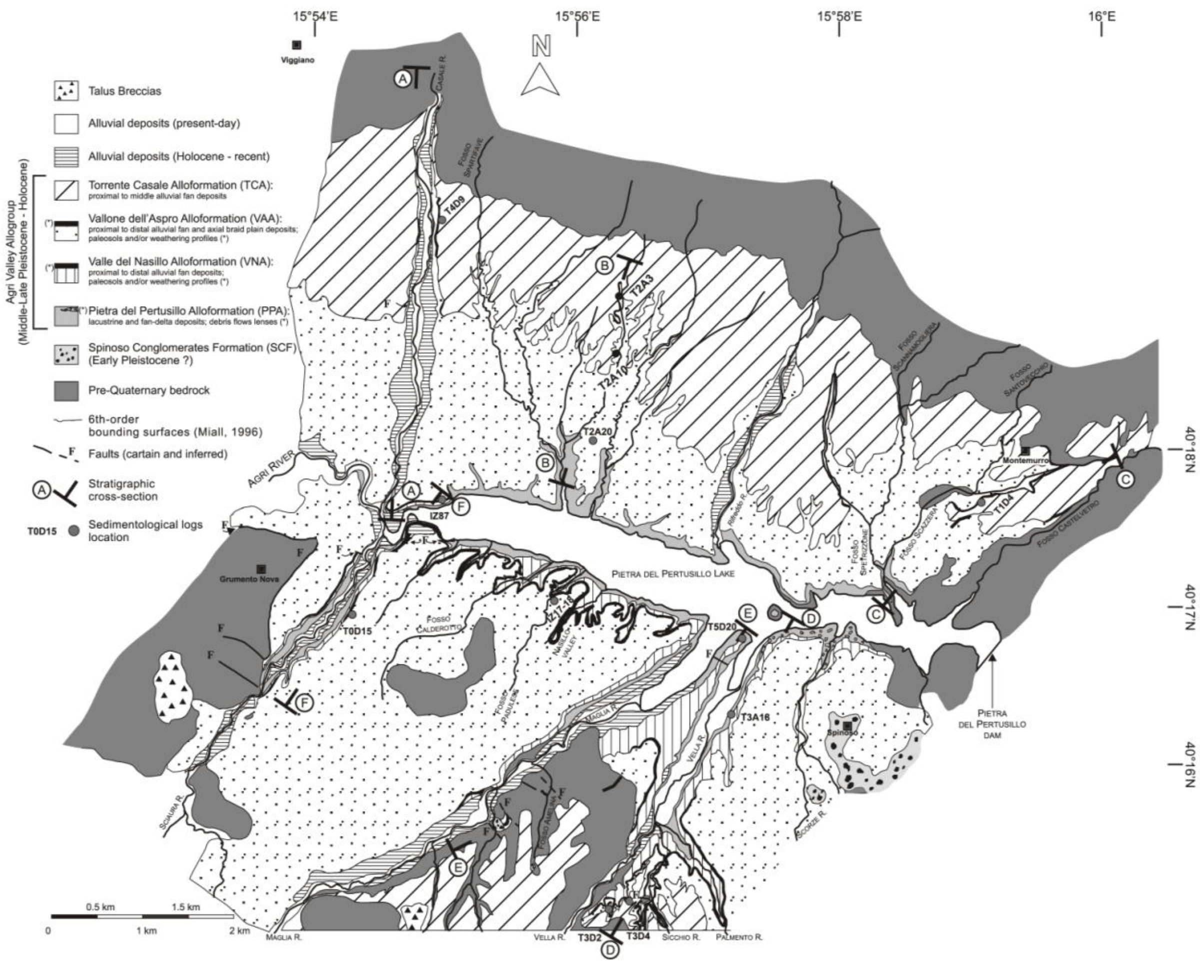

Figure 6. Semplified geological map of the Quaternary deposits outcropping close to the Pertusillo lake (Source: Zembo, 2010).

2.1.3 The structural features

The Southern Apennines represent part of the Africa-vergent Tertiary Alpine orogen formed by progressive collision between Africa and Europe (Dewey et al., 1989; Mazzoli & Helman, 1994; Patacca & Scandone, 1989). As collision progressed from the Miocene through the Pliocene, the Adriatic promontory, a part of the African plate, was detached from its basement and emplaced onto the Adriatic foreland.

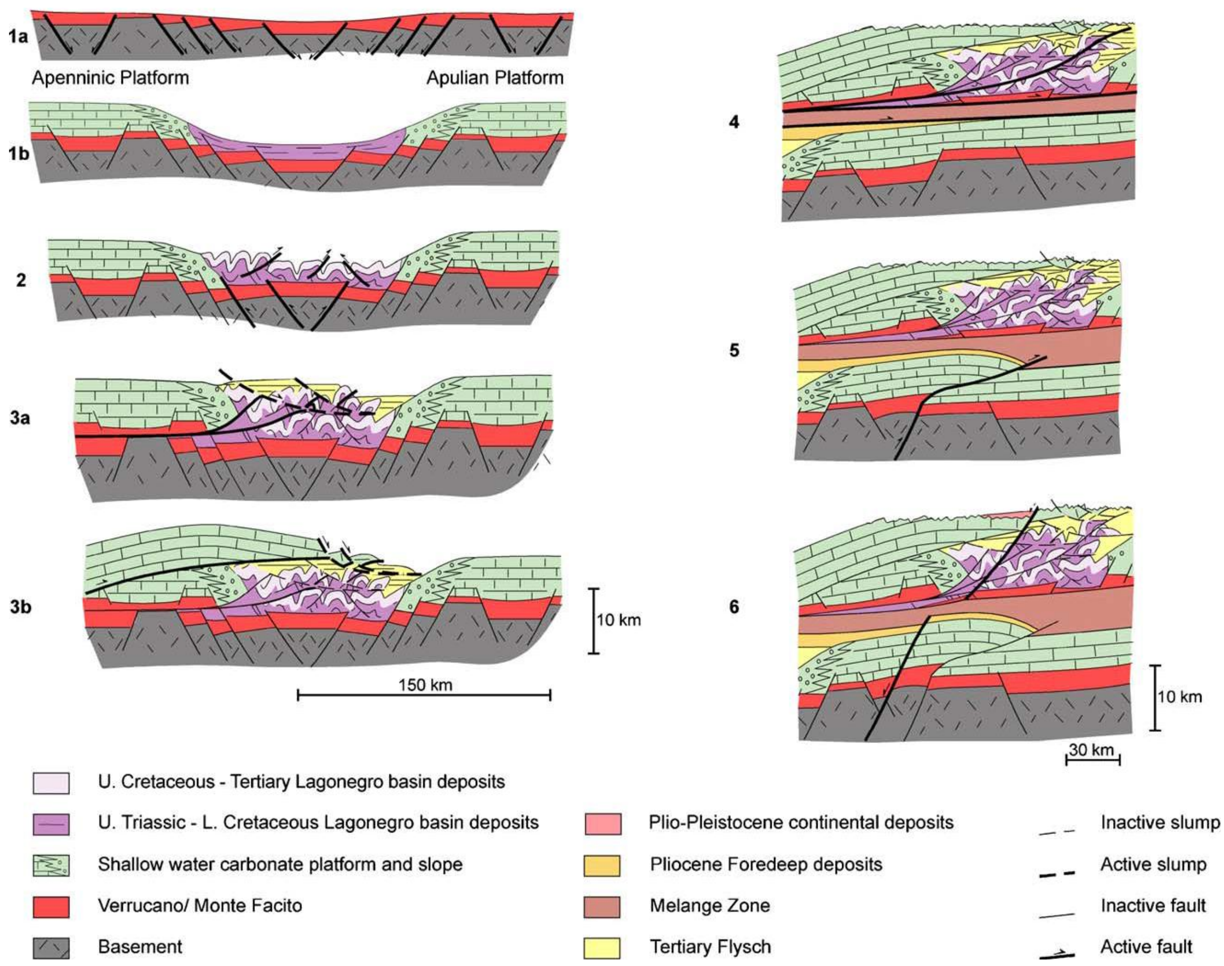

Figure 7. Summary structural model for the evolution of the Southern Apennines from the Permo-Triassic to the present day (Shiner et al, 2004).

The chain was built as an accretionary wedge of Meso-Cenozoic sediments over a sinking and roll-backing slab, which forced the opening of the Tyrrhenian back-arc basin (Malinverno and Ryan, 1986; Doglioni, 1991). The progressive eastward migration of the outer Apennine front, related to the opening of the Tyrrhenian Basin, is considered the main constraint to the large-scale evolution of the Southern Apennine thrust belt (Shiner et al., 2004).

The upper Pliocene–lower Pleistocene tectonic phases of the Southern Apennines, result from strike-slip movements along roughly NNE–SSW trending, right-lateral, and WNW–ESE trending, left-lateral, structures. Since the middle Pleistocene, accretion processes stopped even at the front of the belt and NE–SW extension perpendicular to orogenic axis, along NW–SE striking high-angle normal faults, occurred throughout the chain. The middle Pleistocene age also corresponds to the opening of NW–SE elongated alluvial grabens, i.e. the HAV basin, the acceleration of rapid uplift of the prism, which resulted in the emergence of both the chain and the foredeep and an increase in volcanic activity along the entire Tyrrhenian margin of the Apennines, from Tuscany to Campania (Doglioni, 1991).

The HAV is characterized by a complex pattern of thrusts, folds and normal faults reflecting the superposition of two main tectonic phases. During the Miocene–Early Pleistocene shortening, the Meso-Cenozoic rocks are involved in mainly NW-SE to N-S trending folds and thrusts. This process produced the tectonic superposition of allochthonous units, completely detached from their original substratum, onto the foreland succession of the Apulian Platform. The detachment level between the allochthon and the buried Apulian unit is marked by a mélange zone, several hundreds of meters thick, representing the major décollement at the base of the allochthon.

The formation and evolution of the HAV up to the present is strongly controlled by brittle tectonics, related to WNW-ESE striking, high-angle faults. These, according to Giano et al. (2000), acted as left-lateral strike-slip structures during the Early Pleistocene and are later reactivated, mainly as normal faults, in Middle Pleistocene-Holocene times. A recent (40-20 ky) extensional activity of some of these structures has also been documented by radiocarbon dating of displaced paleosoils by Giano et al. (2000) (fig. 8).

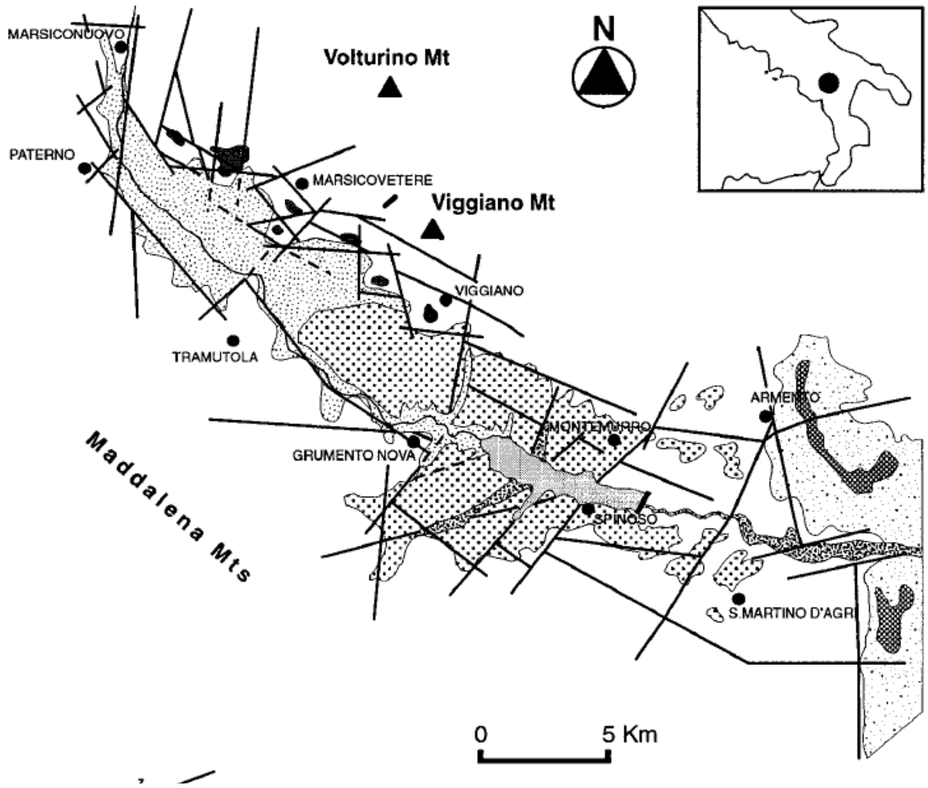

Figure 8. The map shows the major faults in the HAV (Giano et al., 2000).

The geometry and seismogenic potential of these structures are debated: most authors (Benedetti *et al.* 1998; Cello & Mazzoli 1999; Borraccini *et al.* 2002; Cello *et al.* 2003; Barchi *et al.* 2006) consider a morphologically evident NW-trending and SW-dipping normal-fault system, bordering the basin to the east, as the main seismogenic structure (EAFS, Eastern Agri Fault System); conversely, other investigators (Valensise & Pantosti 2001; Maschio *et al.* 2005; Burrato & Valensise 2008) ascribe the seismogenic potential of the area to a fault system located along the Monti della Maddalena ridge to the west of the basin (MMFS, the Mts Maddalena Fault System) (Valoroso L. et al., 2009). The MMFS bounds the HAV to the SW and runs for about 25 km between Pergola and Moliterno villages, whereas the EAFS, which is associated with mature fault-line scarps, bounds the HAV to the NE (figg. 9-10). No detailed definition exists on the length of the EAFS that, based on mapped faults between Pergola and Viggiano villages, is about 25 km (Cello et al., 2003; Maschio et al., 2005; Giocoli et al., 2015).

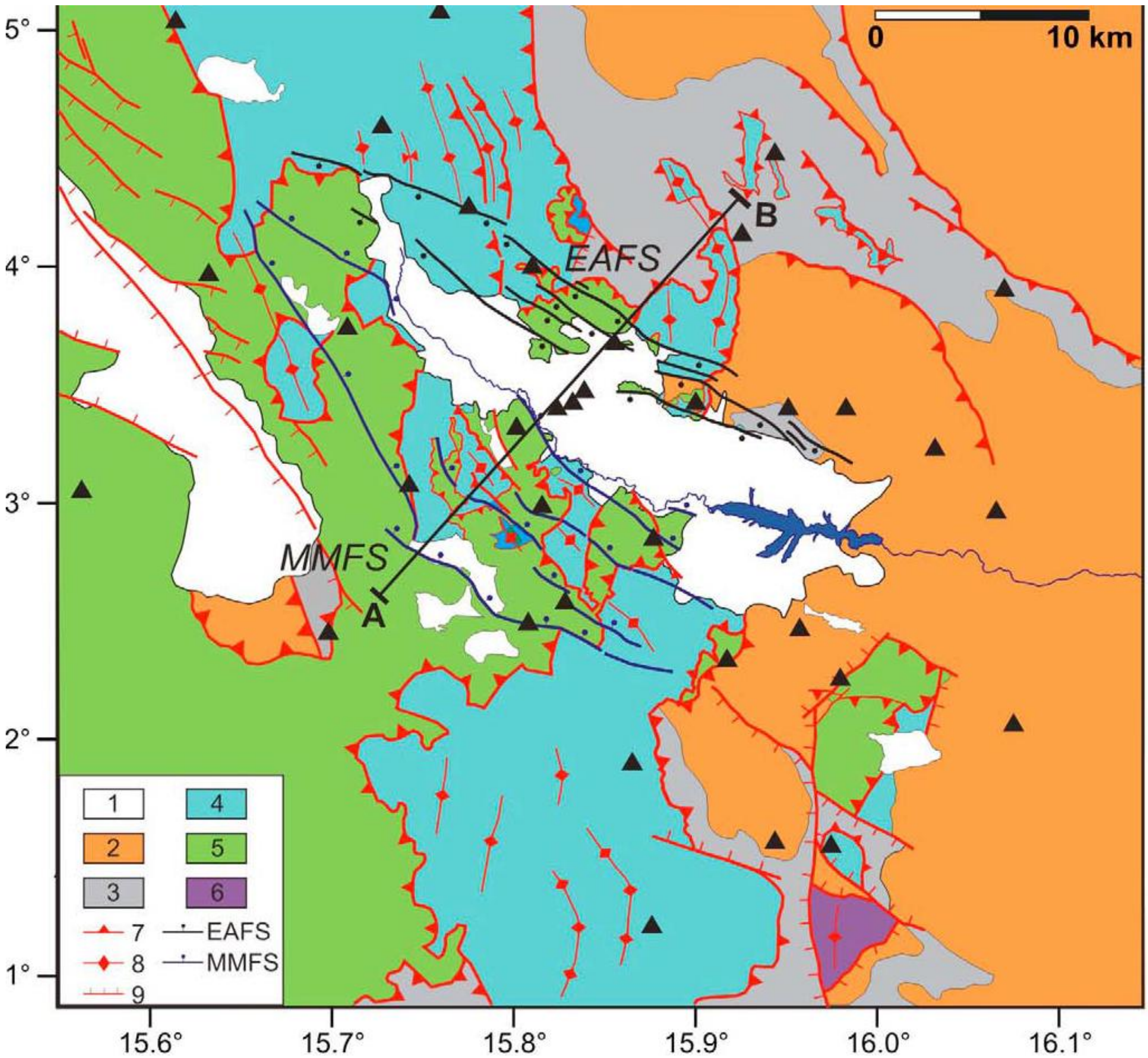

Figure 9. In this map the location of the Eastern Agri Fault System (EAFS) and the Mts. Maddalena Fault System (MMFS). 1) Quaternary continental deposits; 2) Flysch and terrigenous sediments; 3) Pelagic and slope plastic successions; 4) Mesozoic rocks of the Lagonegro Basin; 5) Campania-Lucania Carbonate Platform; 6) Apulia Carbonate Platform exposed in the Mt. Alpi tectonic window; 7) main thrusts and overthrusts; 8) antiform axis; 9) normal faults (Valoroso et al., 2011).

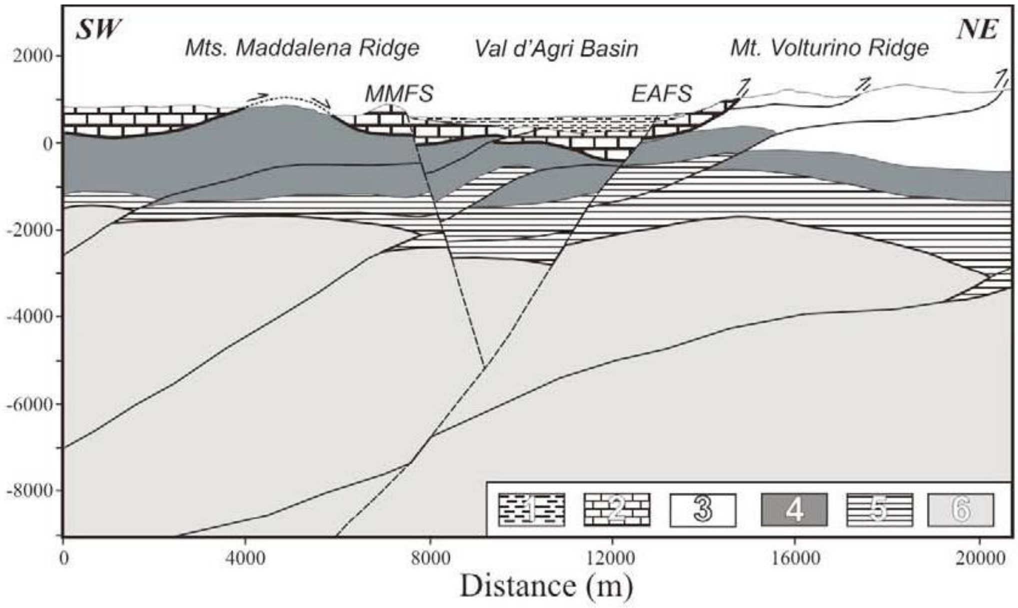

Figure 10. Schematic geologic cross section (A-B of the fig. 9) across the Val d'Agri basin; 1) Quaternary basin infill; 2) Campania-Lucania Carbonate Platform; 3) Mio-Pliocene flysch and sediments of satellite basins, Paleogene clastic successions; 4) Mesozoic rocks of the Lagonegro Basin; 5) Mio-Pliocene foredeep deposits overlying the ACP; region 6, ACP. (Valoroso et al., 2011).

Furthermore the interpretation of seismic surveys and electrical resistivity tomography (ERT) profiles in the HAV basin allowed for the identification of three transverse fault-bounded depocenters: Molinara, Fossa del Lupo and Pertusillo, separated by the transversal intrabasinal highs of Monticello and Grumento (Morandi and Ceragioli, 2002; Lapenna and Rizzo, 2003; Colella et al., 2004; Rizzo et al., 2004).

Figure 11. The highs and depocenters of the HAV basin and their bounded faults (Zembo, 2010).

2.1.4 Geomorphology

The NW–SE elongated Agri Valley basin is bounded to the northeast by the rough peaks of the Mt. Volturino - Il Monte range that reaches elevation of up to 1800 m a.s.l. To the southwest, the low elevated Monti della Maddalena range separates the Val d'Agri from the Quaternary Vallo di Diano basin to the west (Maschio et al., 2005). Topographic profiles across the major axis of the basin, evidenced the different features between the eastern and the western edge (figg. 12-13). The Mts della Maddalena group does not show clear evidences of faults; however, the frequent straight streams and fluvial elbows denote the presence of tectonic structures. The western edge is also characterized by a hat-like topography because of the presence of small intramontane depressions that perched the ridge along its crest; this morphology is produced by swarms of NW–SE striking high-angle faults, belonging to the MMFS (the Monti della Maddalena Fault System). In addition, the rivers, draining to the east, do not build up alluvial fans at the foot of their slopes, but their deposits, together with the Agri River, make up floodplain.

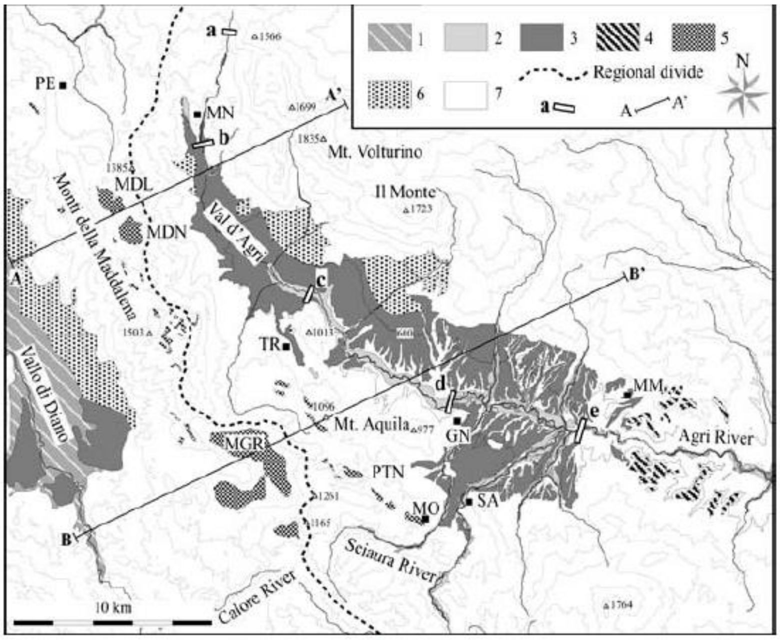

Figure 12. Geomorphologic map of the HAV. 1) Holocene alluvial deposits; 2) Upper Pleistocene alluvial deposits; 3) Middle-Upper Pleistocene alluvial and lacustrine deposits; 4) Middle Pleistocene erosional surface; 5) Upper Pleistocene-Holocene colluvial and lacustrine deposits; 6) Middle Pleistocene fan and breccias deposits; 7) pre-Quaternary bedrock (Maschio et al., 2005).

In contrast, the eastern flank of the Agri Valley displays a rectilinear trend of the mountain front and is characterized by a mature stair-case profile sloping towards the valley. At the foot of the northeastern flank two large alluvial fans are also present, currently deeply reincised by the stream network. These alluvial fans cause a displacement of the Agri River and its consequent asymmetric position in this sector of its alluvial plain.

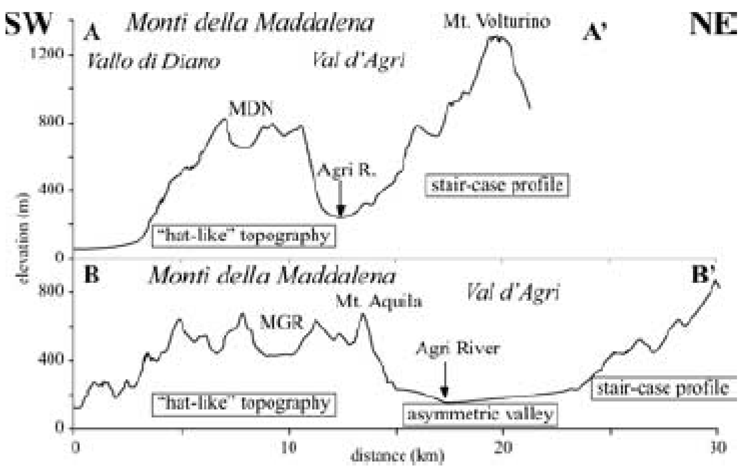

Figure 13. Topographic profile across the Val d'Agri area (traces A-A' and B-B' showed in fig. 12) (Maschio et al., 2005)

Like the other landforms, also the surface hydrography shows different features comparing the right and the left side, mainly caused by the different outcropping lithologies. On the western side, the karsification of the carbonate reliefs results in a poor surface drainage network, badly hierarchical, with few and short streams. On the eastern flank, the streams network, formed at the expense of the less permeable Lagonegro Units, is more hierarchical and consistent.

In both cases, however, the structural control on the hydrographic network is strongly evident and the streams are superimposed on faults or fractures (mainly along the NW-SE system), fold axes and lithological contacts.

Morphological features of the HAV change from North to South: in the higher sector, the Agri River flows in a flat and flooded valley while, downstream, starting from the Villa d'Agri and Tramutola villages, its sides begin to be re-incised and terraced. In the central-eastern sector of the valley, four major fluvial orders of both erosional and depositional terraces (I, II-a, III-a and IV-a) are found, located on both pre-Quaternary bedrock and Quaternary clastic deposits of the Val d'Agri allogroup. The presence of several terraced surfaces testify a fast vertical incision of the Agri Valley allogroup as a consequence of overall regional uplift during the Quaternary, with the consequent lowering of the erosion base level of the Agri River.

The hydrogeological instability differently affects the opposite sides of the valley and in particular involves the eastern portion of the basin, which drains directly in the reservoir. So the streams coming from this area probabily would transport the greatest amount of sediments, as already suggested by Capozza (1963).

Further confirmation comes from the determination of the erosion index obtained by the geomorphic quantitative analysis (Anselmi et al., 1996). The results, shown in fig. 14, prove that the highest values are related to the presence of more erodible lithologies and the presence of the landslides.

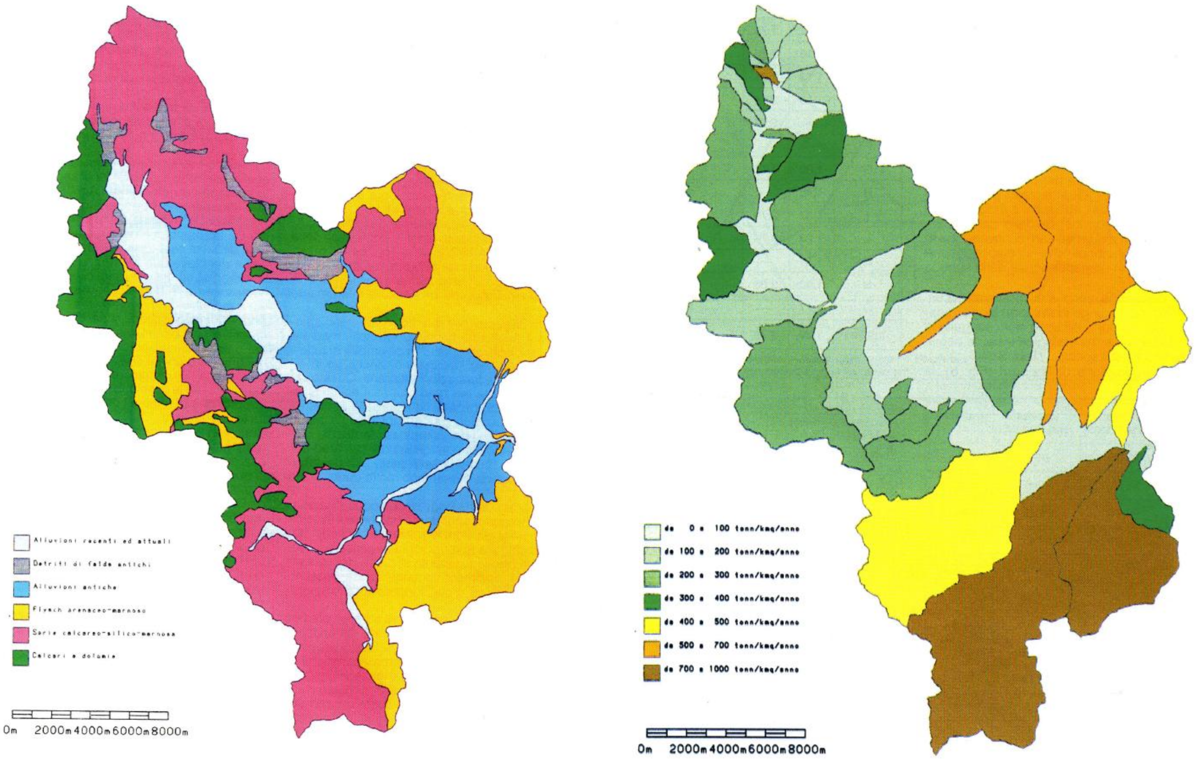

Figure 14. Geolithological scheme (on the left) and erosion index map (on the right) of the HAV (Anselmi et al., 1996)

2.2 The Pietra del Pertusillo reservoir

2.2.1 Geography

The Pietra del Pertusillo fresh-water reservoir is a human-made lake that was formed during the period 1957-1963 (in 1968 the lake reached its maximum level) by building a dam wall across the Agri River, in the upper part of its valley, in the municipalities of Grumento Nova, Montemurro and Spinoso.

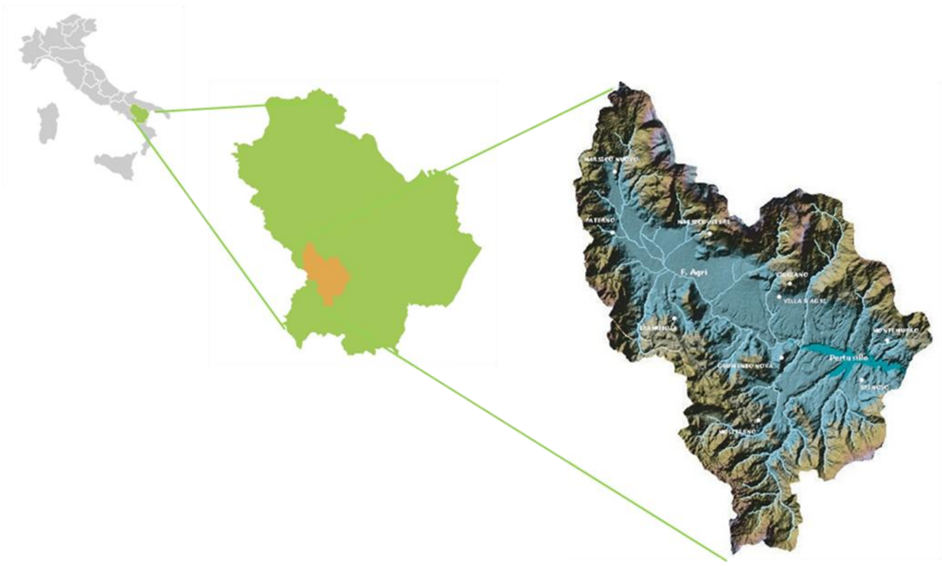

Figure 15. The study area.

The dam is located near “Pietra del Pertusillo”, a locality name derived by the deep gorge where the Agri River flows in this area. It is a concrete arch-gravity dam with a maximum height of 95 m and a crest altitude of 533 m above sea-level. At its maximum storage, the altitude of the lake is 531 m above sea-level while the minimum altitude of the bottom is 453 m and the maximum depth of the dam is 91 m.

Table 1. Technical data about Pietra del Pertusillo.

End of the building	**1963**
Status	Normal conditions
Water uses	Drinking, irrigation, producing hydroelectric energy
Main tributaries	Agri, Sciaura, Casale-Grumentino, Maglia, Vella, Rifreddo, Spetrizzone, Scazzero, Spartifave
Dam's height	95 m
Capacity	155 millions m^3
Maximum altitude	532 m above sea-level
Highest level altitude	531 m above sea-level
Usable capacity	143 millions m^3
Type of the dam	concrete arch-gravity
Surface area	5.27 km^2 (referred to 525 m a.s.l.)

The reservoir, with its surface area of 5.27 km^2, stores approximately 155 million m^3 of water for providing water supply for irrigation, drinking and for producing hydroelectric energy as well (Source: Interregional River Basin Authority of Basilicata). After actuating a hydroelectric plant with an output capacity of about 39 MW, Pertusillo waters are treated to reach Puglia and Basilicata regions (Southern Italy) with a total volume of about 107 millions m^3 (67,7% to satisfy approximately 2 million people). A rate of about 48 millions m^3 (32,3 %) is used for irrigation (the Consortium Bradano-Metaponto through the Gannano dam and the Consortium of High Agri Valley). So, for its capacity and its watershed, the Pertusillo dam is one of the strengths for the regional water supply.

Pertusillo lake is part of Nature 2000, the ecological network of protected areas in the territory of the European Union, aimed at ensuring the long-term survival of Europe’s most endangered species and habitats. It consists of Sites of Community Importance (SCI IT9210143) declared under the Habitats Directive (92/43/EEC) and Special Protected Area for Birds (SPA IT9210270), designed under the Birds Directive (79/409/EEC). The homogeneous area in which the SCI “Pertusillo Lake” is located, is included in a more extensive system of protection that involves the National Park *Appennino Lucano Val D’Agri-Lagonegrese* and the ZPS zone IT9210270 including: Lucanian Apennines, Agri Valley, Sirino Mountain, Raparo Mountain (fig. 16).

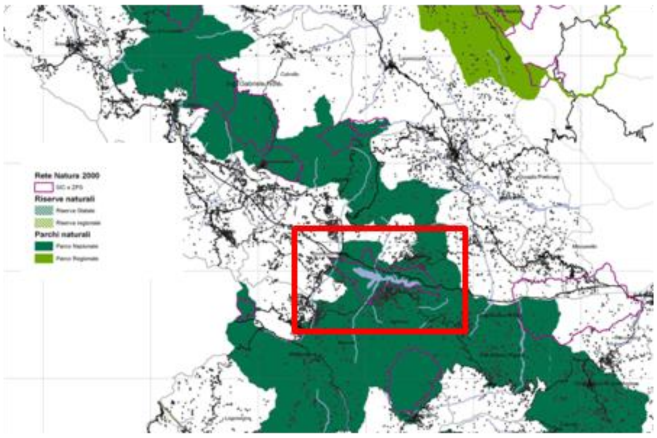

**Figure 16. The wildlife and natural resources in the Province of Potenza.
The red rectangle highlights the Pertusillo lake. (Source: Province of Potenza).**

The Pertusillo SCI provides the ideal habitat for numerous species of animals and plants of significant conservation concern, including*: Ruscus aculeatus*, *Quercus virgiliana*, *Arum lucanum*, *Knautia lucana* and many species of orchids as concern the species of plants and *Lutra lutra*, *Canis lupus*, *Salamandrina terdigitata*, *Hieraetus pennatus*, *Milvus milvus* as concern the species of animals. Moreover the shape of the Pertusillo lake, fairly irregular and with several lateral branches, implies that this reservoir has a strong natural and well integrated appearence in the surrounding area.

Figure 17. The Pietra del Pertusillo reservoir.

2.2.2 Limnology

The Pietra del Pertusillo is a long and narrow fresh-water reservoir with two main arms on its right hand and two small islands (fig. 17): the first one located off of the Vella confluence and the other one off of the Spetrizzone/Scazzero confluence; this last islet joins on the left shore during the drawdown periods. The reservoir is affected by strong seasonal fluctuations of the water level as high as 40 m which correspond to a variation in the reservoir storage of about 80 million m^3 (i.e. about half of the reservoir storage) mainly due to seasonal rainfall/discharge (fig. 18). The extent of drawdown during the last 51 years (i.e. 1964-2015) can be followed according to the data of the Irrigation Institute, with a maximum annual water-level fluctuation of more than 52 m during 1967, when the lake water reached the minimum altitude of about 474 m a.s.l..

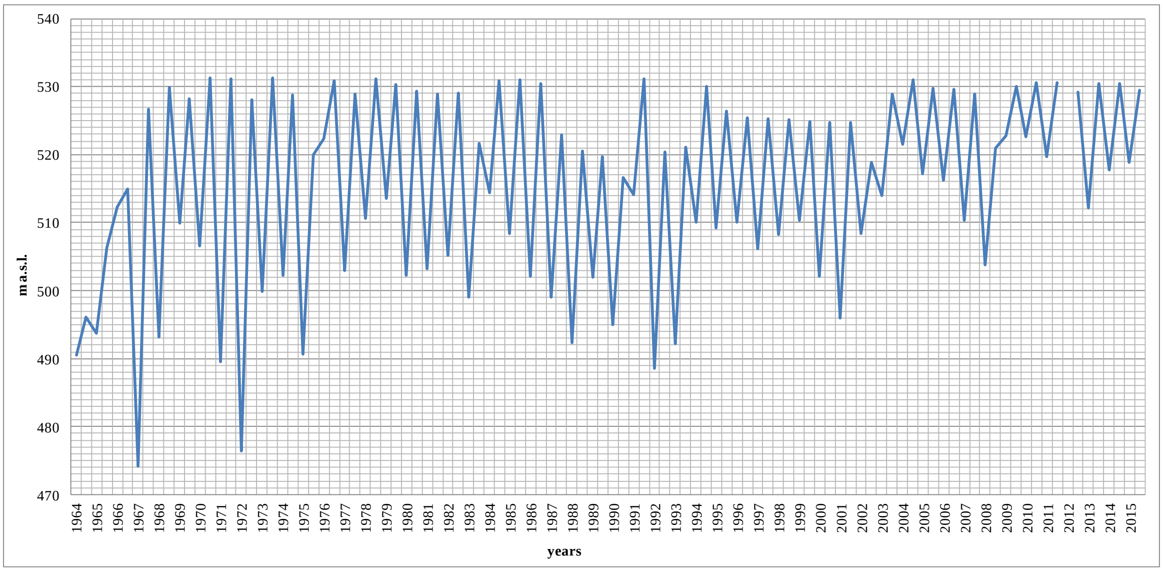

Figure 18. Flood-drawdown cycles during the years 1964-2015 (Data provided by the Irrigation Institute).

The lake level shows an evident annual cycle: it decreases especially in late autumn (October-November), and rises from November to March, as evidenced by the data on the net volume of waters related to the period 2001-2015, published by the Interregional River Basin Authority of Basilicata (fig. 19).

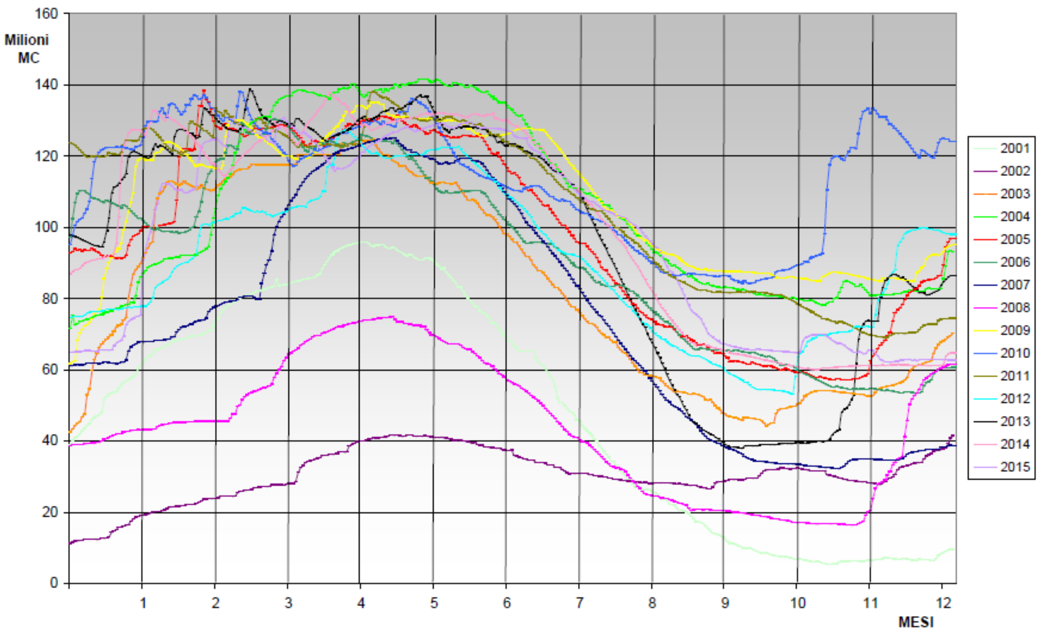

Figure 19. Seasonal changes in reservoir capacity during the period 2001-2015 (Interregional River Basin Authority of Basilicata).

The reservoir is mainly feeded by the Agri River, one of the major rivers of the Basilicata Region, which enters longitudinally the lake basin from the West, whereas other minor lateral tributaries on both northern (Spartifave, Rifreddo, Spetrizzone/Scannamogliera, Scazzero, and Grumentino only during the high-stand periods) and southern (Maglia, Vella, and Sciaura during the high-stand periods) margins are also present, with a torrential-type discharge regime (fig. 20).

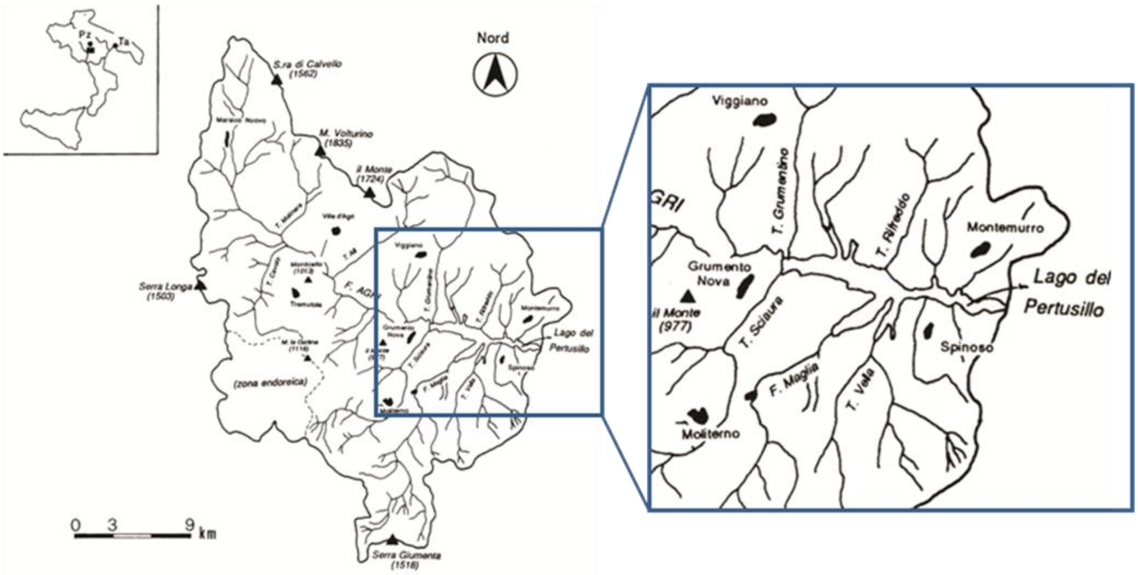

Figure 20. The drenaige basin of the Agri River upstream of the Pertusillo dam on the left and in the enlarged image on the right hand the tributaries of the Pertusillo reservoir (Anselmi et al., 1996).

These tributaries drain areas composed by different lithologic units, so different amounts and types of sediments are introduced at different points in the reservoir. This contrasts with the classical sediment distribution pattern (coarser sediments in shallower regions and finer sediments in deeper regions) typical of natural lakes. Thus, the location of tributaries and the type of sediments they transport are the dominant factors that control the sediment type distribution in the reservoir.

The total volume of sediments accumulated in the reservoir since 1963 to September 2007 was about 7420000 m^3. The dominance of a main stream, the elongated shape and a pronounced lake-bottom topography typical of reservoirs lead to longitudinal gradients in sedimentation rates and grain-size distributions with the greatest sedimentation in the pre-reservoir Agri channel; here the sediment thickness reaches a maximum value of about 8.7 m in the deepest area of the reservoir, near its dam. Consequently it's possible to calculate the approximate average sedimentation rate, that ranges from a value of 4.5 cm/yr up to the first islet to a maximum value of about 19.7 cm/yr near the dam.

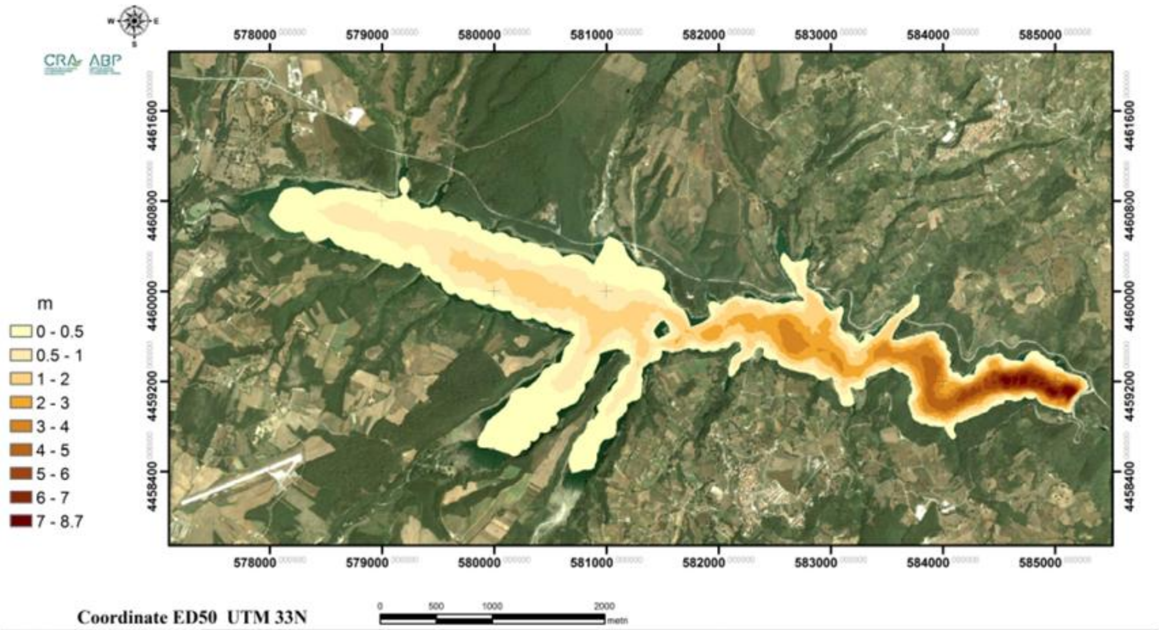

Figure 21. Sediments thickness until September 2007 (Source: CRA-ABP, C*onsiglio per la Ricerca e la Sperimentazione in Agricoltura - Centro per l'Agrobiologia e la Pedologia*, 2007).

Capozza (1963) and Anselmi et al. (1996) concluded that the northern tributaries Rifreddo and Grumentino and the southern tributaries Sciaura, Vella and Maglia probably transport the major amounts of sediments; the suspended sediment yield (T_u) estimated by the second authors for those basins were more than 400 T/km^2/y and more than 700 T/km^2/y for the Vella torrent basin; Lazzari and Schiattarella (2010) calculated a Tu value even more than 900 T/km^2/y for the Rifreddo river basin.

The multiple longitudinal and transversal sediment sources in the area of the lake up to the first islet, together with the water level fluctuations, produce alternating and interdigitated fine-grained sediments sometimes with varves, typical of calm water environments like lakes, and coarse-grained sediments related to fluvial transport in correspondence of the Agri River pre-reservoir channel. At the channel mouths, deposits are arranged in fan deltas with coarse-grained to very coarse-grained sediments, like the Rifreddo fan-delta.

Consequently the spatial distribution of sediments in the area between the mouth of the Agri River and the first islet, where the main tributaries are located is complex and there is no consistent relationship between the spatial distribution of sediment types and water depth. The input of coarse-grained sediments, the multiple sediment sources and the multiple tributaries that input sediments at different points in the reservoir contribute to an inconsistent relationship.

Anselmi et al. 1996 found also a mineralogical variability in the samples collected in the proximal area of the reservoir, with an absence of homogeneity for more than two contiguous samples that strongly reflects the influence of source rocks composition. They highlight a lack of mobility in the reservoir sediments probably due to the significant water-level fluctuations and the frequency of the flood-drawdown cycles.

Basinwards of the first islet, the sediment thickness appears to increase with the increasing water level, as appear if we compare them with the original bathymetry calculated by CRA-ABP (*Consiglio per la Ricerca e la Sperimentazione in Agricoltura - Centro per l'Agrobiologia e la Pedologia*) in September 2007 (figg. 21-22). However there is a lack of sedimentological information about this sector of the lake.

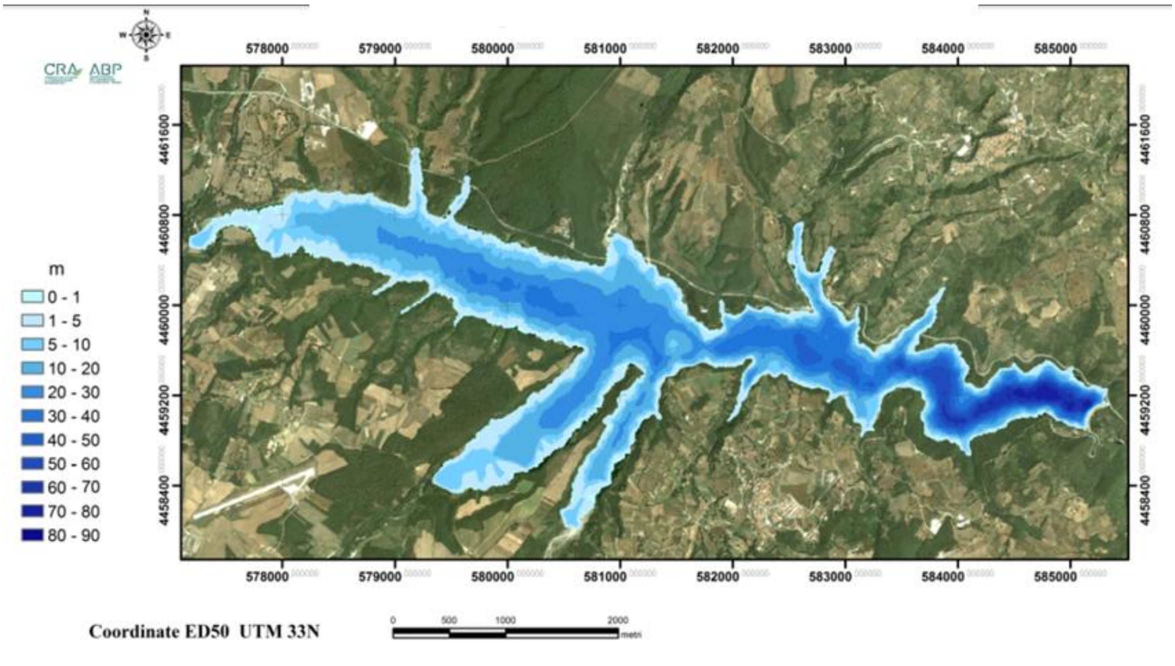

Figure 22. Original bathymetry related to 533 m a.s.l. calculated by CRA-ABP (*Consiglio per la Ricerca e la Sperimentazione in Agricoltura - Centro per l'Agrobiologia e la Pedologia*) in 2007.

2.2.3 Previous monitoring programs of lacustrine sediments

The lacustrine sediments are an important matrix for understanding the anthropogenic pressures to which a specific area is subjected. Technical reports carried out at various times by public bodies on the chemical composition of the Petrusillo lake sediments are given below.

- (2005-2007) - The Metapontum Agrobios Research Centre carried out environmental monitoring of the lacustrine sediments; the samples were taken in a single point located near the dam, with relative chemical analysis of all elements present in table 1/A, Annex 5 of Legislative Decree 152/06, applicable to public, private and residential green sites; the monitoring continued between March 2009 and November 2010, a period in which critical issues were not observed for the investigated metals. Metapontum Agrobios also studied the geochemical distribution of heavy metals in the strategically important soils, including the industrial area of Viggiano. These data are still under validation by the Basilicata Region.
- (2010) - the *Appennino Lucano Val D'Agri-Lagonegrese* National Park authority carried out eco-toxicological analyses on lacustrine sediments to identify the underlying causes of algal bloom, which occurred in the Pertusillo fresh-water reservoir in May 2010;
- (2010) - The Regional Agency for the Protection of the Environment of Basilicata (ARPA-Basilicata) increased the monitoring of the Pertusillo reservoir to determine the chemical, physical and biological characteristics of the reservoir and their variation during an annual cycle. However, at present the only sampling of lacustrine sediments was carried out in March 2012 in seven points of the reservoir, and it shows that a larger contribution of pollutants came from the Agri River.
- (July 2013) - A new survey campaign of various environmental matrices including the surface water environment was started as part of the "*Ecosystem Status Monitoring Project*" regulated by an agreement signed in June 2013 between Eni and ARPAB and carried out by the ARPAB Metapontum Research Centre (formerly, Metapontum

Agrobios). The study includes an investigation of various heavy metals (Ag, Al, As, B, Ba, Be, Cd, Co, Cr tot, Cr VI, Cu, Fe, Hg, Mn, Ni, Pb, Sb, Se, Sn, Tl, V, Zn) analysed on 7 samples taken between September 2013 and September 2014 in 6 points of the Pertusillo basin.

The final report, published in March 2015, shows the comparison between the values found in the stream and lake sediments with national standards (LCR proposed by ISPRA in 2009) and international standards (Standard Quality Guidelines, SQG, calculated in Wisconsin, USA; the Dutch Target and Intervention values). It shows that the concentration of metals regulated by APAT are always below the LCR; Fe and Mn values exceed the American SQG values, while concentrations of Ni, Cu, Co and Ba are between the Dutch T.V. (Target Value) and I. V. (Intervention Value).

A careful reading of these reports and investigation shows that the analyses carried out by various authorities have been discontinuous and fragmented and, in any case, have involved only the surface layer of lacustrine sediments, not taking into account other types of sediments and relationships between them nor the origin of any micro pollutants.

Conversely, this project is based on a more detailed and complete analysis that concern not only the geological formation outcropping in the Pietra del Pertusillo watershed, aims to analyse the different types of sediments in the basin, with greater attention to analyzing lacustrine sediment cores at variable depths sampled in appropriately selected areas. Moreover, this project also provides for a careful study of the sampling and the subsequent analytical phase according to a highly scientific approach.

References

- A.R.P.A.B. – Centro Ricerche di Metaponto, 2015. *Progetto di Monitoraggio dello stato degli Ecosistemi dell'area della Val d'Agri. Acque Superficiali.* http://www.arpab.it/risorse_idriche/public/Relazione_EcosistemiValdAgri11032015.pdf.

- Abraham et al., 1999. *Sediment type distribution in reservoirs: sediment source versus morphometry*. Environmental Geology 38 (2).

- ARPAB (Agenzia Regionale per la Protezione Ambientale della Basilicata), 2012. *Sedimenti, campionamento marzo 2012*. Nell'ambito del progetto: Valutazione dello stato ecologico del lago del Pertusillo. http://www.arpab.it/risorse_idriche/public/SedimentiMarzo2012.pdf.

- Anselmi et al., 1996. *La sedimentazione nell'invaso artificiale del Pertusillo (fiume Agri, Basilicata)*. Geologia Tecnica & Ambientale, 4.

- Autorità Interregionale di Bacino della Basilicata 2005. *Piano di bacino stralcio del bilancio idrico e del deflusso minimo vitale.*

- Barchi et al., 2006. *Extensional tectonics and seismicity in the axial zone of the Southern Apennines*. In *CROP-04,* Vol. 7, pp. 47–56, eds Mazzotti, A., Patacca, E. & Scandone, P., Boll. Soc. Geol. It., Spec. Issue.

- Ben-Avraham et al., 1990. *Principali domini strutturali originatisi dalla collisione neogenico-quaternaria nel Mediterraneo centrale*. Mem. Soc. Geol. It. 45, 453– 462.

- Benedetti et al., 1998. *Surface rupture due to the 1857 Southern Italian Earthquake*. *Terra Nova,* **10**(4), 206–210.

- Bersezio et al., 2007. *Aquifer analogues to assist modeling of groundwater flow: the Pleistocene Aquifer Complex of the Agri Valley (Basilicata)*. Mem. Descr. Carta Geol. d'It. LXXVI, pp. 51-66.

- Bertinelli et al., 2005. *Stratigraphic evolution of the Triassic-Jurassic Sasso di Castalda succession (Lagonegro Basin, Southern Apennines, Italy)*. Boll. Soc. Geol. It., 124, 161-175.

- Bianca M. & Caputo, 2003. A*nalisi morfotettonica ed evoluzione quaternaria della Val d'Agri, Appennino Meridionale.* Il Quaternario, Italian Journal of Quaternary Sciences 16(2 158-170.

- Boezi et al., 2004. *Polyphase geomorphological evolution and uplift rates of the south-western side of the Agri high Valley (southern Apennines)*. Boll. Soc. Geol. Ital. 123, 357—372 (in Italian).

- Bonardi et al., 1985. *La formazione di Albidona nell'Appennino calabro-lucano: ulteriori dati biostratigrafici e relazioni con le unità esterne appenniniche*. Boll. Soc. Geol. It., v. 104, p. 539–549.

- Borraccini et al., 2002. *3D Model of the active extensional fault system of the high Agri River valley, Southern Apennines, Italy*. In: Jessell, M. W. 2002 General Contributions. Journal of the Virtual Explorer, 6, 1-6.

- Burrato & Valensise, 2008. *Rise and fall of a hypothesized seismic gap: source complexity in the Mw 7.0 16 December 1857 Southern Italy Earthquake*. *Bull. seism. Soc. Am.,* **98,** 139–148, doi:10.1785/ 0120070094.

- Capozza 1963. *Influenza del fattore geomorfologico e litologico sul trasporto solido del f. Agri a monte della diga del Pertusillo*. Rass. Lav. Pubbl., n. 12, 1235- 1258.

- Carbone et al., 1991. *Presentazione della Carta Geologica del Bacino del fiume Agri (Basilicata)*. Mem. Soc. Geol. It., 47, 129 - 143.

- Catalano & Monaco. *Affinità composizionali tra la Formazione del Saraceno ed il Flysch di Albidona nell'Appennino calabro-lucano*. Rendiconti della Società Geologica Italiana, num.13, pagg. 85-88, figg. 4.

- Cello & Mazzoli, 1999. *Apennine tectonics in southern Italy*: a review. *J. Geodyn.,* **27,** 191–211.

- Cello et al., 2000. *Fault zone characteristics and scaling properties of the Val d'Agri Fault System (Southern Apennines, Italy)*. Journal of Geodynamics 29 (2000) 293±307.

- Cello et al., 2003. *Active tectonics and earthquake sources in the epicentral area of the 1857 Basilicata earthquake (Southern Italy)*. *J. Geodyn.,* **36,** 37–50.

- Colella et al., 2004. *High-resolution imaging of the High Agri Valley Basin (Southern Italy) with electrical* *resistivity tomography*. Tectonophysics 386, 29– 40.

- CRA-ABP (Firenze). *Invaso Pertusillo (PZ) Rilievi batimetrici e sedimentometrici al 29 settembre 2007*. Nell'ambito del progetto REL: Attività tecnico-scientifiche nell'ambito del Progetto Operativo "Attività di assistenza tecnica e supporto agli enti concessionari nel settore dekll'uso irriguo delle risorse idriche".

- D'Argenio et al., 1972. *Schema geologico dell'Appennino Meridionale (Campania e Lucania)*. Atti del Conv. Moderne vedute sulla geologia dell'Appennino (Roma 16-18 Febbraio 1972), Accad. Naz. Lincei, Quad., 183, 49-72.

- Dewey et al., 1989. *Kinematics of the Western Mediterranean*. In: Coward M. P., Dietrich D. & Park R. G. (eds), Alpine Tectonics, Geol. Soc. Spec. Publ., 45, 265-283.

- Di Niro & Giano, 1995: *Geomorphological evolution of the eastern side of the Agri high Valley (Basilicata)*. Studi Geologici Camerti, Spec. Vol. 1995/2, 207—218 (in Italian).

- Di Niro et al., 1992: *Preliminary notes on the geomorphological and sedimentary evolutions of the Agri high basin (Basilicata)*. Studi Geologici Camerti, Spec. Vol. 1992/1, 257—263.

- Doglioni, 1991. *A proposal modelling of W-dipping subduction possible application to the Tyrrhenian-Apennines system*. Terra Nova, 3: 423-434.

- Doglioni et al., 1996. *A geodynamic model of the Southern Apennines accretionary prism*s. Terra Nova 8, 540–547.

- Ente Parco Appennino Lucano Val d'Agri Lagonegrese, 2010. *In Bloom. Studio sulla fioritura algale nel bacino idrico artificiale del Pertusillo.*

- Giano et al., 1997. *Nuovi dati geologici e geofisici sull'assetto strutturale dei depositi continentali quaternari dell'alta Val d'Agri (Basilicata)*. Il quaternario, Italian Journal of Quaternary Sciences, 10 (2), 589-594.

- Giano et al., 2000. *Radiocarbon dating of active faulting in the Agri high valley, southern Italy*. Journal of Geodynamics 29, 371-386.

- Giano, 2011. *Quaternary alluvial fan systems of the Agri intermontane basin (southern Italy): tectonic* *and climatic controls.* Geologica Carpathica, 62, 1, 65-76 doi: 10.2478/v10096-011-0006-y.

- Giocoli et al., 2015. *Geological and geophysical characterization of the High Agri Valley*. Nat. Hazards Earth Syst. Sci., 15, 315–323. www.nat-hazards-earth-syst-sci.net/15/315/2015/ doi:10.5194/nhess-15-315-2015.

- Grasso et al., 2006. *Caratteri strutturali e significato tettonico di un melange continentale nell'Alta Val d'Agri (Appennino Lucano)*. *Rend*. Soc. Geol. It., 2, Nuova Serie, 146-147.

- Gueguen et al., 2015. *The Verdesca landslide in the Agri Valley (Basilicata, southern Italy).* Nat. Hazards Earth Syst. Sci., 15, 2585–2595. www.nat-hazards-earth-syst-sci.net/15/2585/2015/ doi:10.5194/nhess-15-2585-2015.

- Lapenna & Rizzo (2003) - *Tomografie geoelettriche dipolari del Bacino dell'Alta Val d'Agri.* In: A. COLELLA (Ed.): "*Le risorse idriche sotterranee dell'Alta Val d'Agri*". Autorità Interregionale di Bacino della Basilicata, Collana Editoriale di Studi e ricerche, n. **3**: 87 - 112, Potenza.

- Lazzari and Schiattarella 2010. *Estimating Long to Short-Term Erosion Rates of Fluvial vs Mass Movement Processes: An Example from the Axial Zone of the Southern Italian Apennines*. Ital. J. Agron. / Riv. Agron., 2010, 3 Suppl.:57-66.

- Lechler et al., 2012. *Stratigraphic setting of a segment from the Eastern margin of the Apennine platform (Monte di Viggiano, Southern Apennines).* Rend. Online Soc. Geol. It., Vol. 21, pp. 1012-1013.

- Lentini et al., 1987. *Confronti sedimentologici-petrografici e posizione strutturale dei Flysch di Albidona e di Gorgoglione nella media Val d'Agri (Appennino Lucano).* Mem. Soc. Geol. It., 38 (1987), 259-273, 6 ff., 1 tab.

- LISUT, Scuola di Ingegneria – UNIBAS, 2014. *Contributi al Piano Strategico Intercomunale della Val d'Agri. Il quadro conoscitivo: il sistema socio-demografico e insediativo.* http://www.lisut.org/it/public/[Download]/file/Analisi%20di%20contesto%20val%20d'agri.pdf

- Loperte and Cosmi, 2015. *The environmental balance of the Alta Val d'Agri: a contribution to the evaluation of the industrial risk and strategic sustainable development*. Nat. Hazards Earth Syst. Sci., 15, 1941–1954, www.nat-hazards-earth-syst-sci.net/15/1941/2015/ doi:10.5194/nhess-15-1941-2015.

- Malinverno & Ryan (1986). *Extension in the Tyrrhenian Sea and shortening in the Apennines as a result of arc migration driven by sinking of the lithosphere*. Tectonics, 5: 227-245.

- Marsella et al., 1995. *Tectonic history of the Lagonegro Domain and Southern Apennine thrust belt evolution*. Tectonophysics, 252, 307-330.

- Maschio et al., 2005. *Active extension in Val d'Agri area, Southern Apennines, Italy: implications for the geometry of the seismogenic belt*. Geophys. J. Int. 162, 591–609.

- Mazzoli and Helman (1994). *Neogene patterns of relative plate motion for Africa-Europe: some implications for recent Central Mediterranean tectonics*. Geologische Rundschau, 83, 464-468.

- Menardi-Noguera & Rea, 2000. *Deep structure of the Campanian-Lucanian Arc (Southern Apennine, Italy).* Tectonophysics, 324, 239-265.

- Metapontum Agrobios, 2007. *Progetto Val D'Agri. Rete di monitoraggio ambientale nelle aree a rischio di inquinamento da idrocarburi*. Relazione finale.

- Monaco et al., 1998. *Structural evolution of the Lucanian Apennines, Southern Italy*. Journal of Structural Geology 20 (5), 617–638.

- Morandi and Ceragioli, 2002. *Integrated interpretation of seismic and resistivity images across the «Val d'Agri» graben (Italy)*. Annals of Geophysics, vol. 45, N. 2.

- Nehyba et al. 2011. *Depositional rates and dating techniques of modern deposits in the Brno reservoir (Czech Republic) during the last 70 years*. J Paleolimnol. 45:41–55 DOI 10.1007/s10933-010-9478-5.

- Ogniben, 1969. *Schema introduttivo alla geologia del confine calabro-lucano.* Mem. Soc. Geol. Ital., 8, 453-763.

- Palladino et al., 2008. *Tectonic control on the deposition of the Lower Miocene sediments of the Monti della Maddalena ridge (Southern Apennines): synsedimentary extensional deformation in a foreland setting.* Boll. Soc. Geol. It. (*Ital. J. Geosci.*), Vol. 127, No. 2, pp. 317-335.

- Patacca & Scandone, 1989. *Post-Tortonian mountain building in the Apennines. The role of the passive sinking of a relic lithospheric slab.* In: Boriani A., M. Bonafede M., Piccardo G.B., Vai G.B. Eds. "The lithosphere in Italy. Advances in Earth Science Research".

- Patacca et al., 1990. *Tyrrhenian basin and Apenninic arcs: kinematic relations since Late Tortonian times*. Mem. Soc. Geol. Ital., 45, 425-451.

- Patacca et al., 1992b. *La zona di giunzione tra l'arco appenninico settentrionale e l'arco appenninico meridionale nell'Abruzzo e nel Molise*. In: TOZZI M., CAVINATO G.P. & PAROTTO M. Eds., «Studi preliminari all'acquisizione dati del profilo CROP 11 Civitavecchia-Vasto», AGIP-CNR-ENEL. Studi Geol. Camerti, Vol. Spec. 1991-2, 417-441.

- Patacca & Scandone, 2007. *Geology of the Southern Apennines*. Boll. Soc. Geol. It. (*Ital.J.Geosci.*), Spec. Issue No. 7, pp. 75-119. CROP-04 (ed. by A. Mazzotti, E. Patacca and P. Scandone).

- Pavan & Pirini, 1963. *Microfossili cretacici ed eocenici nella zona di M. Falapato (Lucania)*. Mem. Soc. Geol. It., vol. 4, 6 pp., 2 figg., 6 tavole.

- Pescatore et al., 1988. *La sedimentazione miocenica nell'Appennino Campano-Lucano*. Mem. Soc. Geol. Ital., 41, 37-46.

- Pescatore et al., 1999a. *Stratigraphic and structural relationships between Meso-Cenozoic Lagonegro basin and coeval carbonate platforms in southern Apennines, Italy*. Tectonophysics, 315, 269-286.

- Provincia di Potenza 2009. Piano strutturale provinciale.

- Prosser et al., 1996. Una sezione rappresentativa dell'Appennino Meridionale. Conferenza sulla Ricerca Scientifica in Basilicata, Potenza, 29 febbraio-1 marzo.

- Prosser, 2012. *Introduzione alla geologia dell'Appennino meridionale*. In: Atti del 1° Congresso dell'Ordine dei Geologi di Basilicata. Potenza, 30 Novembre - 2 Dicembre 2012.

- Rete Natura 2000 - Regione Basilicata - Piano di gestione Area 3 - ATO 13 – *Scheda di sintesi del rapporto n°1- SIC Lago PERTUSILLO IT9210143*.

- Rizzo et al., (2004). *High-resolution images of the faultcontrolled High Agri Valley basin (Southern Italy) with deep and shallow electrical resistivity tomographies*. Phys. Chem. Earth, 29, 321-327.

- Scandone, 1967. *Studi sulla geologia lucana: le serie calcareo-silicomarnosa e i suoi rapporti con l'Appennino Calcareo*. Bollettino della Società dei Naturalisti in Napoli 76, 1–175.

- Scandone, 1972. *Studi di geologia lucana: carta dei terreni della serie calcareo-silico-marnosa e note illustrative*. Boll. Soc. Natur. Napoli, **81**, 225-300.

- Selli, 1962. *Il Paleogene nel quadro della geologia dell'Italia Meridionale*. Mem. Soc. Geol. It.,3, 737-789.

- Sgrosso, 1986. *Criteri ed elementi per una ricostruzione paleogeografica delle zone esterne dell'Appennino centro-meridionale*. Mem. Soc. Geol. Ital., 35, 203-219.

- Shiner et al., 2004. *Thin-skinned versus thick-skinned structural models for Apulian carbonate reservoirs: constraints from the Val d'Agri Fields, S Apennines, Italy*. Marine and Petroleum Geology, 805–827.

- Shotbolt et al. 2001. *Establishing the sediment stratigraphy of reservoirs in the Southern Pennines, Uk*. Hydrological Sciences-Journal des sciences hydrologiques, 46(5).

- Shotbolt et al. 2005. *The use of reservoir sediments as environmental archives of catchment inputs and atmospheric pollution*. Progress in Physical Geography 29, 3, pp. 337–361.

- Simoniello et al., 2015. *Land cover changes and forest landscape evolution (1985–2009) in a typical Mediterranean agroforestry system (high Agri Valley)*. Nat. Hazards Earth Syst. Sci., 15, 1201–1214, www.nat-hazards-earth-syst-sci.net/15/1201/2015/ doi:10.5194/nhess-15-1201-2015.

- Valensise & Pantosti, 2001. *The investigation of potential earthquake sources in peninsular Italy: a review. J. Seism.,* **5,** 287–306.

- Valoroso et al., 2009. *Active faults and induced seismicity in the Val d'Agri area (Southern Apennines, Italy)*. Geophys. J. Int. 178, 488–502.

- Valoroso et al., 2011. *Upper crustal structure, seismicity and pore pressure variations in an extensional seismic belt through 3D and 4D VP and VP/VS models: The example of the Val d'Agri area (southern Italy)*. Journal of geophysical research, vol. 116, xxxxxx, doi:10.1029/2010jb007661, 2011.

- Van Metre et al., 2001. *Differences in lake and reservoir sedimentation – implications for sediment coring studies*. Proceedings of the Seventh Federal Interagency Sedimentation Conference, Reno, Nevada.

- Vezzani, 1970. *Il flysch di Albidona nell'area del confine tra Calabria e Lucania*. Geol. Rom., 9, pp. 101-126.

- Zembo, 2010. *Stratigraphic architecture and quaternary evolution of the Val d'Agri intermontane basin (Southern Apennines, Italy)*. Sedimentary Geology 223 (2010) 206–234.

- Zembo, 2006. Evoluzione quaternaria del bacino intermontano alta Val d'Agri. Tesi di dottorato.

MATERIALS & METHODS

3. Materials and methods

3.1 Sampling

The Meso-Cenozoic formations with a predominate siliciclastic pelitic fraction and the Quaternary fluvio-lacustrine deposits outcropping in the Pietra del Pertusillo catchment, the fluvio-lacustrine sediments of the main Pietra del Pertusillo tributaries, close to the supply entry-points and the lacustrine long-cores were collected.

3.1.1 The bedrock

The Meso-Cenozoic formations and the Quaternary deposits outcropping in the Pietra del Pertusillo catchment were sampled in order to determine the background values of elements. 46 samples were analyzed: 31 pelitic samples belonging to the different lithoid formations and 15 samples to the Pleistocene fluvio-lacustrine deposits (fig. 23).

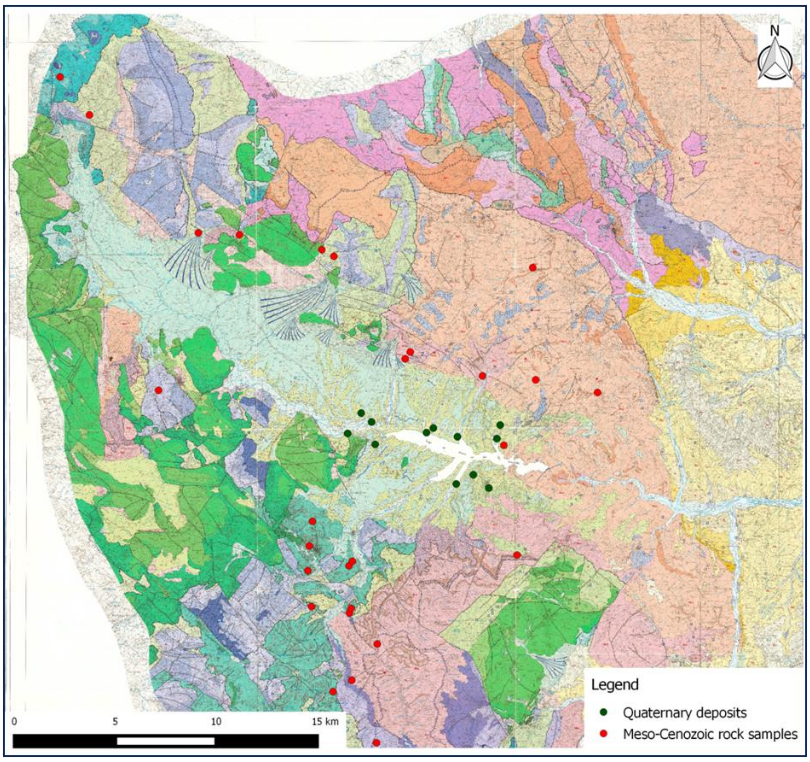

Figure 23. Location of the bedrock samples (Geological map from Lentini et al., 1991).

Meso-Cenozoic formations

31 samples with a predominate siliciclastic pelitic fraction were selected; due to its intrinsic features, this fraction contains the highest content of minor and trace elements, and more readily tend to release the elements into the environment. Lithologies with a dominant carbonate component were analysed at a lower extent. In particular, the following geological formations were taken into consideration: Scisti Silicei, Galestri, Monte Facito Formation, Moliterno Succession, the Ligurian Complex (Crete Nere Formation and Saraceno Formation), Albidona and Gorgoglione Flysches. So, we considered as bedrock only the lithologies having a significant pelitic fraction that commonly is thought to be responsible for the uptake and absorption of minor and trace elements.

Figure 24. The Albidona Flysch (on the left) and the Gorgoglione Flysch (on the right).

Quaternary deposits

The Quaternary incoherent deposits were sampled in the drainage basin and, during the low-standing periods, along the shores of the reservoir between the confluences of the Spartifave and Vallone dell'Aspro Streams as well as at the confluence of the Rifreddo and of the Vella Streams (fig. 26).

15 samples were collected from 18 outcrops, and subjected to subsequent chemical analyses, taking into consideration: the closer location of the outcrop to the reservoir, the

finer grain size (preference was given to the analysis of sandy-clay samples rather than conglomerates) and the more areally exposed lithologies. For each outcrop a data sheet was made up, containing: the location of the outcrop, its lithological description, the picture and the type of material collected.

Chemical analyses were performed on the bedrock samples in order to achieve a representative value of the geogenic contribution of each element. Chemical analyses were performed on the bulk fraction of the 31 lithoid samples and on the silty-clay fraction (< 63 μm) of the 15 incoherent quaternary samples.

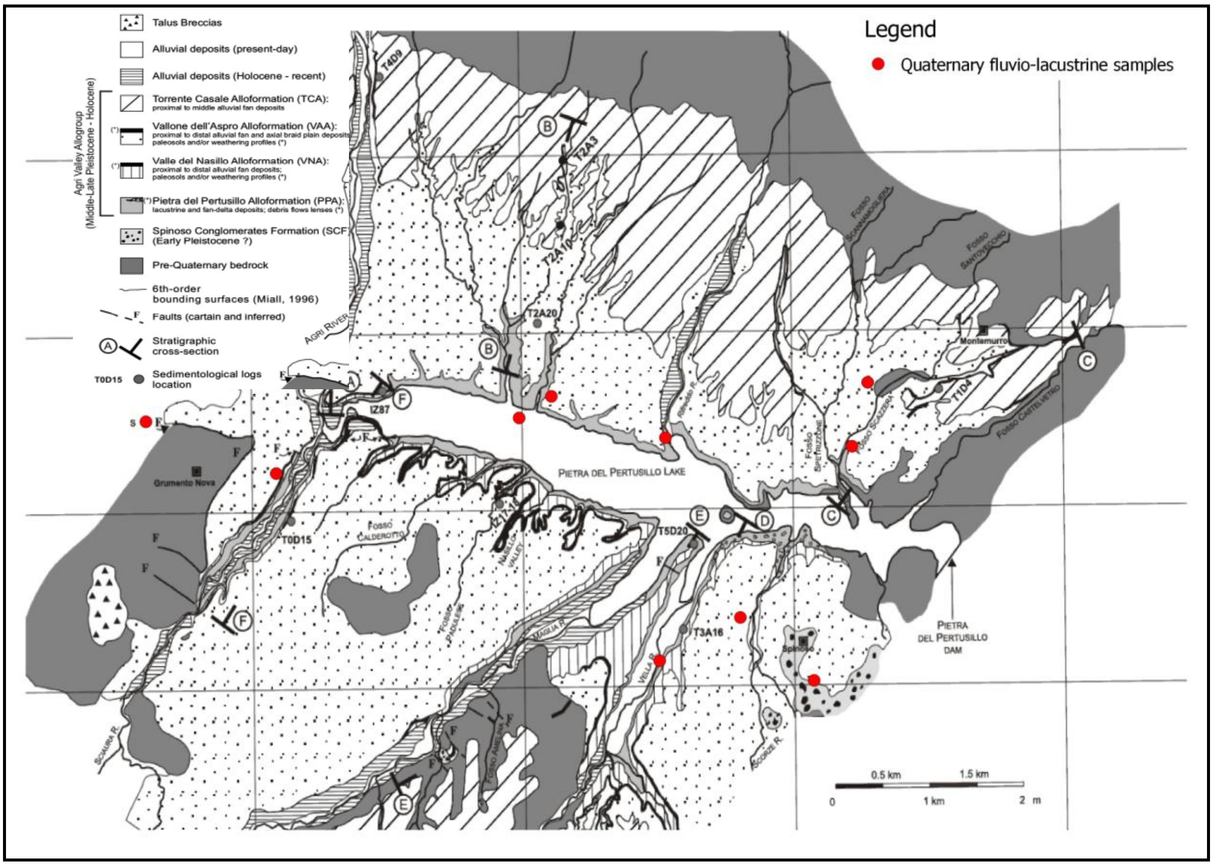

Figure 25. Location of the Quaternary fluvio-lacustrine samples
(Semplified geological map from Zembo, 2010).

Figure 26. Quaternary deposits outcropping: along the SP11 to Montemurro (on the left) and close to the Pertusillo lake, between the confluences of the Spartifave and Vallone dell'Aspro Streams (on the right).

3.1.2 The fluvio-lacustrine sediments

Recent scientific papers (*Miller J. R. and Miller S. M., 2007; Ladd S.C. et al., 1998*) stressed the importance of speciation of metals and trace elements in river sediments and, more specifically, the transport and deposit of contaminants and especially of metals in various types of river channels, their mechanisms of distribution among the different fluvial morphological units and the implications for sampling. Therefore, the factors that influence the distribution of metals and other trace elements in the active river channels, are mainly the grain size and the presence of silty-clay material in a single river channel. Other papers were also analysed in order to assess the heavy metals in soils in the water-level fluctuation zone (WLFZ) close to the reservoirs (*Chen Y. et al., 2011*; *Junjie Lin, 2012; Shiliang Liu, 2014*); however, to date, we have not found any papers concerning the trend of metals in the streams collected at the confluences between rivers and artificial reservoirs, affected by significant water level fluctuations.

In the case of an artificial reservoir such as the Pertusillo, the peri-lacual zone is a very dynamic system. Therefore, before sampling the surface sediments and in the absence of an official method or literary studies, we decided to carry out 3 surveys along the beaches, close to the confluences of the major tributaries. The surveys were carried out during the low-standing of the autumn 2013; in particular the following streams were investigated: the

Agri River, which represents the main tributary of the reservoir; Spartifave, Vallone dell'Aspro, Rifreddo, Spetrizzone and Scazzero on the left side of the reservoir; the Maglia river and the Vella Stream on the right side.

Among these, Spartifave, Vallone dell'Aspro, Rifreddo and Vella showed typical torrential features since they were dry during the summer months and in particular, during 2013, up to the beginning of November, after which the intensification of autumn rainfall determined their reactivation. Therefore, having ascertained an inconsistent hydraulic system and in order to obtain an homogeneous chemical data set, we decided to only sample sediments of active channels. The sediment samples were taken upstream of the confluences since higher quantities of finer sediment fractions have been registered in these areas (fig. 27).

Figure 27. Sampling points of the fluvio-lacustrine sediments.

Sampling was carried out in November 2013. The sediment samples were collected in the central part of the channel, below a water column of at least 10-15 cm and using a polyethylene unpainted shovel, placed in plastic bags, sealed, kept at a temperature of 4°C and transported to cold storage within 24 hours (fig. 28). As concern the Agri River, 3 samples were taken along the fluvial channel in the section that goes from the mouth of its last tributary, the Sciaura Stream, up to the confluence with the reservoir. A fourth point was sampled approximately 30 m off the coast (EFF15) with a boat and a *Van Veen* type bucket (fig. 29).

Figure 28. Sampling of the Maglia River. (Left)

Figure 29. Sample EFF15 collected with a boat and a Van Veen grab sampler. (Right)

3.1.3 The lacustrine core sediments

Based on the sediment thickness data proposed by CRA-ABP, 2007 (*Consiglio per la Ricerca e la Sperimentazione in Agricoltura - Centro per l'Agrobiologia e la Pedologia*) and the main anthropogenic pressures acting in the immediate vicinity of the reservoir, 15 core sampling points were selected. It was decided to sample close to the confluences of the main tributaries, in order to intercept the sediment contributions coming from the different drainage basins. In particular it was decided to locate a larger number of cores basinward of the Agri River confluence (cores: A, B, F, F_1) and of the northern tributaries (Rifreddo cores: H, L; Spetrizzone-Scazzero cores: Q, R), due to the important human pressure which insists in their respective basins. As for the southern tributaries, it was decided to collect a core in each of the two arms: the core I in the Maglia river arm and the core M in the Vella stream arm.

The selection of the other core sampling points was a balance between the following factors:

- the presence of high sedimentation rates and consequent high sediment thickness, which improve the reconstruction of temporal trend, reduce the effects of post-depositional mixing effects and also the time in which the sediments remain in contact with water;

- the presence of undisturbed and homogeneous finer-grained sediments, due to the constant submersion of the area also during low-standing periods.

The redistribution action of a reservoir usually involves very homogeneous and finer-grained sediments in its middle and lower portions, that normally correspond to the accumulating zone. Regarding the Pertusillo reservoir, the pachymetrical map proposed by CRA-ABP (2007) shows the highest sediment thicknesses in the central portion of the lake, in the pre-reservoir stream channel and in its middle and lower portions, basinwards the first islet to the SE. So, the other cores (N, P, S, T, V) were located in this portion of the lake (fig. 30). In correspondence of the F, I, Q, V sampled points, two cores were collected, one of which was intended for the analysis of hydrocarbons, which however is not the object of this study. Coordinates, length and approximate water depth for each sampling point are in table 2.

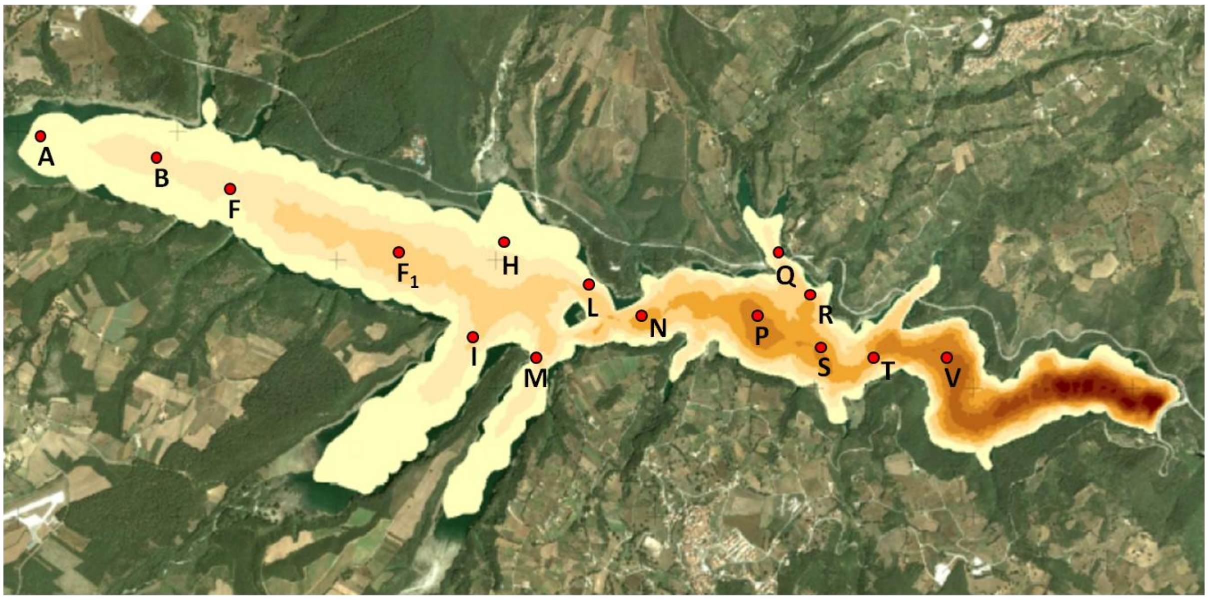

Figure 30. Core sampling points.

Table 2. Coordinates, length and approximate water depth for each sampling point.

Sampling point	Longitude	Latitude	Length (cm)	Approximate water depth (m)
A	578019.10	4460549.77	65	10
B	578792.32	4460446.81	50	12.5
F	579229.09	4460229.37	69	13
F_1	580289.34	4459787.92	50	17
H	580973.26	4459874.80	32	13
I	580757.62	4459283.51	150	18
L	581467.64	4459581.02	55	22
M	581200.77	4459143.34	130	20
N	581820.88	4459455.33	180	26
P	582550.69	4459450.96	120	30
Q	582714.28	4459822.80	50	20
R	582897.10	4459519.52	175	35
S	582923.67	4459251.54	143	
T	583259.88	4459175.07	160	55
V	583770.75	4459109.81	140	65

On the basis of national and international guidelines (*EPA, 2001; IAEA, 2003; IRSA CNR, 2005; ISPRA, 2009*) a gravity corer, which is indicate as the most suitable instrument for sampling soft finer-grained sediments (silt and clay) at limited depths in order to minimize the disturbance, was selected. The sampling cruise was undertaken in May 2014 with the logistic support of the Austrian company UWITEC, who also supplied all the equipment for sampling, which consists of the following material:

- a motorized aluminium platform (3.6 x 2.8 m) with a tripod for the vertical descent of the corer;
- a gravity corer provided with 2 weights of 7 kg each and a drill of the same weight to enable the progressive insertion in the sediment;
- no. 20 transparent PVC tubes with a length of 2 metres each and a diameter of 90 mm, in order to obtain greater quantities of sample for laboratory analysis;
- no. 20 caps and sponges to plug cores respectively at the top and bottom;
- also: a manual winch, an anchor, 120 metres of rope with a thickness of 8 mm capable of supporting a weight of 5000 kg.

Appendix 4 contains a detailed core drilling operation description.
Each core was measured, sealed, labelled and, at the end of each sampling day, brought into cold storage until the time of splitting. The cores were stored in the dark at a temperature of 4°C in order to limit possible biological activity and in vertical position to prevent mixing of the top layer of the core, which is characterized by higher water content and unconsolidated material.

At the time of sub-sampling, each core was removed individually from the cold storage and the tube was cut with the help of an electric milling machine and splitted. The two halves obtained were photographed and subsequently the stratigraphic and sedimentation description was carried out on one half of the core; the colour determination was performed using comparative tables (*Munsell soil colour charts*). These operations enabled to identify the horizons to be sampled. The surface patina was removed and all levels identified were sampled for each core for a total number of 147 samples. The sediment fractions collected were placed in containers of high density polyethylene (HDPE) and frozen at -20 ° C; this temperature precludes the development of potential bacterial activity (*EPA, 2001*). Half of the core not sampled was wrapped in parafilm, and also frozen at -20 ° C, and preserved as a standard.

The splitting and sub-sampling operations of the different core sediments were carried out in the thin sections laboratory of the Science Department at the University of Basilicata and they are described in detail in Appendix 4.

3.2 Analytical tecniques

Grain size, mineralogical and chemical analyses were carried out on the fluvio-lacustrine and lacustrine core sediments. Only chemical analyses were performed on the bedrock samples in order to achieve a representative value of the geogenic contribution of each element.

3.2.1 Grain size analysis

The granulometric soil characterization was performed using the *Grain Size Analyser* (fig. 31), an instrument that enables to detect the finer fraction of the soil (between 0.1 mm and 1µ) by measuring the progressive reduction in the density of soil suspension resulting from the sedimentation of material particles over time. The instrument is managed by a software and enables the collection and processing of the acquired data, which is returned either by granulometric curve or in summary form (amount in g/kg for each fraction). Analysis were performed at the sedimentology laboratory of the Department of Science at the University of Basilicata.

For the purposes of this study, the samples were treated as follows: 62.5 ml of a sodium hexametaphosphate at 4% solution was added to 25 g of each soil sample (where present) and left to react for 24 hours. Once this time was completed, the solution was poured into a cylinder provided by the instrument and distilled water was added up to the reference mark on the cylinder. The time of each measure is of about 6 hours.

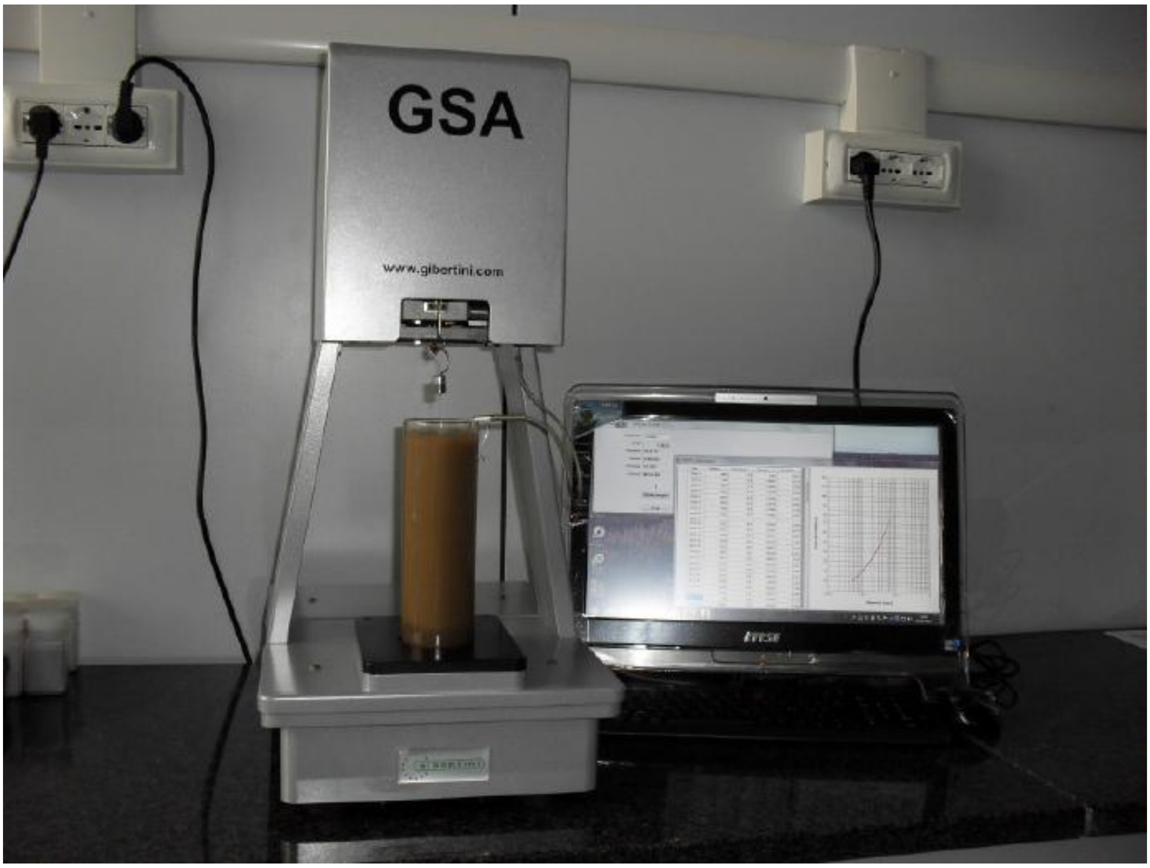

Figure 31. Grain size analyzer.

3.2.2 XRPD (X-Ray Powder Diffraction)

The overall mineralogical composition of the sediment fraction lower than 63 µm was determined by the X-ray diffraction on non-oriented powders (*random powder*). The disorientation of the powder was obtained with the "top-loading" method of the sample holder; once powdered and distributed in a plexiglass sample holder, the powder was pressed using a planar glass slide and was placed in a X'Pert PRO PAnalitycal diffractometer for powders (40 kV, 30 mA) (fig. 32). The X'Pert Data Collector is the Software provided and used to manage the diffractometer and the acquisition of data. Analysis were performed at the diffraction laboratory of the Department of Science at the University of Basilicata.

The software allows to collect data through a continuous scan and to establish the experimental conditions (namely the scan axis, angular interval, temporal acquisition interval, acquisition time and speed of rotation) depending on the sample and the research objectives. The X-ray diffraction analysis of the fluvio-lacustrine sediments (17 samples) was carried out at a scan interval of 2-70° 2ϑ, using acquisition steps of 0.02° 2ϑ; the analysis time for each sample is approximately 56 minutes; on the lacustrine sediments (147 samples) the scan interval was 5-35° 2ϑ, using acquisition steps of 0.01° 2ϑ, time per step = 1 s; the analysis time for each sample is approximately 50 minutes. Copper radiation Cu-K$\alpha_{1,2}$ = 1.54184 was used.

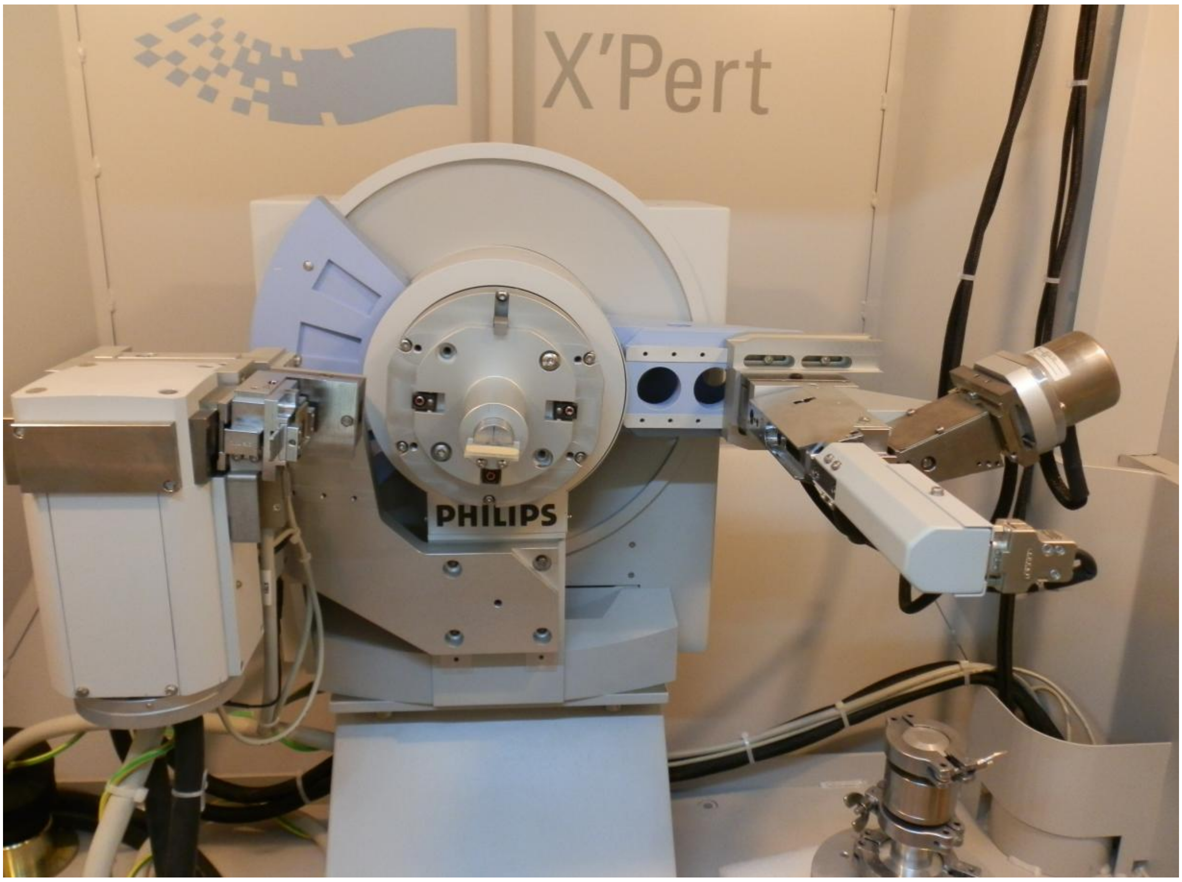

Figure 32. X'Pert PRO PAnalitycal diffractometer for powders.

Among the 147 core sediments submitted for mineralogical analysis, 24 were selected to perform chemical analysis from among those that showed the highest peaks of interstratified clay minerals together with illite peaks opened at low 2ϑ angles, indicating a degradation of the illite for the benefit of the interstratified clay minerals, as shown in figure

33 for the sample R18. The choice is based on the hypothesis that an higher content of interstratified clay minerals corresponds to a higher concentration of trace elements.

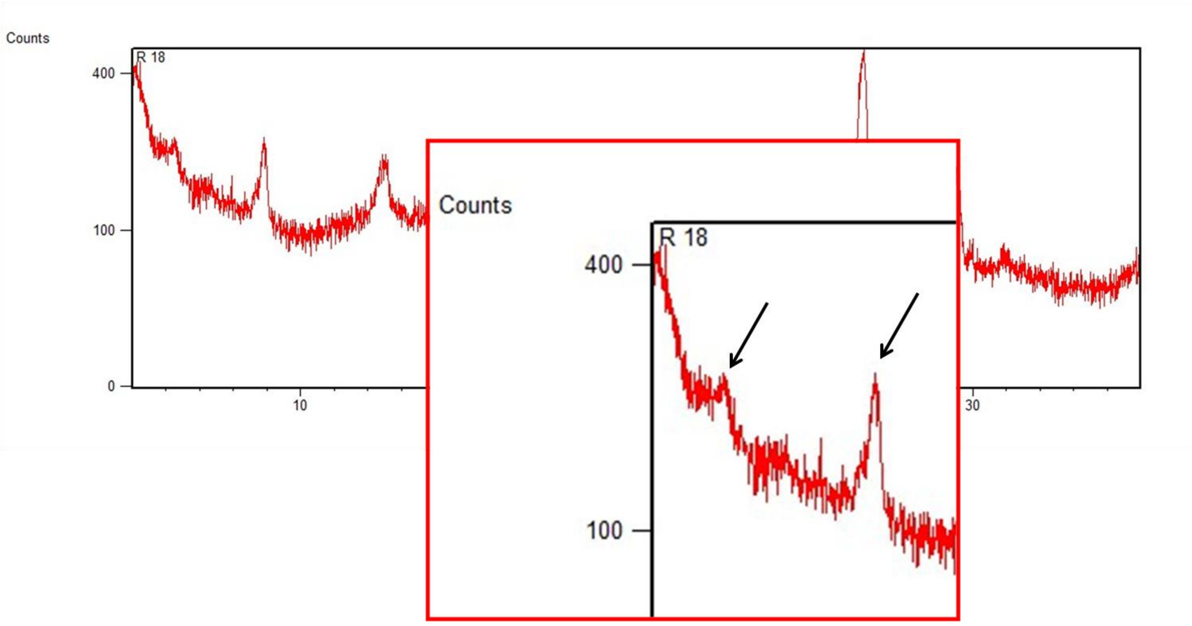

Figure 33. (From left to right) The peaks of interstratified clay minerals and of illite.

The selected samples were wet sieved with stainless steel sieves no. 230 to obtain the fraction lower than 63 microns which, according to the scientific literature, is the widely acknowledged sand-silt separation limit. Starting from sieve no. 230, fractionated sedimentation of the fraction of less than 4 µm was carried out; the clay minerals and iron and manganese oxides/hydroxides, in fact, constitute the most reactive phase of the aqueous environment with regard to the adsorption of metal ions and anionic complexes.

The fractionated sedimentation technique uses the speed of a body falling in fluid under the action of gravity that, according to Stokes' law:

$$V_T = \frac{g(\rho_p - \rho_l)D^2}{18\eta}$$

and, by expressing the speed V_T as a ratio between time t and the drop height h, we obtain:

$$t = \frac{18\eta h}{g(\rho_p - \rho_l)D^2}$$

where D is the particle diameter in cm, η expresses the viscosity of a liquid at a certain temperature, ρ_p- ρ_l is the difference between the density of the particle and the fluid, typically water.

Based on the aforementioned law, to separate a fraction lower than 4 µm, the samples, after mechanical agitation of 15 minutes, were left to settle for a time of 1h 57 minutes (the time calculated for a temperature of 22°C which is the temperature recorded in the laboratory during the extraction procedures) from a drop height of 10 cm; once this time lapsed, the suspension was removed by siphoning. Extraction (mechanical agitation + siphoning) was repeated until complete removal of the suspended solid.

All selected samples are reported in the following table:

Table 3. The core sediment samples for the chemical analyses.

Core	Sample n°	Level
A	A1	0 - 3
B	B1t	14 - 19
F	F4	39,50 - 41
F_1	$F_1$3	9 - 12
	$F_1$6	22 - 24,50
	$F_1$12	45 - 48
I	I2	5 - 6
	I12	122 - 127

Core	Sample n°	Level
L	4L	26 - 29
M	M2	46 - 68,5
R	a/R	12,5 - 14,5
	R9	69 - 77
	R12	124 - 126
	R18	176,5 - 178
S	S7 t	64 - 68
	S7 b	76 - 81
T	T1	9 - 13
	a/T	16 - 17,5
	c/T	59,5 - 60,5
V	a/V	32,25 - 33,5
	V1	44 - 45
	d/V	68 - 70
	b/V	75 - 77
	c/V	89,5 - 92,25
	V2	96,5 - 97,5
	V3	124 - 126,5

3.2.3 Chemical analyses (ICP-MS)

The chemical analyses of sediments were carried out at Activation Laboratories Ltd. (Actlabs) laboratory. Special attention was given to the instrumental detection limits for each chemical element, the type of chemical treatment to subject the sample before analysis, the instruments used and the average values of analytical uncertainty provided for each single element. A further check on the quality of the data obtained from a single laboratory was achieved through the anonymous comparison of duplicate analysis of the same sample.

Meso-Cenozoic rocks

The lithoid samples were crushed in plastic bags, quartered and pulverized in agate mill. This procedure was chosen by analysing the data for 4 test samples (a radiolarite, a calcarenite, a limestone and a shale) selected to assess the *cross contamination* and prepared in two different ways (crusher + tungsten carbide mill and hammer + agate mill). The second sample treatment method (red rectangles in figure 34) returned minor alteration for most of the investigated trace elements except for Ba and Sr, which are in greater concentration in the samples milled in the agate mill. So this last method was chosen for lithoid samples preparation.

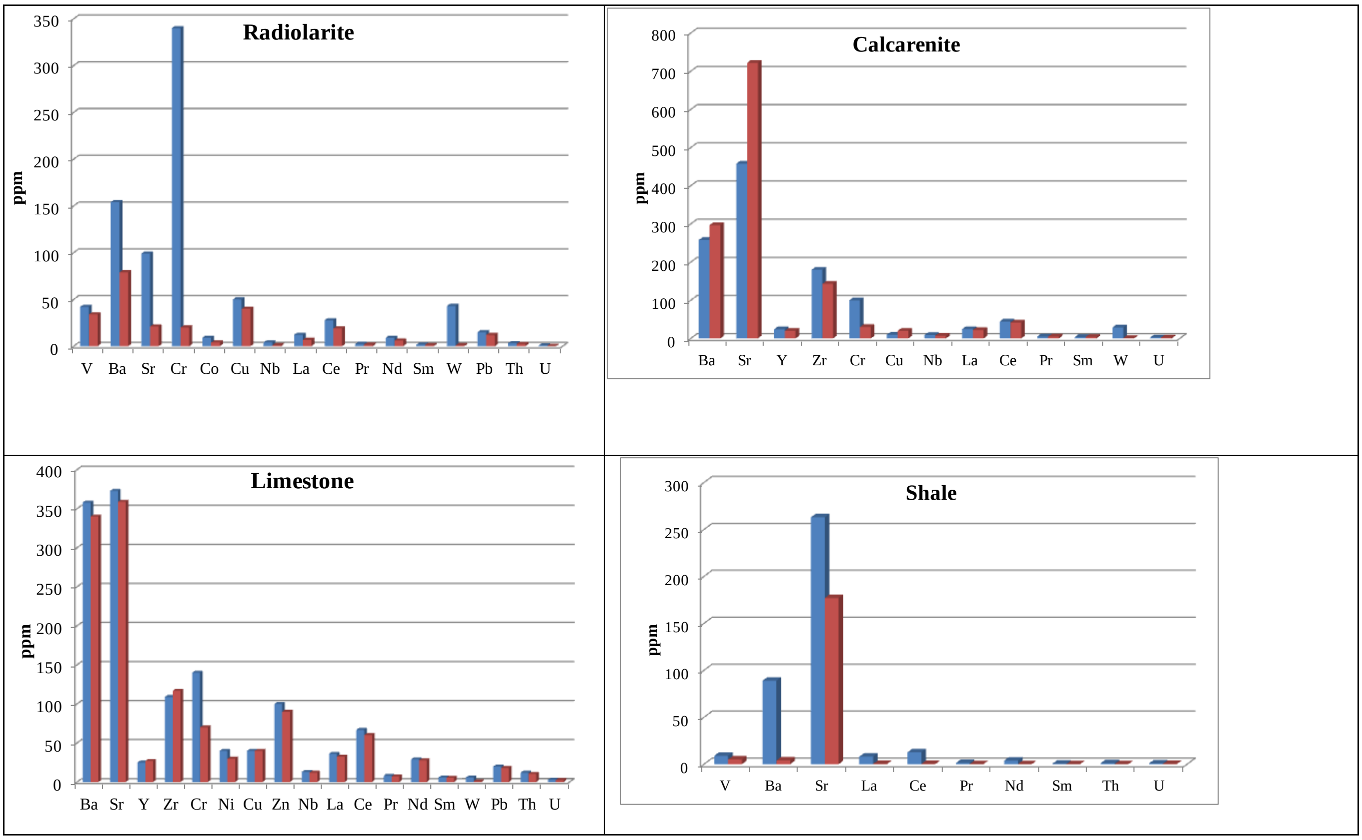

Figure 34. Comparison between the concentration of the trace elements analyzed after the preparation throught the two methods (the diagrams contain only the trace elements, whose concentrations differ).

Quaternary and fluvio-lacustrine sediments

The Quaternary and present-day fluvio-lacustrine sediments were wet sieved, using the stainless steel ASTM sieves. The grain size separation was performed through sieve no.10 (hole diameter: 2 mm) to separate the gravel from the sand and sieve no. 230 (hole diameter: 0.063 mm) to separate the sand from the silt-clay fraction. The sandy samples were dried at 105°C, while the silt and clay fractions at room temperature for a few weeks and, at the end of that period, in some cases, were put in an oven at 30°C until completely dry. The temperature was kept below of 30°C for the silt and clay samples to avoid deconstruction of the clays. Once dried, all samples were quartered (if the quantity was suitable), and the resulting aliquots were pulverized in agate mill. The pulverization time was 3 minutes, thus obtaining a powder with a consistency of talcum. If 3 minutes were not sufficient to obtain a powder with these features, pulverization continued for another 2 minutes. In any case, the pulverization time was taken into consideration for each sample. All sample preparations were carried out in the laboratories of the Department of Science at the University of Basilicata.

Lacustrine core sediments

Stratigraphic-sedimentological description

After splitting, the two halves of each core were photographed. A bed-by-bed description of each core was then performed on the basis of various macroscopic features, including: grain size, colour, sedimentary and biogenic structures, other organic and inorganic components. The informations from each core were then graphically represented in logs, with all the descriptive relevant details. The sediment colour was determined using comparative tables (*Munsell soil colour charts*), after removing a thin superficial lamina where the original colour could have been altered.

Each powdered sample (bedrock, Quaternary and fluvio-lacustrine and lacustrine core samples) was analysed at the Activation Laboratories Ltd. (Actlabs) laboratory. The selected method was WRA+trace 4Litho, which consists of blending with metaborate/lithium tetraborate. The samples were prepared and analysed in sequence. Each sequence contains a blank sample, a certified reference material and 17% repeats. The samples are mixed with a metaborate and lithium tetraborate flush and melted in an induction oven. The melted product obtained was immediately poured in a 5% nitric acid solution containing an internal standard and mixed until complete dissolution (about 30 minutes). The samples were processed in inductively coupled plasma mass spectrometry (ICP/MS). Moreover, 3 blank samples and five control samples (2 before the sample set and 3 after the sample set) were analysed for each group of samples. Each 15 samples were melted and duplicates were analysed, while the instrument recalibrated every 40 analysis.

The results of the chemical analyses of the different samples were included in the *box and whiskers plot* diagrams, which represent the distribution of data between the 25th and 75th percentile (interquartile differences), including 50% of the data (*the box*); the line inside each box is the median. The two outer lines of the box that extend up to the higher value (at the top) and down to the smallest value (bottom) are called *whiskers* and cover the data range between the 75th percentile (and down between the 25th percentile) representing the limit of the box, up to the value equal to one and a half times the interquartile range. The values that falling outside the whiskers, both above and below, are called *outliers* and represent abnormal values compared to the rest of the data distribution. In this study, the *box and whiskers plots* were used both to describe the trend of the major elements expressed as oxides in weight % and of the minor and trace elements of environmental interest expressed in ppm and to identify any *outliers*.

TOC (Total Organic Carbon)

Loss-on-ignition technique was used to evaluate total organic content in the lacustrine samples.

A ceramic crucible was pre-weighed after: washing, placing in a drying oven at 110 °C for 10 minutes, placing in a muffle furnace at 800 °C for 30 minutes and after cooling for 30 minutes in a desiccator. Those operations were repeated for three times in three different days.

On the data obtained, the average values were estimate for each sample. At the end of this step, about 3 g of wet sediment was placed into each crucible. The crucibles were then placed in a drying oven set to 60°C and allowed to dry for 48 hours. They were be cool in a desiccator, so as to prevent the absorption of atmospheric moisture, before being weighed for estimate the dry weight. Subsequently they were placed in the muffle furnace at 500°C for 8 hours. At the end of this time, each crucible was allowed to cool in a desiccators and weighted for the dried sediment without organic matter. After a week, the crucibles were replaced in the muffle furnace at 500°C for 8 hours and then reweighted.

The percentage of organic matter was calculated by the following formula (Hakanson and Janson, 1983):

$$TOC = \frac{wt_{(60°C)} - wt_{(500°C)}}{wt_{(60°C)}} \times 100$$

References

- Actlabs, 2016 *Canadian Schedule of Services and Fees*.

- Chen et al., 2011. *Assessing soil heavy metal pollution in the water-level fluctuation zone of the Three Gorges Reservoir, China*. Journal of Hazardous Materials 191. 366-372.

- CNR-ISE, 2011. *Protocollo di campionamento ed analisi chimica di sedimenti lacustri*. Progetto LIFE+ 2008 ENV/IT/000413 INHABIT.

- CRA-ABP (Firenze), 2007. *Invaso Pertusillo (PZ) Rilievi batimetrici e sedimentometrici al 29 settembre 2007*. Nell'ambito del progetto REL: Attività tecnico-scientifiche nell'ambito del Progetto Operativo "Attività di assistenza tecnica e supporto agli enti concessionari nel settore dekll'uso irriguo delle risorse idriche".

- EPA (United States Environmental Protection Agency), 2001. *Methods for Collection, Storage and Manipulation of Sediments for Chemicaland Toxicological Analyses: Technical Manual*. EPA-823-B-01-002.

- Hakanson, Jansson, 1983. *Principles of lake sedimentology*. Springer-Verlag Berlin Heidelberg.

- IAEA (International Atomic Energy Agency), 2003. *Collection and preparation of bottom sediment samples for analysis of radionuclides and trace elements*. ISBN 92–0–109003–X. ISSN 1011–4289.

- IRSA CNR, 2005. *Gli ecosistemi e i sedimenti: linee guida, protocolli operativi, attività sperimentali*. Progetto Nazionale di Monitoraggio delle Acque, ed. on-line.

- ISPRA, 2009. *Proposta per la valutazione dello stato qualitativo dei sedimenti fluviali nel sito di interesse nazionale Fiumi Saline ed Alento*. ISPRA, 2009. http://www.isprambiente.gov.it/files/temi/protocollo-sedimenti-saline-alento-rev1.pdf.

- Ladd, 1998. *Differences in trace metal concentrations among fluvial morphological units and implications for sampling*. Environmental Geology 36 (3-4).

- Lin et al., 2012. *Heavy Metal Contamination in the Water-Level Fluctuating Zone of the Yangtze River* *within Wanzhou Section, China*. Biological Trace Element Research, Volume 145, Issue 2, pp 268-272.

- Liu et al., 2014. *Assessing the heavy metal contamination of soils in the water-level fluctuation zone upstream and downstream of the Manwan Dam, Lancang River*. J Soils Sediments, 14:1147–1157 DOI 10.1007/s11368-014-0855-y.

- Miller and Miller, 2007 *Contaminated rivers*. *A Geomorphological-Geochemical Approach to Site Assessment and Remediation*. Ed. Online Springer. ISBN: ISBN 978-1-4020-5602-4.

- Zembo, 2010. *Stratigraphic architecture and quaternary evolution of the Val d'Agri intermontane basin (Southern Apennines, Italy)*. Sedimentary Geology 223, 206–234.

RESULTS

4. Results

The results of the multy-proxy (sedimentological, mineralogical and chemical) approach are illustrated for the fluvio-lacustrine and lacustrine core sediments. The latter represent the main topic of this study, so a detailed stratigraphical analysis was also carried out.

4.1 The fluvio-lacustrine sediments

The following streams were investigated: the Agri River, which represents the main tributary of the reservoir; Spartifave, Vallone dell'Aspro, Rifreddo, Spetrizzone and Scazzero on the left side of the reservoir; the Maglia River and the Vella Stream on the right side for a total of 17 fluvio-lacustrine sample.

According to the Shephard diagram (Shephard et al., 1954; Anselmi et a., 1996), the grain size distribution of the fluvio-lacustrine samples vary from clayey silt to silt (fig. 35). The silty fraction is the most abundant in the examined samples. However, for the purposes of the project, the clay fraction is the most important component as it drives the mobility of elements in aqueous systems (De Vivo et al., 2004). The clay fraction in the analysed sediments varies from 30 g/kg (sample EFF13) to 320 g/kg (sample EFF6) (tab. 4).

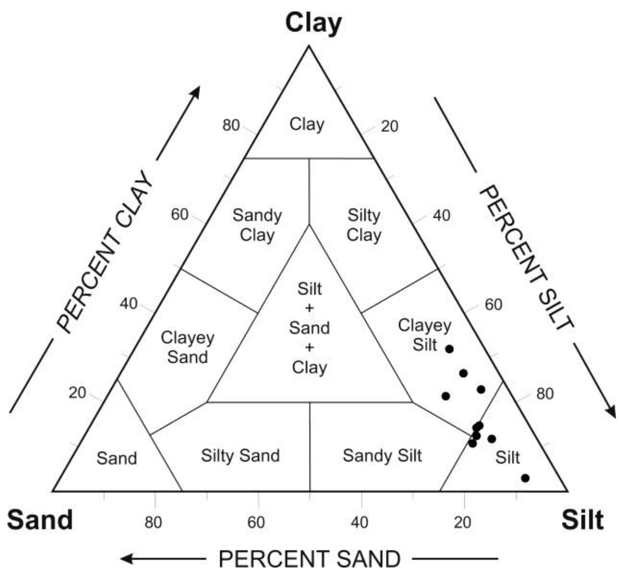

Figure 35. Ternary diagram showing the grain-size distribution for the fluvio-lacustrine sediment samples.

The representative granulometric curve of a selected sediment is shown in fig. 36. The granulometric fractions for the same sample are reported in the Table 4. The granulometric curves of all fluvio-lacustrine sediment samples are reported in Appendix 5.

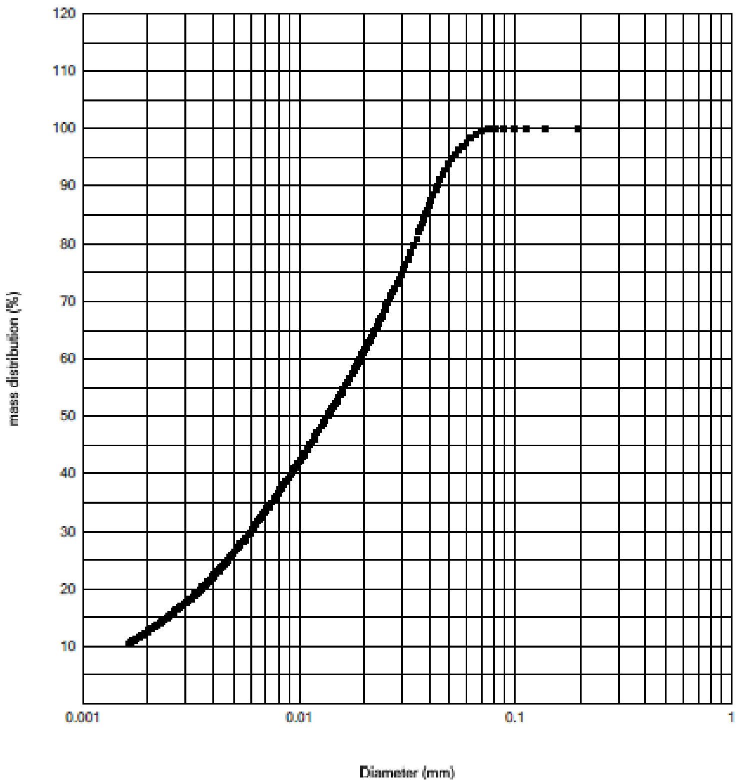

Figure 36. The granulometric curve of a fluvio-lacustrine sediment sample (EFF2).

Table 4. The granulometric fractions of the fluvio-lacustrine sediment samples.

Sample	Sand > 100 µ (g/kg)	Sand 100 - 50 µ (g/kg)	Coarse silt 50 - 20 µ (g/kg)	Fine silt 20 - 2 µ (g/kg)	Clay < 2 µ (g/kg)
EFF2	0	88	323	471	118
EFF3	48	57	284	468	143
EFF4	53	61	303	458	125
EFF6	29	40	87	525	320
EFF7	26	27	117	601	229
EFF8	52	45	167	588	148
EFF9	76	54	281	481	108
EFF10	23	106	303	354	214
EFF11	23	46	59	606	265
EFF13	5	62	229	674	30

The minerological data are in Table 5. The analysed samples show the presence of quartz as the main mineral phase followed by calcite and feldspars. The 2:1 type phillosilicates (such as muscovite and/or illite), chlorite and interstratified minerals are also present (fig. 37). The dolomite is only in samples of the Agri River. The diffraction patterns of all fluvio-lacustrine sediment samples are reported in Appendix 6.

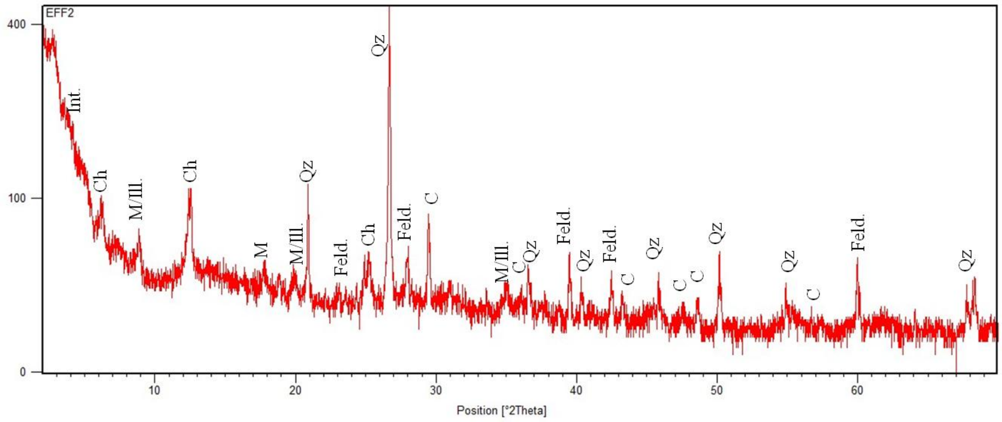

Figure 37. An example of a diffractogram of the sample EFF2.

Table 5. Mineralogical composition of the fluvio-lacustrine sediments.

	Quartz	Calcite	Dolomite	Feldspar	Muscovite/ Illite	Chlorite	Interstratified minerals
EFF1	X	X		X	X	X	X
EFF2	X	X		X	X	X	X
EFF3	X	X		X	X	X	X
EFF4	X	X		X	X	X	X
EFF5	X	X		X	X	X	X
EFF6	X	X		X	X	X	X
EFF7	X	X		X	X	X	X
EFF8	X	X		X	X	X	X
EFF9	X	X		X	X	X	X
EFF10	X	X		X	X	X	X
EFF11	X	X		X	X	X	X
EFF13	X	X		X	X	X	X
EFF14	X	X		X	X	X	X
EFF15	X	X	X	X	X	X	X
EFF16	X	X	X	X	X	X	X
EFF17	X	X	X	X	X	X	X

EFF18	X	X	X	X	X	X	X

4.2 Lacustrine sediments

15 cores, up to 2 m long, distributed across the whole fresh-water reservoir were subject to a stratigraphic analysis in order to provide a reconstruction of the depositional settings. The detailed sedimentary logs obtained from a bed-by bed description are in Appendix 7. In the following map (fig. 38), synthetic logs illustrate the general sedimentary features across the Pietra del Pertusillo lake. Particular care has been taken in the lithofacies description.

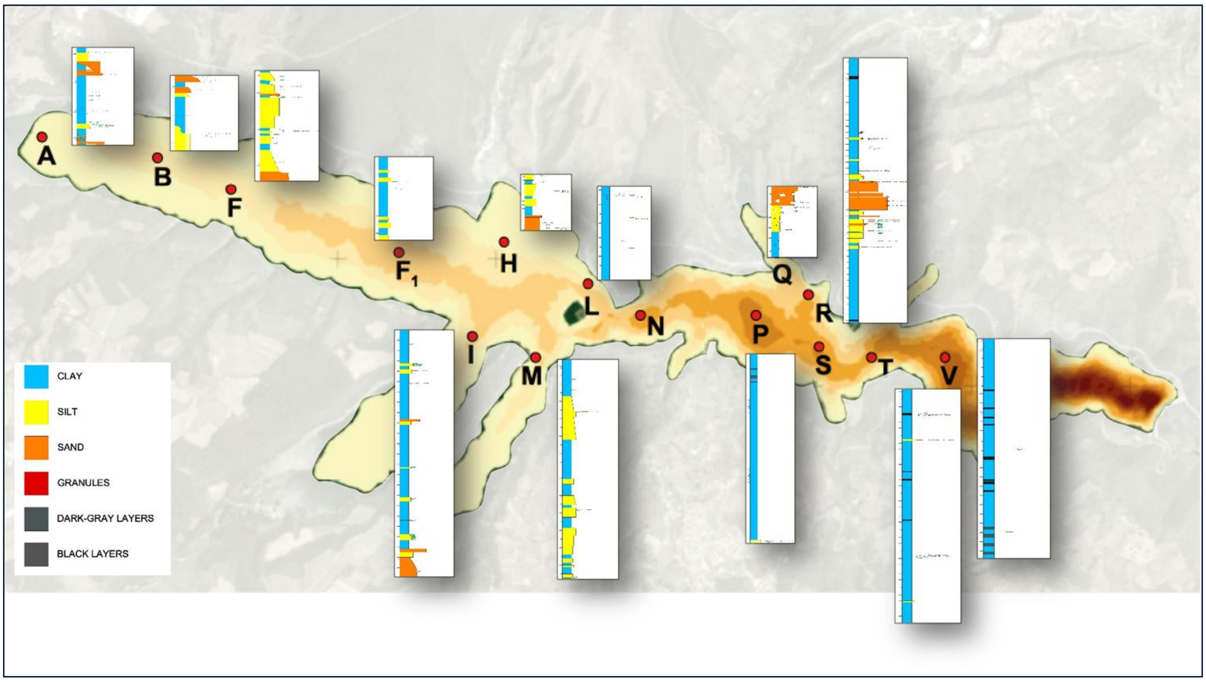

Figure 38. Synthetic logs summarizing the sedimentological features of the Pietra del Pertusillo infill.

Eleven sedimentary facies have been identified on the basis of the macroscopic features and are described below.

Facies A. Cm-to dm-bedded, massive mud. This is the most abundant facies in our lake system. It consists mostly of clay with a quite homogeneous colour in each unit; colour varies from ocher, reddish, greenish in the proximal cores and becomes grey in the distal cores, basinward of the first islet. In the cores collected basinward of the tributaries this facies becomes more silty. In the core Q, heterometric (until 2 cm larger in diameter), rounded and angular granules and predominantly sandstone pebbles are widespread across the core; also a white shell was found. Except for the core B and Q, this facies occurs at the top of each core, where it shows a major clay and water contents. In the proximal cores, red and black spherules, and organic matter (branches, leaves) are widespread; the frustules decrease in the other distal cores. The major rates were found in the proximal cores western of the core N, in which one bed reaches about 70 cm thickness.

Facies B. Cm-bedded, massive mud with organic matter. This facies was found only in cores A and I as clayey silt with abundant frustules, leaves and roots, intercalated to muds of facies A. Sediment thickness is almost < 2 cm and boundaries are irregular.

Facies C. Variegated cm-to-dm bedded mud. The facies always consists of clays, whose main features is the variegated colour; in the proximal core the colour is ocher-orange that becomes grey and dark grey in the distal sector. These clays were found in several cores, from F to T, with thickness increasing in the centre of the reservoir (core I, P, R) and decreasing up to few centimetres and disappearing at both lake margins. In the core L and P thick black laminae were found at different depths.

Facies D. Finely laminated mud. This facies occurs in the core B, F_1, I, L, N, P and S. Laminae colour, thickness, sharpness vary gradually from the proximal to the distal cores, becoming sharper, thicker and darker basinward. In the cores B and N, the laminae became silty; branches and leaves are also present. The facies reaches its maximum total thickness of about 29 cm in the core I. It is always associated with facies C, except in the core L, where a bed of facies A is intercalated between them.

Facies E. Dark grey to black cm-to-mm-bedded mud. This facies becomes increasingly abundant in the basinward direction from core F_1 and is characterised by dark grey to black beds, whose thickness, quantity and colour intensity increase basinwards, becoming progressively darker. In core F_1 only a dark grey bed was found; in cores L, I, M, N very thin darker laminae, whereas basinwards dark black cm-bedded beds frequently occur, reaching the maximum number of 14 in core V.

Facies F. Graded mud. This facies occurs in cores B, F, I, M, N as beds of (sandy) silt grading upwards into clayey silt, reaching the maximum thickness of 13 cm in the core M. In the proximal cores B and F, beds show frequently erosional bases.

Facies G. Cm-bedded massive sandy mud. The facies is mainly developed in the cores collected in the central portion of the lake, H, I and M. It consists of beds of sandy mud up to 6 cm thick; in core H several branches, leaves and black-purple powdery agglomerates are widespread.

Facies H. Dm-bedded graded silty sand. This facies occurs at the bottom of cores F and I, with a thickness of respectively 15 and 11,5 cm and becames coarser in the core R; here it consists of coarse to fine sand, 5 - 7 cm thick with rare frustules. It consist of two beds of fine sand (with rare granules), that gradually becomes muddier upwards.

Facies I. Cm-bedded massive sand. It is not limited to a particular sector of the reservoir, and was found both in the proximal core A, in the central core I, in the core Q and in distal core R. This facies consists of medium to coarse well-selected sand, often with granules, up to 7 mm in diameter in the core A, and up to 1 cm in cores R and Q. In core A locally beds have erosional bases.

Facies L. Granules. Only one bed was recognized in core N. The bed, 3 cm thick, occurs at the bottom of the core and consists of rounded red-brown and subangular white clasts.

Facies Dm. Massive breccia. It is well developed in core S, where large angular sandstone clasts, up to 5 cm in diameter, occur in a sandy-clay matrix. The bed reaches a maximum thickness of about 24 cm in core S, while is thinner in core Q (about 6 cm).

4.3 Grain size distribution, XRPD and TOC

4 of 15 cores were not take into consideration for the following analyses (grain size, XRPD, TOC and ICP-MS) due to the high percentage of coarse facies (Q and H) or to their distance from the months (N and P).

147 core sediments belonging to the muddy facies A, C, D, E and F were submitted for mineralogical analysis. 24 samples were selected to perform chemical analysis: in particular those that showed the highest peaks of interstratified clay minerals together with illite peaks open towards low angles, indicating a degradation of the illite for the benefit of the interstratified clay minerals, as shown in figure 33 for the sample R18. The choice is based on the hypothesis that an higher content of interstratified clay minerals corresponds to an higher concentration of trace elements. By granulometrical analysis, the lacustrine sediments can be defined as silty clay and clayey silt (fig. 39), except a sample from the proximal core F resulting a sandy silt.

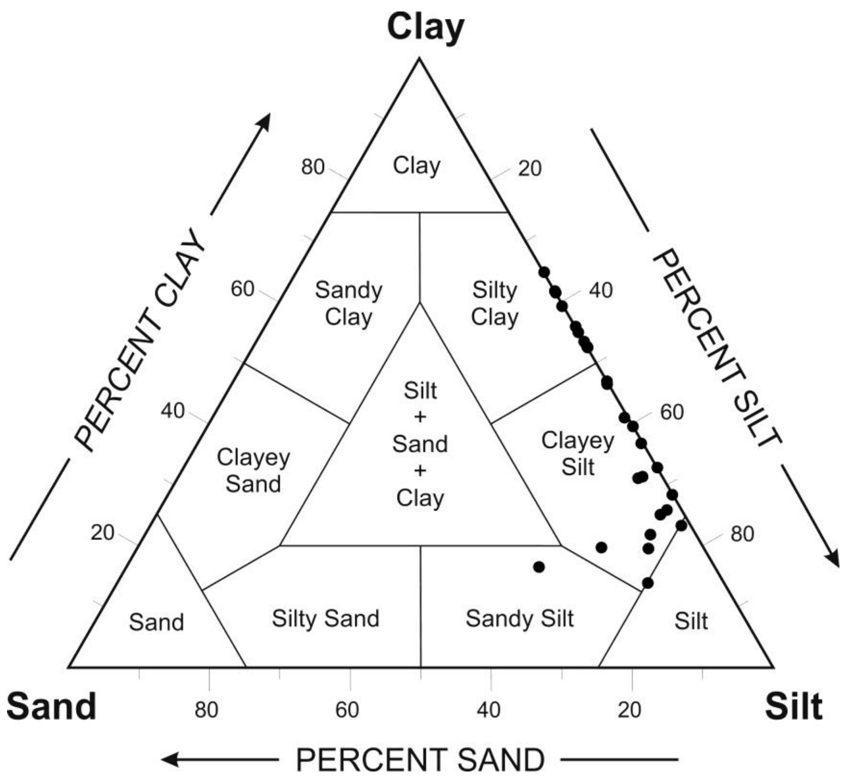

Figure 39. Ternary diagram showing the grain-size distribution for the lacustrine core sediments.

The percentage of sand decreases eastwards; it is high in the proximal cores and decreases almost to zero values in the deepest cores (L, S, T and V).

The proximal and central sectors have the highest percentages of silt, which drastically decreases in correspondence of the core S. However, the V1 and V2 samples contain high amounts of silt fraction (fig. 40 and tab. 6)

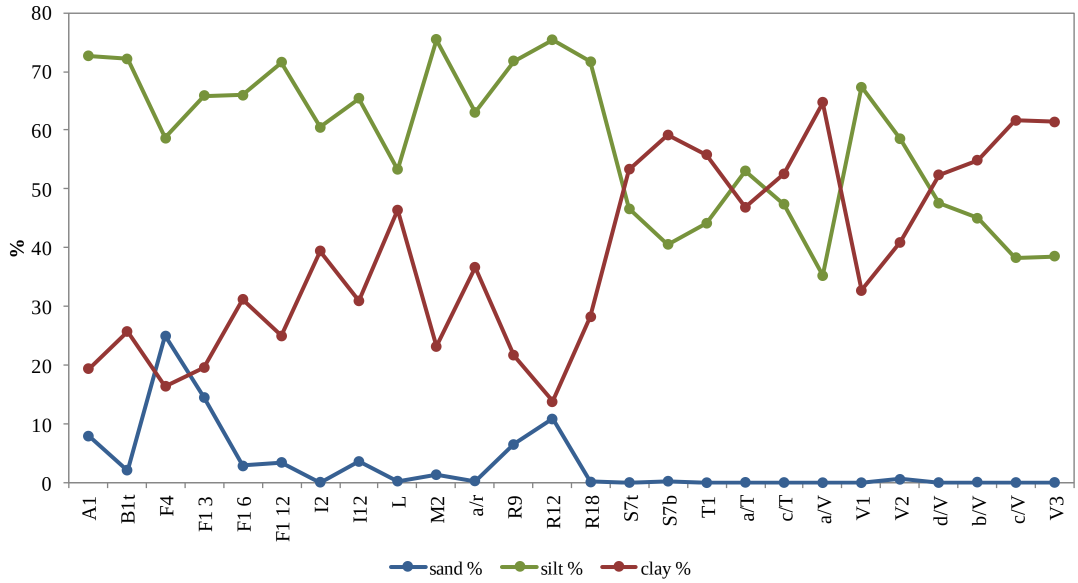

Figure 40. The grain size distribution in the lacustrine samples from the proximal (left) to the distal cores (right).

Table 6. Percentages of sand, silt and clay in the lacustrine samples.

Sample	Sand %	Silt %	Clay %
A1	7,92	72,66	19,42
B1t	2,14	72,13	25,74
F4	24,96	58,63	16,41
F_1 3	14,50	65,90	19,60
F_1 6	2,84	65,95	31,21
F_1 12	3,45	71,58	24,97
I2	0,08	60,46	39,45

I12	3,61	65,44	30,95
L	0,26	53,34	46,40
M2	1,36	75,46	23,18
a/r	0,30	63,03	36,67
R9	6,49	71,80	21,71
R12	10,84	75,39	13,77
R18	0,11	71,65	28,24
S7t	0,03	46,60	53,37
S7b	0,25	40,57	59,18
Sample	**Sand %**	**Silt %**	Clay %
T1	0,00	44,16	55,84
a/T	0,06	53,07	46,87
c/T	0,03	47,41	52,56
a/V	0,00	35,24	64,76
V1	0,00	67,30	32,70
V2	0,57	58,54	40,89
d/V	0,02	47,57	52,41
b/V	0,10	45,01	54,90
c/V	0,03	38,31	61,66
V3	0,04	38,56	61,39

The mineralogical phases identified by XRPD are similar throughout all the analysed cores. Quartz (Qz), calcite (C), feldspar (Feld.), muscovite/illite (M/Ill.), chlorite (Ch) and minor amount of mixed-layered clay minerals were identified. The only exception is dolomite (D) that is only in samples of the cores A, B, F, F_1 basinward of the confluence of the Agri River (fig. 41).

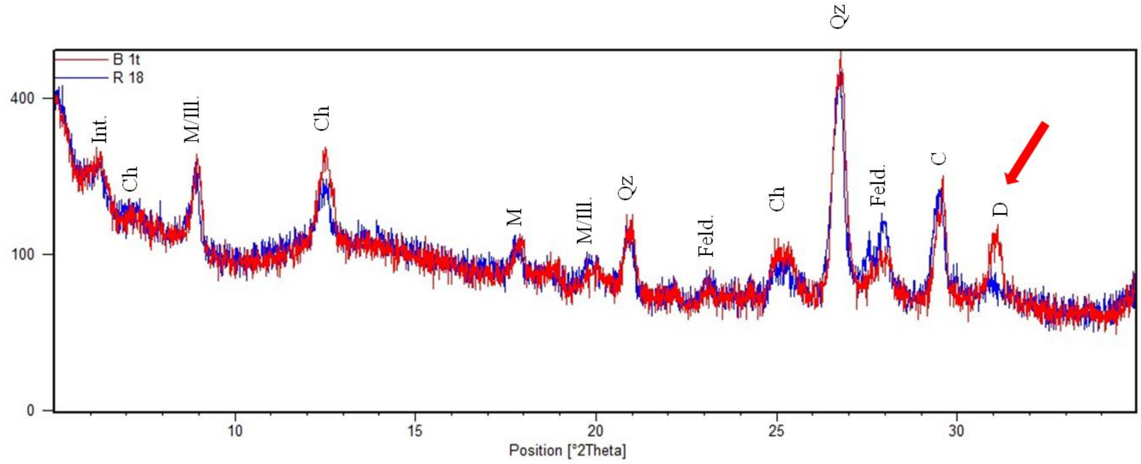

Figure 41. Comparison between diffractograms of B1t (core B) and R18 samples (core R) collected in different areas.

Total Organic Carbon (TOC) content ranges between 3.7% (sample M2) and 9.8% (c/T) and increases in the deeper part of the reservoir (fig. 42). The black layers show the higher TOC contents (all higher than 6%), with a maximum in the core T.

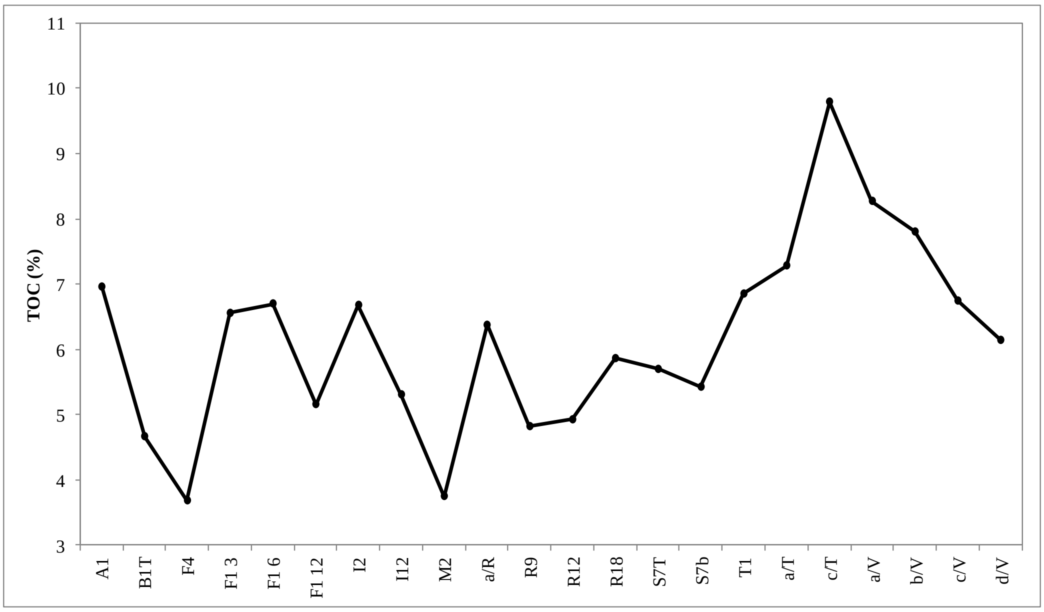

Figure 42. TOC content in the lacustrine sediments.

4.4 Chemical composition of sediments and rocks.

The maximum, minimum, and median concentrations for major and trace elements in the local bedrock, in the fluvio-lacustrine and lacustrine sediments are presented in Table 4. Regarding to the lacustrine sediments, chemical analyses have been performed on samples selected based on the presence of both interstratified clay minerals and illite peaks opened at low °2θ (fig. 43). The < 4 μm fraction was also extracted from these samples and in turn analysed.

Below the description of each detected element (major and trace elements) is presented.

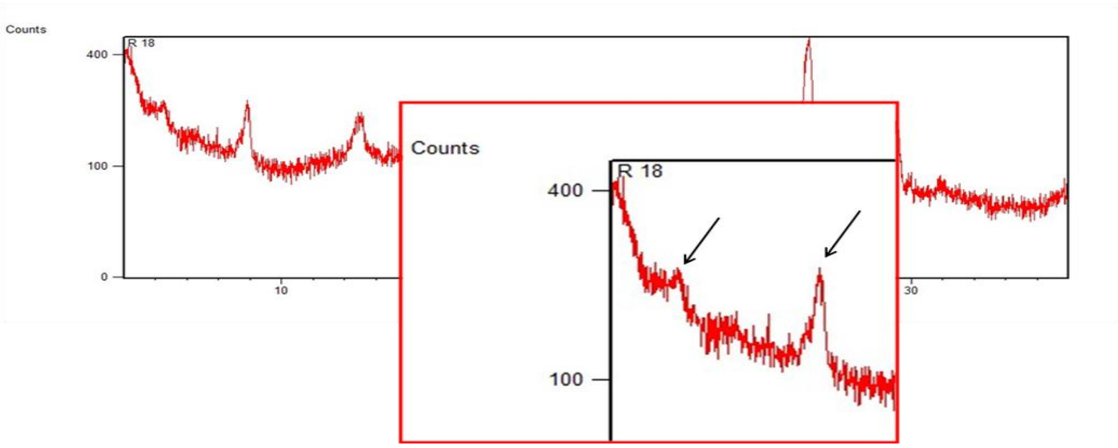

Figure 43. The peaks of the illite and the mixed-layered clay minerals in the sample R18.

Table 7. Concentration values for major and trace elements in: the local bedrock, fluvio-lacustrine sediments, lacustrine core sediments, UCC (Upper Continental Crust).

Elements	Local bedrock (n=38)		Fluvio-lacustrine sediments (n=17) (<63 µm)		Lacustrine core sediments (n=24)				UCC[1]
					(bulk)		(<4 µm)		
Major (wt%)	**range**	**median**	**range**	**median**	**range**	**median**	**range**	**median**	
SiO_2	48.37-66.47	54.77	46.96-56.51	50.21	39.88-59.03	45.68	43.81-47.99	46.17	65.89
Al_2O_3	9.04-22.55	16.31	12.49-15.65	14.56	12.7-18.52	15.17	18.38-22.71	20.11	15.17
Fe_2O_3 (T)	2.99-8.54	6.22	4.12-6.22	5.13	4.18-6.34	5.41	6.47-7.51	6.96	4.49
MnO	0.02-0.268	0.07	0.05-0.12	0.076	0.055-0.119	0.078	0.063-0.16	0.086	0.08
MgO	0.73-2.51	1.71	1.18-2.77	1.73	1.46-2.35	1.81	1.8-2.27	2.045	2.2
CaO	0.13-11.53	3.15	5.42-9.65	8.3	4.24-12.72	8.025	2.03-3.67	2.66	4.19
Na_2O	0.23-1.24	0.78	0.75-1.38	1	0.42-1.26	0.62	0.37-0.52	0.42	3.89
K_2O	1.44-4.75	2.88	2.04-3.04	2.43	2.06-3.21	2.495	2.67-3.66	3.15	3.39
TiO_2	0.43-1.164	0.75	0.57-0.728	0.681	0.558-0.781	0.67	0.679-0.892	0.782	0.5
P_2O_5	0.05-0.18	0.13	0.14-0.33	0.17	0.1-0.26	0.17	0.16-0.3	0.22	0.2
Trace (ppm)									
Ba	117-747	394	307-516	412	327-463	389.5	389-541	455	550
V	74-176	125	86-119	107	81-139	111.5	144-169	157	107
Pb	5-50	21	17-33	23	20-29	25	31-49	42	17
Cu	10-70	40	30-50	40	-	-	50-70	50	25
Zn	40-150	110	80-130	110	80-140	110	130-160	140	71
Co	4-27	16	9-17	13	10-16	14	15-19	16	17
Ni	20-80	40	30-50	40	30-50	40	50-70	50	44
Cr	40-120	90	60-90	80	70-120	100	110-130	125	83
As	5-15	5.5	-	-	-	-	5-11	8	1.5

[11] McLennan et al., 2006.

SiO_2

The bedrock samples (fig. 44) show silica content ranging from 48.37 to 66.47%, with a median of 54.77%. The highest values belong to Calcari con Selce (74.67%), Scisti Silicei Formations (75.06%, 69.49%) and sandy portion of the Vallone dell'Aspro Alloformation (69.14%). The lowest values are in two samples belonging respectively to the Galestri (38.7%) and the Albidona (41.41%) Formations that are enriched in carbonate minerals. In the fluvio-lacustrine sediments the silica content range from 46.96% to 56.51% with median value of 50.21%; in the lacustrine bulk fraction, the values still decreases to a median value of 45.68% ranging from 39.88-to 59.03%. In the clay fraction the percentage of SiO_2 shows a very little variability from 43.81 to 47.99%, with a median of 46.17%.

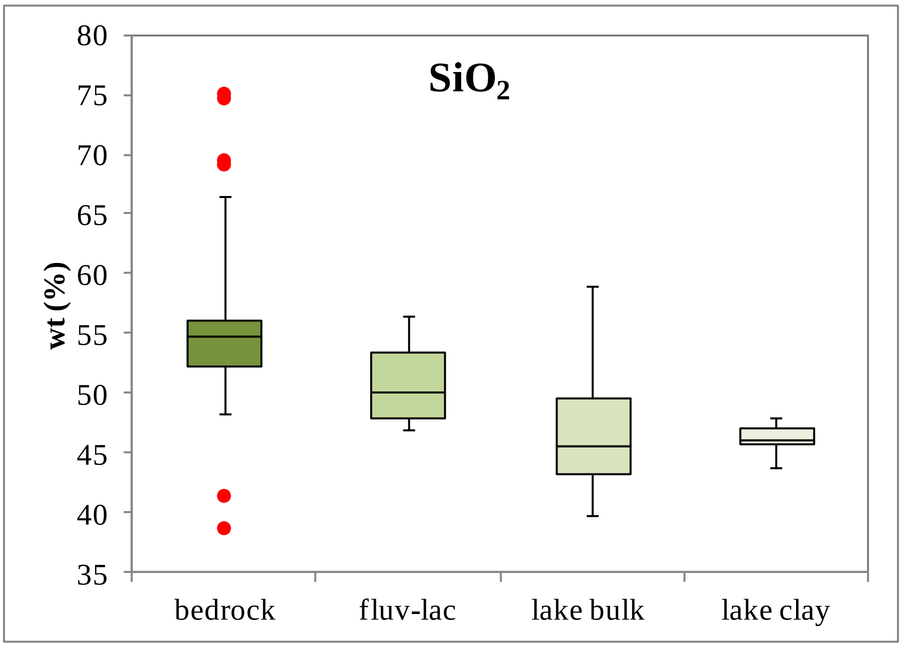

Figure 44. Boxplot of SiO_2 contents in the different sample types.

Al_2O_3

Aluminium oxide shows its greatest variability in the bedrock samples (fig. 45) from 9.04 to 22.55%, with a median value of 16.31% probably due to the different average values of the Al_2O_3 in the different rock types collected. The median value of the lithoid rocks (15.07%) slightly differs from the Quaternary deposits one (16.89 %).

In the fluvio-lacustrine sediments, Al_2O_3 median value is 14.56 %, ranging from 12.49 % to 15.65%,

In the lacustrine bulk fraction, the median value is similar to that of lacustrine samples (15.17%) with minimum and maximum values of 12.7 and 18.52% respectively. The maximum values are found in the core L and basinward of the core S and can be correlated to the higher clay percentages.

The highest concentrations of Al_2O_3 were observed in the clay fraction (<4 µm) of the lacustrine sediments (median value=20.11, min =18.38, max =22.71%).

The maximum values were found at the bottom of the core I, in the core L and S.

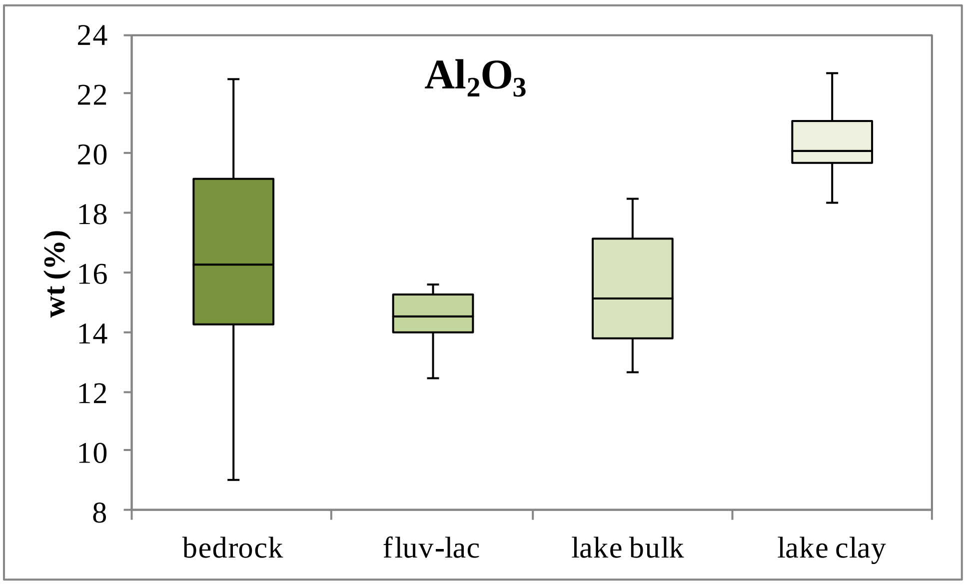

Figure 45. Boxplot of Al_2O_3 contents in the different sample types.

Fe_2O_3 (T)

The iron oxide content of bedrock shows a slight variability (2.99 % to 8.54 %) and a median value of 6.22 % (fig. 46). Two outliers were also observed: the upper one is related to samples from the Galestri Formation (11.58%); the lower one is from a Quaternary sandy sample (1.98%), also depleted in iron and aluminium oxides and in most of the trace elements.

In the fluvio-lacustrine sediments (median = 5.13 %; range 4.12 - 6.22 %) the iron oxide concentrations are similar to those of the bulk lacustrine sediments (median = 5.41 %; range 4.18 - 6.34 %).the Fe_2O_3 contents increase in the clay fraction (median value of 6.96 %) ranging from 6.47 to 7.51 %.

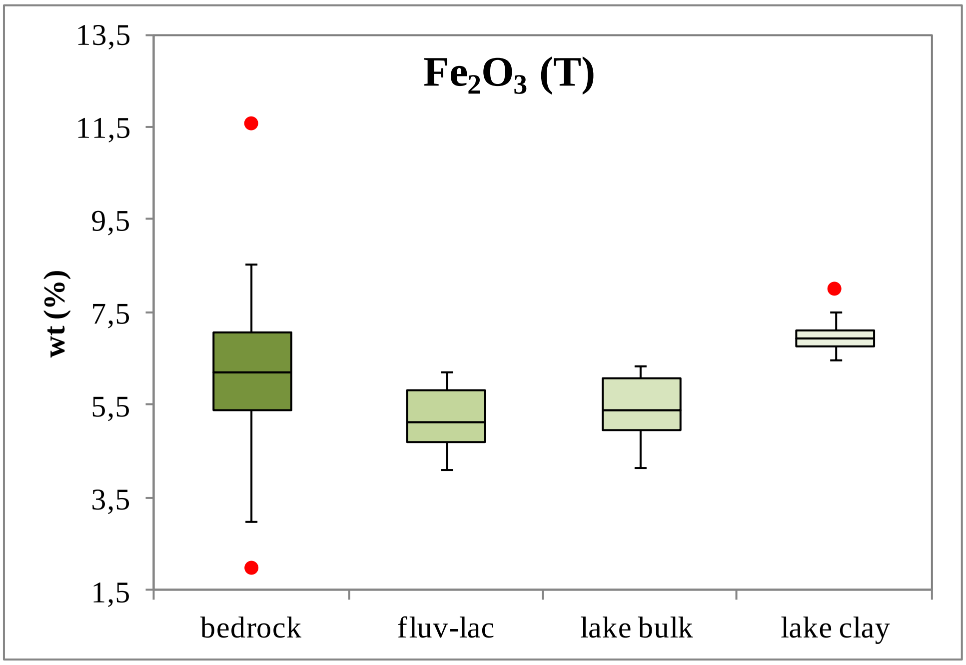

Figure 46. Boxplot of Fe_2O_3 (T) contents in the different sample types.

MnO

The median manganese oxide values are quite comparable in the different sample types (fig. 47). In the bedrock samples, an high dispersion of the values was observed (0.02 - 0.268% with median value of 0.07. The highest values belong to Scisti Silicei Formation and the Quaternary deposits. In the fluvio-lacustrine sediments one outlier was observed. It is probably related to the Quaternary sample EF 65, outcropping just upstream of the mouth of the Rifreddo Stream.

The bulk fraction of the lacustrine sediments shows a little variability (from 0.055 and 0.119, with a median value of 0.078%). The highest value (0.134%) was perfomed into a black layer into the core V.

In the clay fraction, although the median concentration of MnO (0.086%) is similar to the other samples, a larger variability was observed. The outlier is related to the coarser sample F4 (0.185%), collected in proximal sector, affected by strong seasonal fluctuations of the water level.

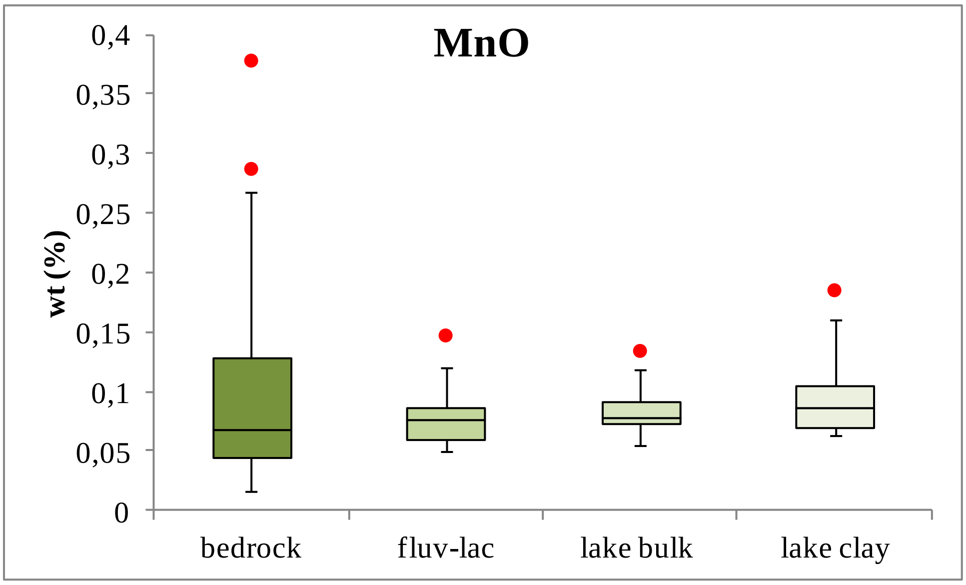

Figure 47. Boxplot of MnO contents in the different sample types.

MgO

Magnesium ranges from 0.73 to 2.51% (fig. 48), with a median value of 1.71%. MgO is more abundant in the lithoid rocks (median value = 1.87%) and in particular in a more calcareous portion of the Albidona Flysch (3.02%) than in the Quaternary deposits (median = 1.6%), whose major amount were found in the Vella catchment.

In the fluvio-lacustrine sediments, MgO median value is similar (1.73%) and it ranges between 1.18% and 2.77%. Two outliers are found at the month of Agri (3.16% 3.37.

In the lacustrine bulk, MgO median increases (1.81%); two outliers (2.83% and 3.02%) both at the Agri-month are present.

MgO reaches its maximum in the clay fraction (median = 2.045%), ranging from 1.8% and 2.27%.

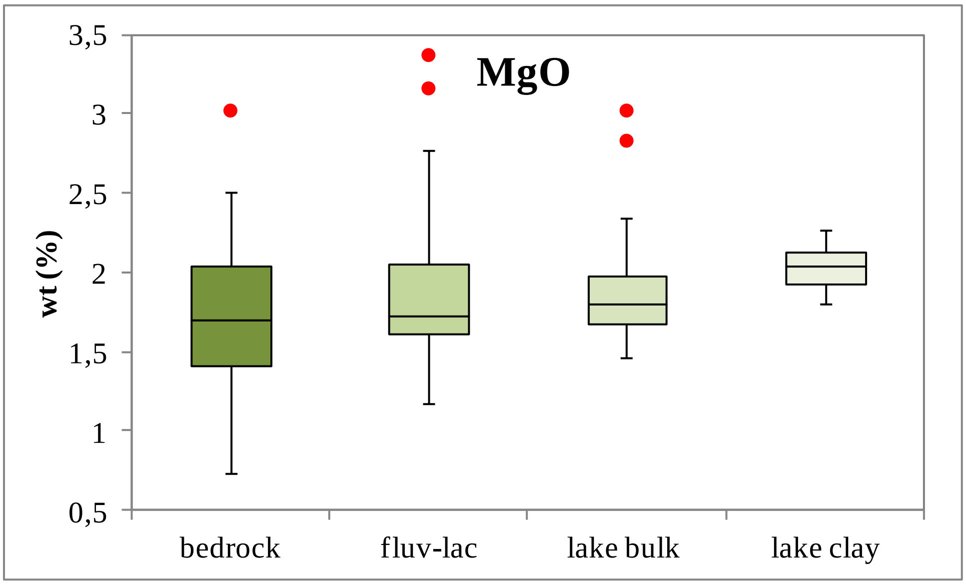

Figure 48. Boxplot of MgO contents in the different sample types.

CaO

In the bedrock samples, calcium oxide shows the highest dispersion among the major elements, ranging over three orders of magnitude (0.13% - 11.53%) (fig. 49). The lithoid rocks shows a lower median value (2.67%), that quite doubles in the Quaternary deposits (4.01%). The more calcareous portions of the Albidona and the Galestri Formations show three outliers (18.7%, 15.83 and 20.62%, respectively).

In the fluvio-lacustrine sediments, CaO variation decreases from 5.42% to 9.65% with a median value of 8.3%; the major amount are in the Rifreddo and in the Agri rivers.

In the lacustrine bulk, CaO slightly decreases (median value = 8.025%) and ranges from 4.24% to 12.72%. In the clays, the median value greatly decreases (2.66%) together with its range, from 2.03% to 3.67%. The rate of calcium oxide increases in correspondence of the black layers, where an outlier was found (4.4%).

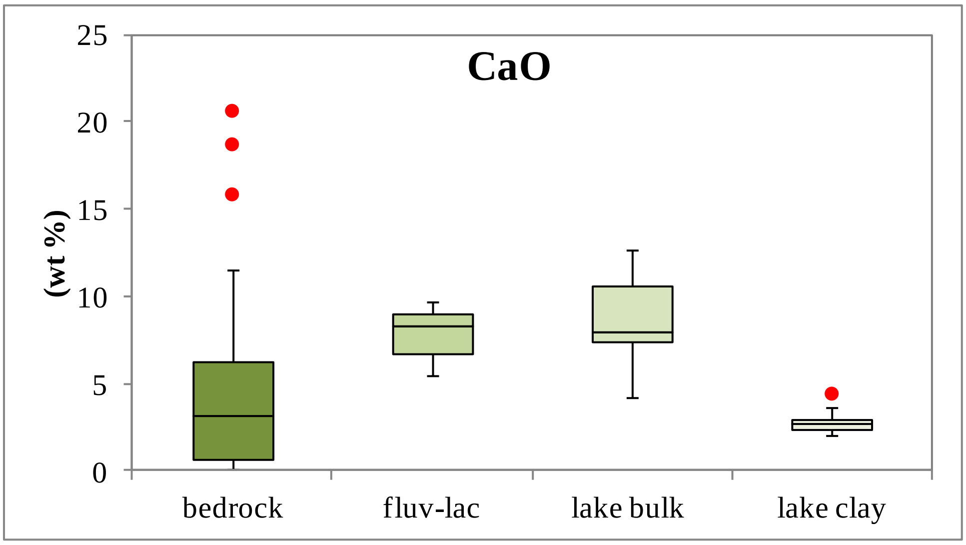

Figure 49. Boxplot of CaO contents in the different sample types.

Na_2O

In the bedrock samples the median Na_2O content is 0.78% and it content ranges from 0.23% to 1.24% (fig. 50). The median value of the lithoid rocks (0.77%) is quite equal to that of Quaternary deposits (0.81%) and both show outliers: the first related to the Gorgoglione Flysch and the second to a coarse sample from the Vallone dell'Aspro Alloformation.

The fluvio-lacustrine samples exhibit the maximum median value (1%) and Na_2O varies from 0.75% to 1.38%; the major percentages are found at the Montemurro and Vella months.

In the lacustrine sediments, Na_2O clearly decreases, with a median value of 0.62% and a range between 0.42% and 1.26%; the major values are related to the core M and R, collected respectively basinward of Vella and Scazzero-Spetrizzone months.

In the clay fraction the sodium content is low (median = 0.42%) and its variability scarce (0.37% - 0.52%); the only outlier is related to the sample I12 (0.64%), in the Maglia arm.

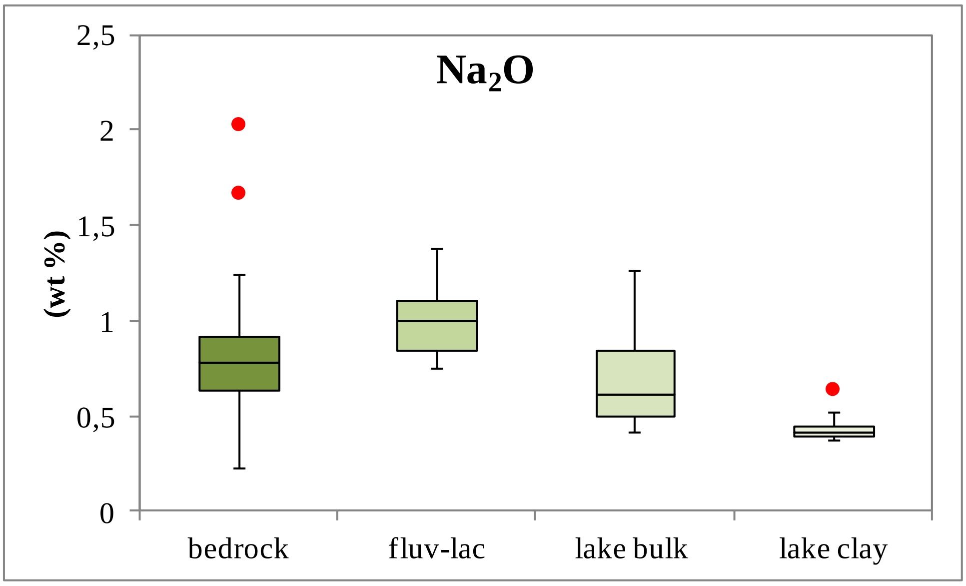

Figure 50. Boxplot of Na_2O contents in the different sample types.

K_2O

In the bedrock, the median potassium oxide content is 2.88%, with a range between 1.44% and 4.75% (fig. 51). In the lithoid rocks, K_2O median value is higher (2.94%) than the Quaternary deposits (median = 2.61%); its major values are found in the Crete Nere Formation and in the Moliterno Succession. In the Quaternary deposits the maximum values are related to the Vella catchment.

In the fluvio lacustrine samples, K_2O median value (2.43%) and its range (2.04% - 3.04%) decreases; the maximum percentages are related to the Scazzero Stream.

In the lacustrine bulk, K_2O median value is quite equal (2.495%) and its range as well (2.06% - 3.21%), with its maximum in the cores L and S.

In the clay fraction, the K_2O increases (median = 3.15%; range = 2.67 - 3.66%); here it reaches its maximum value in the core M (3.99%), collected in the Vella arm.

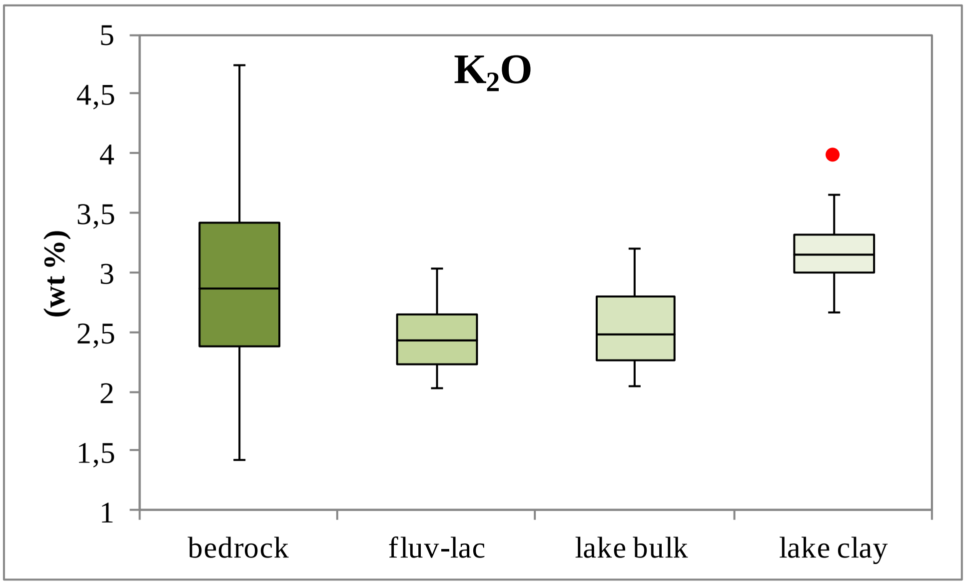

Figure 51. Boxplot of K_2O contents in the different sample types.

TiO_2

In the bedrock samples, the TiO_2 median value is 0.75%, ranging between 0.43% and 1.164% (fig. 52); in the Meso-Cenozoic rocks, the maximum percentages of TiO_2 are related to the Galestri Formation; however the TiO_2 median value in the lithoid rocks (0.713%) is lower than that of the Quaternary deposits (0.82%), among which an outcrop close to the Rifreddo month shows the major percentage.

In the fluvio-lacustrine samples, the median value (0.681%) and its range (0.57 - 0.728%) decrease; here three outliers are found, all related to the samples collected at the Maglia confluence.

The lacustrine bulk and clay fraction confirm the previous evidence, showing the maximum value (respectively 0.885 and 1.072%) in the same sample of the core I, collected in the Maglia arm. In general, in the lacustrine bulk the TiO_2 content slightly decreases (median = 0.67), varing between 0.558 and 0.781% and then increase in the clay fraction, with a median value of 0.782% and a range between 0.679% and 0.892%.

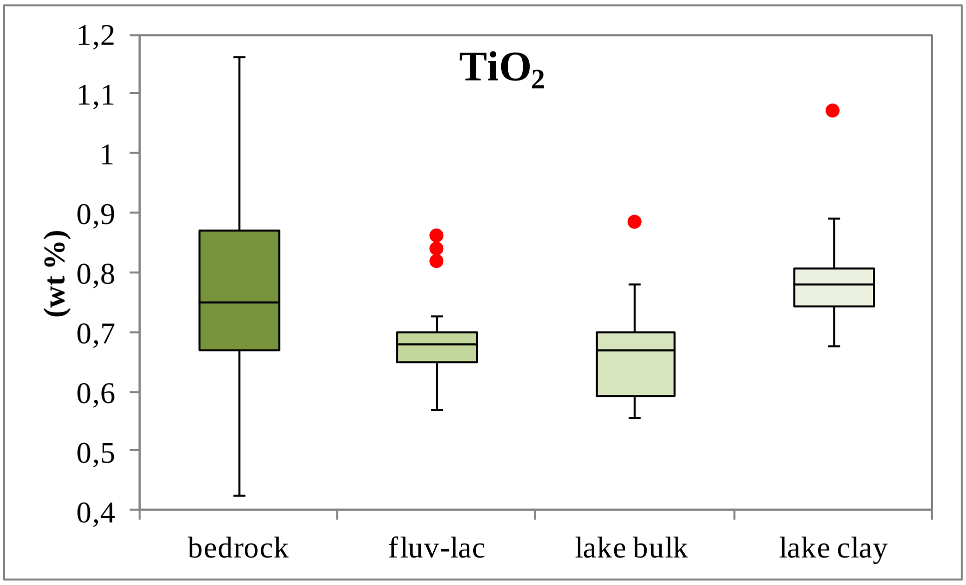

Figure 52. Boxplot of TiO_2 contents in the different sample types.

P_2O_5

In the bedrock, P_2O_5 median content is 0.13%, with a range from 0.05% and 0.18% (fig. 53); the lithoid component shows lower P_2O_5 values (median = 0.12%) than Quaternary deposits (median = 0.15%).

The P_2O_5 maximum values are found in the fluvio-lacustrine sediments (median = 0.17%; range = 0.14 - 0.33%), and in particular in the Scazzero Stream. The fluvio-lacustrine sediments collected at the month of the Agri River are also characterized by higher P_2O_5 percentages, which decrease towards the lake.

The median value of the lacustrine bulk (0.17%) is equal to that of the fluvio-lacustrine sediments; the major concentrations are in the core R and in the distal cores T and V.

In the lacustrine clays the P_2O_5 increases to a median value of 0.22% and ranges between 0.16% and 0.3% with its maximum values in the distal cores and in the black layers.

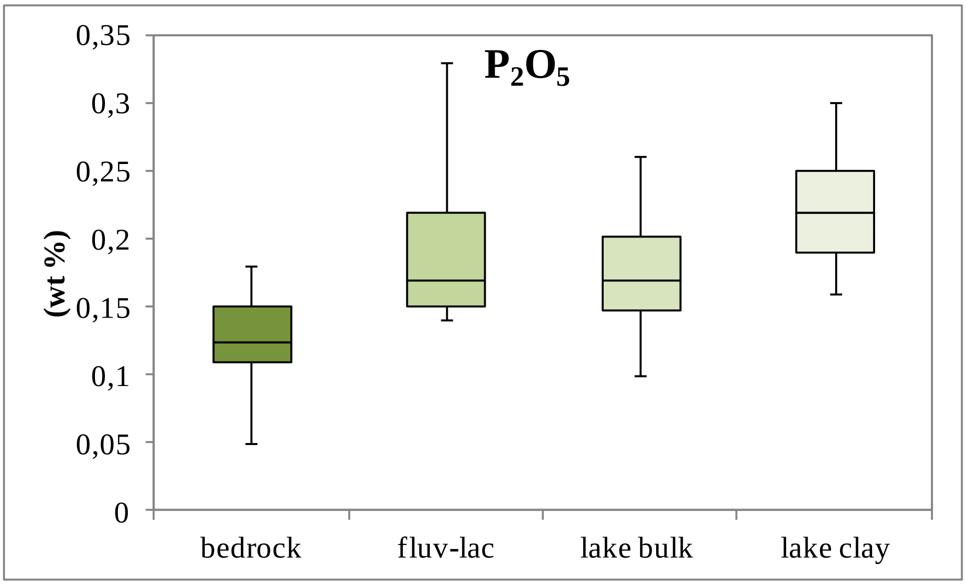

Figure 53. Boxplot of P_2O_5 contents in the different sample types.

Next pages show the chemical results of the main environmental interest elements (vanadium, chromium, cobalt, nickel, copper, zinc, lead, barium and arsenic) in the different sediment-types.

Barium (Ba)

In the local bedrock, barium content ranges from 117 ppm and 747 ppm with a median value of 394 ppm (fig. 54). The lithoid rocks show Ba contents (median value = 340 ppm) lower than the Quaternary deposits (median value = 463 ppm). The highest concentrations are in the Vella catchment. Two outliers were identified: the lowest value is related to a Quaternary outcrop, collected close to the Vella confluence; the highest bedrock value (2759 ppm) is related to an outcrop of the Gorgoglione Flysch collected near the northern ridge of the valley.

In the fluvio-lacustrine sediments, the Ba median value is 412 ppm and the range from 307 ppm to 516 ppm, while in the lacustrine bulk fraction the Ba median value is 389.5 ppm and its range from 327 ppm to 463 ppm.

Ba increases in the lacustrine clays, where reaches a median value of 455 ppm and a range of 389 - 541 ppm. In the core M, collected into the Vella arm, an anomalous value was found (615 ppm).

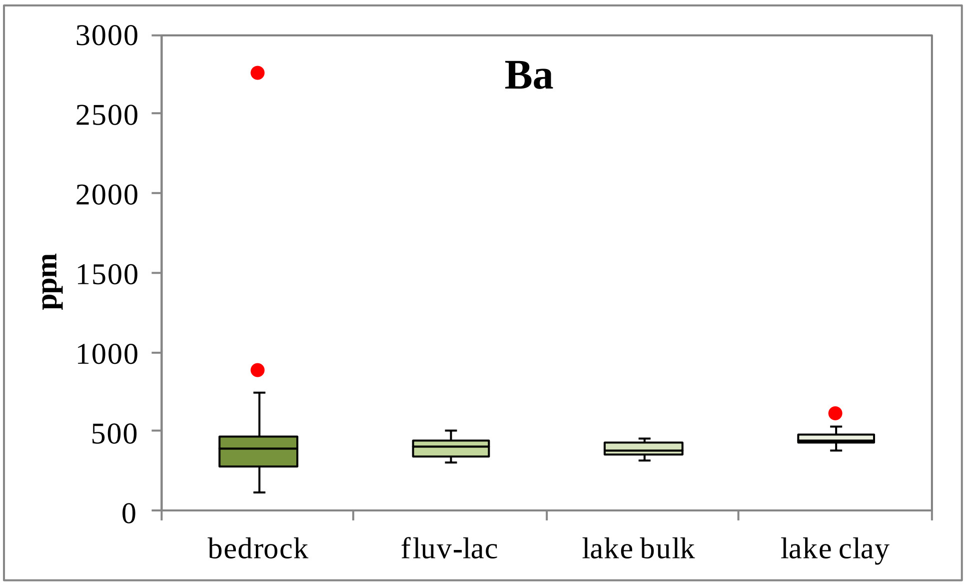

Figure 54. Boxplot of Ba contents in the different sample types.

Vanadium (V)

In the local bedrock, vanadium median value is 125 ppm and its content ranges from 74 ppm and 176 ppm (fig. 55). In the lithoid rocks, the V median value (116 ppm) is quite similar to that of the Quaternary deposits (127 ppm). The two outliers are related to a cherty sample of the Scisti Silicei Formation and a more sandy Quaternary sample.

In the fluvio-lacustrine sediments vanadium range decreases from 86 ppm to 119 ppm; the median value is 107 ppm.

In the bulk lacustrine fraction, vanadium median is 111.5 ppm and is quite similar to that of the fluvio-lacustrine sediments, while its variability increases (81-139 ppm). The coarse samples shows the lowest V concentrations, while the samples of the cores L, S, T and V are more enriched.

The lacustrine clays contains the greatest amount of vanadium with a median value of 157 ppm and a range of 144 - 169 ppm.

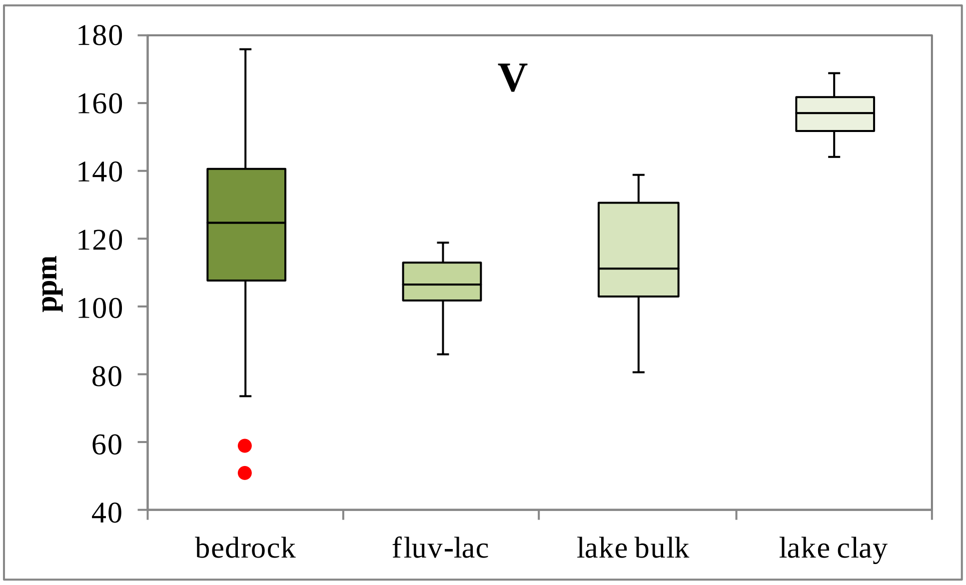

Figure 55. Boxplot of V contents in the different sample types.

Chromium (Cr)

In the local bedrock, chromium median value is 90 ppm and its content ranges from 40 and 120 ppm (fig. 56). In the lithoid rocks and in the Quaternary deposits Cr median value has the same value (90 ppm).

The fluvio-lacustrine sediments show the lowest Cr contents; here the median is 80 ppm and it ranges from 60 to 90 ppm; the maximum values were found at the month of the Agri and the Maglia rivers.

In the bulk lacustrine fraction, chromium median reaches 100 ppm, while its variability increases (70-120 ppm). The highest values are in a sample of the core B and I and in the distal cores R, S, T, V. The lacustrine clays contain the greatest amount of chromium with a median value of 125 ppm and a range of 110 - 130 ppm, that exceed the bedrock values. It has no outlier values.

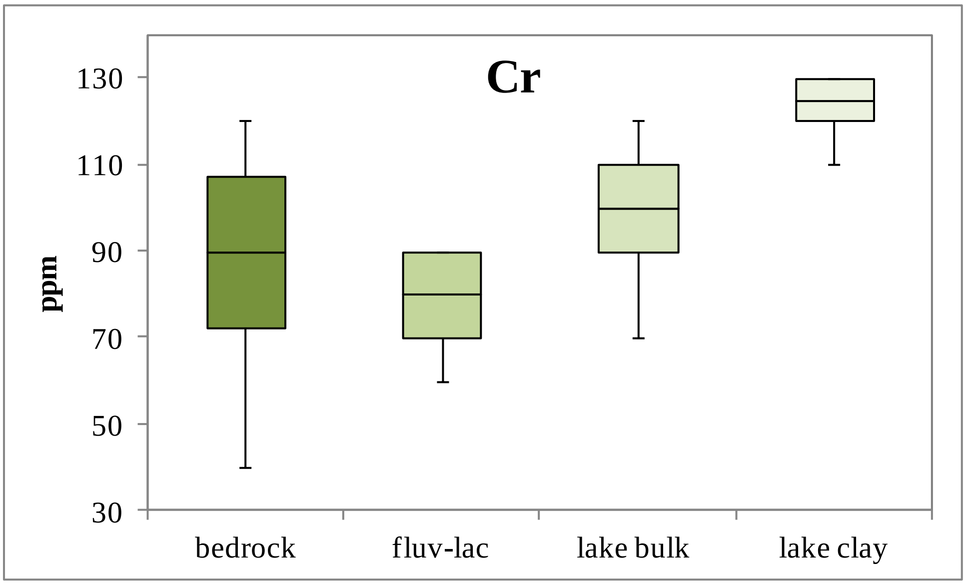

Figure 56. Boxplot of Cr ontents in the different sample types.

Cobalt (Co)

In the local bedrock, cobalt median value is 16 ppm and its content ranges from 4 and 27 ppm (fig. 57). Co median value in the lithoid rocks (15 ppm) is quite similar to that of the Quaternary deposits (18 ppm). The Galestri Formation shows the three greatest Co values, reaching a maximum of 100 ppm.

The fluvio-lacustrine sediments show the lowest Co contents; here the median is 13 ppm and it ranges from 9 ppm to 17 ppm.

In the bulk lacustrine fraction, cobalt median is 14 ppm, while its variability slightly decreases (10-16 ppm). The highest value was found in a sample of the core I.

The lacustrine clays contains the greatest Co amount, with a median value of 16 ppm and a range of 15 - 19 ppm. The outliers have quite low values (down to 20 ppm) and are related to three cores collected basinward of the Agri and Maglia months.

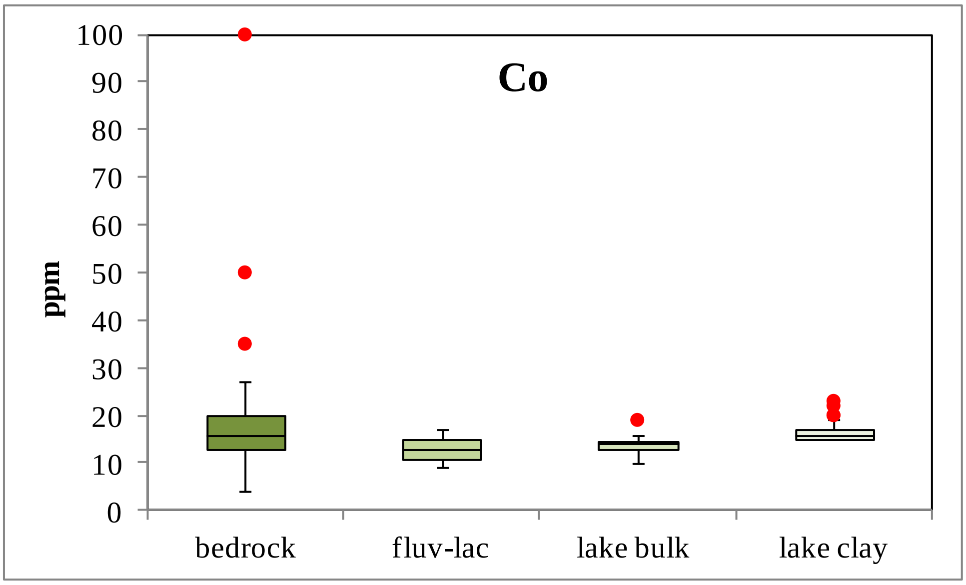

Figure 57. Boxplot of Co contents in the different sample types.

Nickel (Ni)

In the local bedrock, nickel median value is 40 ppm and its content ranges from 20 and 80 ppm (fig. 58). Its maximum value is 100 ppm and was found in the Galestri Formation. In the lithoid rocks and in the Quaternary deposits, Ni median has the same value (40 ppm).

The fluvio-lacustrine sediments exhibit the lowest Ni contents; the median is 40 ppm and it range from 30 ppm to 50 ppm; the maximum values were found at the Maglia month.

In the bulk lacustrine fraction, Ni median keeps the same value of 40 ppm, and the same range (30 - 50 ppm). In the lacustrine clays, Ni content slightly increases, reaching a median value of 50 ppm and a range of 50 - 70 ppm.

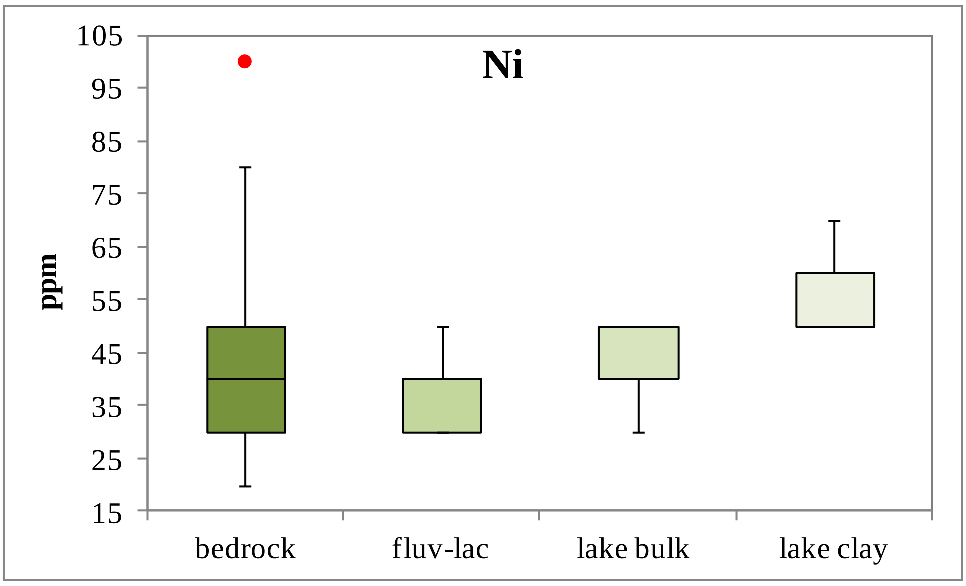

Figure 58. Boxplot of Ni contents in the different sample types.

Copper (Cu)

In the bedrock, Cu median value is 40 ppm and its range very broad, extending from 10 and 70 ppm (fig. 59). The Galestri Formation shows two outliers (110 and 90 ppm respectively); the other outlier is related to the Crete Nere Formation (90 ppm).

In the fluvio-lacustrine sediments the median value is 40 ppm and it ranges from 30 ppm to 50 ppm; its maximum value was found in a sample collected at the Maglia mouth.

Due to their scarce variability, it is impossible to graph the Cu distribution in the lacustrine bulk.

In the lacustrine clays, copper slightly increases, reaching a median value of 50 ppm and a range of 50 - 70 ppm. The values are very homogeneous, with a only maximum found in the black layer of the core R (a/R).

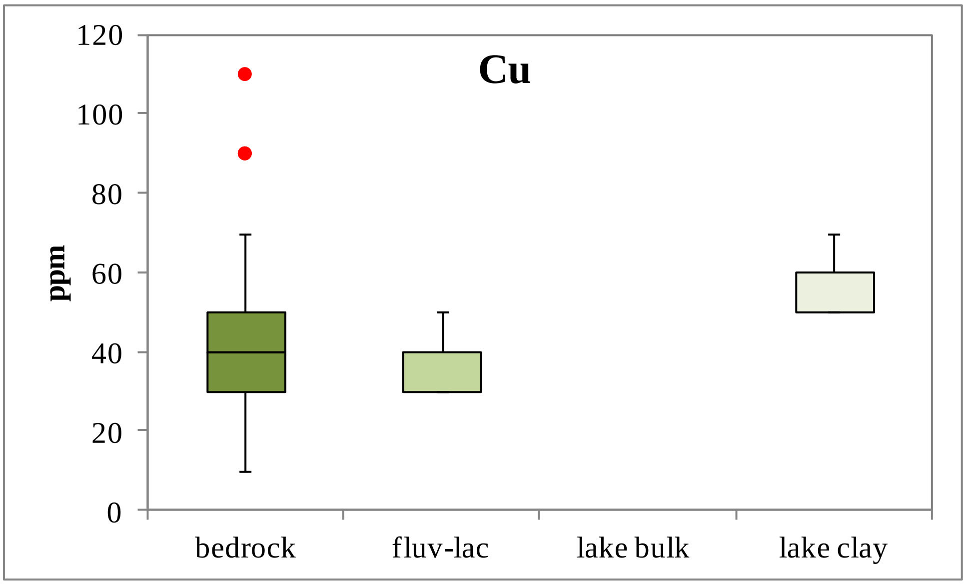

Figure 59. Boxplot of Cu contents in the different sample types.

Zinc (Zn)

In the local bedrock, zinc median value is 110 ppm and its content ranges between 40 ppm and 150 ppm (fig. 60).

In the lithoid rocks, Zn median value (100 ppm) is lower than that of the Quaternary deposits (120 ppm); the maximum values are related to the Galestri Formation while the minimum was found in a more cherty lithoid sample.

In the fluvio-lacustrine sediments, the Zn median value is 110 ppm and its range 80 - 130 ppm. Three outliers are found, two of which belonging to the samples EFF8 and EFF9 collected basinward of the Montemurro waste water treatment plant; the other outlier was found in the sample EFF16 collected at the Agri mouth.

In the lacustrine bulk, Zn contents remain quite equal, with the same median value of 110 ppm and the slightly larger range (80 - 140 ppm); the values are homogeneous with an unique low value in a coarse sample.

In the lacustrine clays, Zn concentrations increase, reaching a median value of 140 ppm and a range of 130 - 160 ppm. The sample a/R in the core R, shows the highest Zn value (220 ppm).

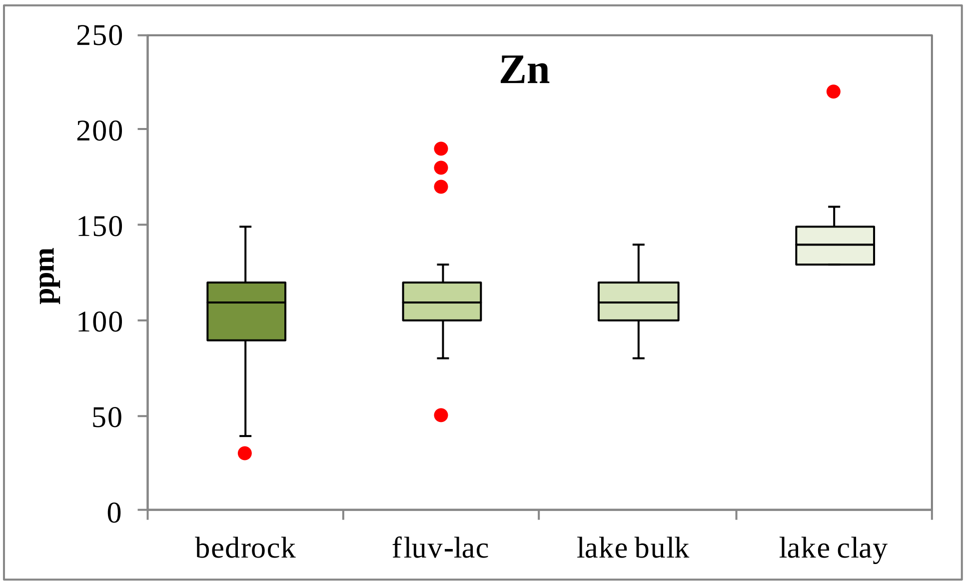

Figure 60. Boxplot of Zn contents in the different sample types.

Lead (Pb)

In the local bedrock, lead median value is 21 ppm and its content ranges from 5 and 50 ppm (fig. 61). In the lithoid rocks, Pb median value (16 ppm) greatly differs from that of the Quaternary deposits (31 ppm). Three outcrops show the highest Pb contents: an outcrop belonging to the Albidona Formation showing basic elements (pillow lavas,..) located close to the Agri River, with the highest value of 79 ppm; a Quaternary outcrop (60 ppm) belonging to the Spinoso Conglomerate Formation (the Pb concentration is also significant in the other outcrop of the same Formation), another Quaternary outcrop (64 ppm) located close to the Sciaura Stream.

In the fluvio-lacustrine sediments, the Pb median value is 23 ppm and it ranges from 17 ppm to 33 ppm. The highest Pb concentrations were found in three samples, at the Agri, Rifreddo and Vella months respectively.

In the lacustrine bulk, Pb contents slightly increases with a median value of 25 ppm and a range of 20 - 29 ppm; the outlier, found in the sample T1 at the top of the core T, has a relatively low concentration (35 ppm).

In the clay fraction, Pb reaches a median value of 42 ppm and it ranges between 31 - 49 ppm. Pb variations seem to be more regular, with only one outlier related to a black sample collected in the core I (69 ppm).

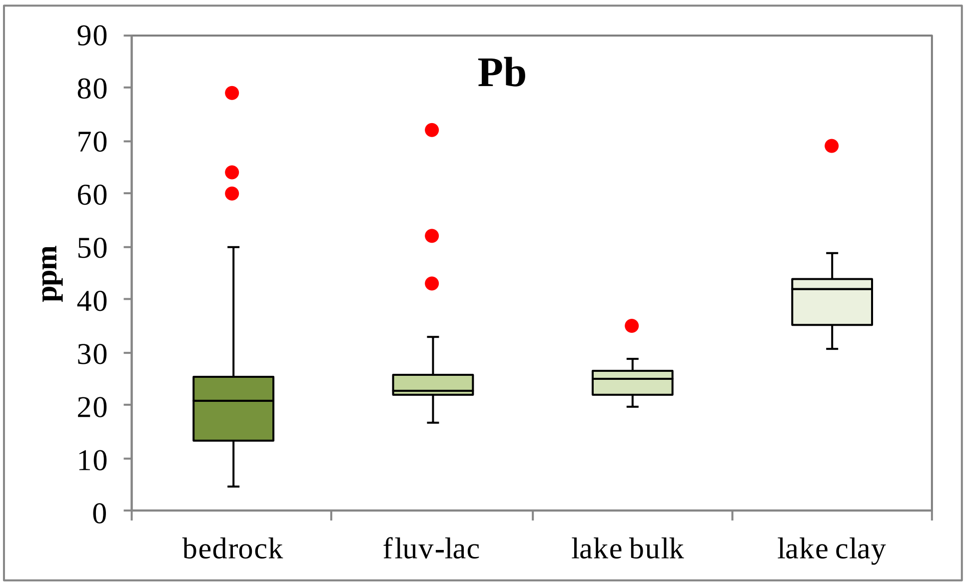

Figure 61. Boxplot of Pb contents in the different sample types.

Arsenic (As)

In the local bedrock, As median value is 5.5 ppm and its content ranges from 5 ppm to 15 ppm (fig. 62).

However, among the Meso-Cenozoic items, 15 on 23 samples show As contents under the detection limits. The asymmetrical box plot confirms the difference between the As concentration in the lithoid rocks and the Quaternary incoherent deposits, whose median value double to a value of 10 ppm. In a Quaternary outcrop it reaches the maximum value of 26 ppm. The other outliers is related to the Scisti Silicei Formation.

In the fluvio-lacustrine and in the bulk lacustrine sediments, the As content is quite always under the detection limit.

In the lacustrine clays, the As values slightly increase, ranging between 5 ppm and 11 ppm, with a median value of 8 ppm.

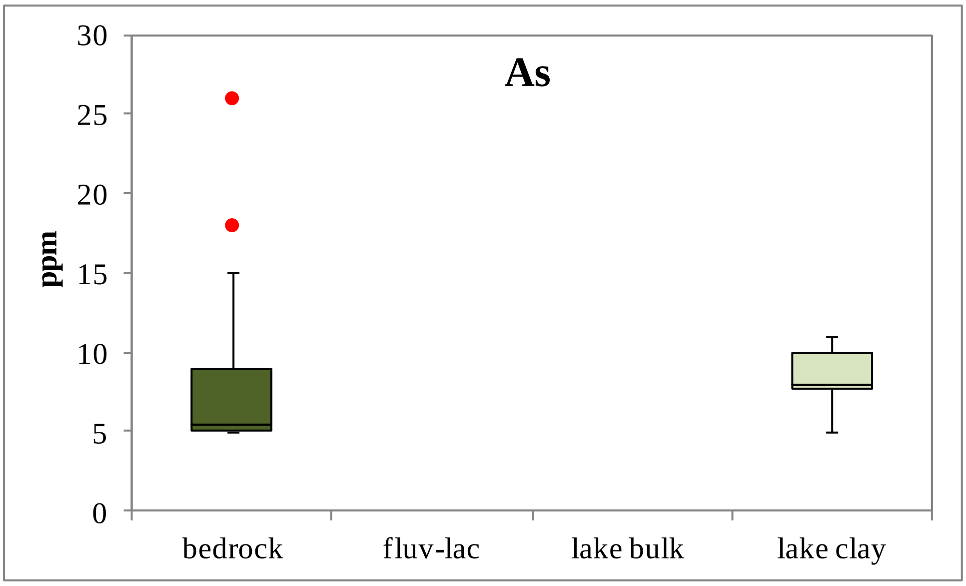

Figure 62. Boxplot of As contents in the different sample types.

4.5 Enrichment factors

In order to evaluate the possible contamination of the Pietra del Pertusillo reservoir sediments the enrichment factors of the environmental interest metals were calculated.

The enrichment factor, hereafter EF, for a given element (X) is determined using the following equation (Reimann and De Caritat, 2005):

$$EF = \frac{\left[\frac{X}{Ti}\right]_{sample}}{\left[\frac{X}{Ti}\right]_{crust}}$$

where X and Ti are the weight percentages of an element and titanium, respectively. Titanium was used as the normalizing element because it is associated with crustal rock sources with little mobility during diagenesis and it is less altered anthropogenically (Callender, 2003).

Generaly, the subscript “crust” identifies the reference standard used for the calculation. In the present study, the EFs were calculated using bedrock ($EF_{bedrock}$) and upper continental crust (UCC, Mc Lennan, 2006) (EF_{UCC}) element concentrations.

On the basis of the enrichment factor, five categories are recognized as follows (Sutherland, 2000): EF < 2 is depletion to minimal enrichment; EF 2–5 is moderate enrichment; EF 5–20 is significant enrichment; EF 20–40 is very high enrichment; EF > 40 extremely high enrichment.

The EF_{UCC} and the $EF_{bedrock}$ values calculated for both bulk and clay fractions of the lacustrine sediments are given in Tables 8 and 9.

The $EF_{(bedrock)}$ values are greater than the $EF_{(UCC)}$ ones due to its higher percentages of titanium. Cu, Zn and As are the exceptions: Cu and Zn show identical enrichment factor values in the UCC and in the local bedrock while As is depleted in the local bedrock, and in particular in the Meso-Cenozoic rocks. As a consequence, we preferred to use the EFs normalized by bedrock values in order to detail the distribution of environment interest metals and consequently to define the origin.

In the two following paragraphs, we present the vertical profiles of the EF for the cores F_1, R, T and V, that show a major number of samples.

4.5.1 Vertical profiles

In this paragraph, we compare the vertical profiles of the $EF_{(UCC)}$ and the $EF_{(bedrock)}$ for both bulk (figg. 63-66, tab. 8) and clay fraction (figg. 67-70, tab. 9) of the cores F_1, R, T and V; for each of these cores, in fact, a greater number of samples were analyzed.

Bulk fraction

Almost all the analyzed trace elements of the core $\underline{F_1}$ show EFs<2. The major enrichments is in general related to the sample $F_1$6, a black layer with an higher total organic carbon percentage.

The samples from the core R show an identical situation and EFs are always <2. V, Co, Cu and Cr exhibit the same trend, becaming depleted in the two samples R9 and R12 (-73 cm and -125 cm respectively), while Ba and Pb are enriched in the same samples.

As concern the core T, V, Ba, Co increase downwards, reaching the maximum in the deepest sample c/T, the black layer with the highest TOC content. Cr as well shows the maximum value in the sample c/T, while Ni, Cu and Pb became enriched in the shallowest sample T_1.

Finally, in the core V, EFs are always <2. The sample d/V (-69 cm) is slightly enriched in Ni, Cr and Pb, while Co and V exhibit the same trend and a tiny enrichment in the sample b/V (-76 cm).

Table 8. Enrichment factors $EF_{(UCC)}$ (against the Upper Continental Crust values) and $EF_{(bedrock)}$ (against the local bedrock values) in the lacustrine bulk fraction.

Core	Sample	Depth (cm)	V		Ba		Cr		Co		Ni		Cu		Zn		Pb	
			$EF_{(UCC)}$	$EF_{(bedrock)}$	$EF_{(UCC)}$	$EF_{(bedrock)}$	$EF_{(UCC)}$	$EF_{(bedrock)}$	$EF_{(UCC)}$	$EF_{(bedrock)}$	$EF_{(UCC)}$	$EF_{(bedrock)}$	$EF_{(UCC)}$	$EF_{(bedrock)}$	$EF_{(UCC)}$	$EF_{(bedrock)}$	$EF_{(UCC)}$	$EF_{(bedrock)}$
A	A1	0 - 3	0,69	0,90	0,50	1,09	0,80	1,16	0,61	1,02	0,67	1,08	1,19	1,20	1,15	1,20	1,00	1,25
B	B1t	14 - 19	0,71	0,93	0,47	1,02	0,84	1,22	0,62	1,03	0,79	1,27	1,12	1,14	0,98	1,03	1,07	1,34
F	F4	39,50 - 41	0,65	0,85	0,66	1,44	0,71	1,02	0,64	1,07	0,76	1,22	1,00	1,02	0,94	0,98	1,13	1,41
F_1	$F_1$3	9 - 12	0.71	0.92	0.49	1.08	0.80	1.16	0.64	1.06	0.57	0.91	1.33	1.35	1.17	1.22	1.08	1.35
	$F_1$6	22-24,5	0.79	1.03	0.51	1.11	0.87	1.26	0.62	1.03	0.73	1.17	1.29	1.31	1.25	1.30	1.09	1.36
	$F_1$12	45-48	0.70	0.91	0.48	1.06	0.79	1.15	0.65	1.08	0.67	1.06	1.17	1.19	1.03	1.08	1.08	1.35
I	I2	5 - 6	0,72	0,94	0,47	1,03	0,79	1,15	0,56	0,93	0,67	1,07	1,17	1,19	1,03	1,08	0,86	1,08
	I12	122 - 127	0,63	0,82	0,36	0,79	0,68	0,99	0,63	1,05	0,64	1,03	1,13	1,15	0,95	1,00	0,83	1,04
L	4L	26 - 29	0,83	1,09	0,54	1,18	0,93	1,34	0,60	1,00	0,73	1,16	1,28	1,30	1,08	1,13	1,09	1,36
M	M2	46 - 68,5	0,65	0,85	0,56	1,22	0,64	0,93	0,55	0,92	0,61	0,97	1,07	1,09	1,04	1,08	1,02	1,28
R	a/R	12,5-14,5	0.84	1.10	0.56	1.23	0.89	1.29	0.63	1.05	0.75	1.20	1.32	1.34	1.39	1.45	1.07	1.33
	R9	69-77	0.77	1.00	0.68	1.48	0.85	1.23	0.52	0.86	0.80	1.28	1.06	1.07	1.24	1.29	1.24	1.55

Core	Sample	Depth (cm)	V		Ba		Cr		Co		Ni		Cu		Zn		Pb	
			$EF_{(UCC)}$	$EF_{(bedrock)}$	$EF_{(UCC)}$	$EF_{(bedrock)}$	$EF_{(UCC)}$	$EF_{(bedrock)}$	$EF_{(UCC)}$	$EF_{(bedrock)}$	$EF_{(UCC)}$	$EF_{(bedrock)}$	$EF_{(UCC)}$	$EF_{(bedrock)}$	$EF_{(UCC)}$	$EF_{(bedrock)}$	$EF_{(UCC)}$	$EF_{(bedrock)}$
R	**R12**	124-126	0.68	0.88	0.67	1.47	0.86	1.25	0.53	0.88	0.61	0.98	1.07	1.09	1.39	1.45	1.37	1.71
	R18	176,5-178	0.81	1.06	0.61	1.34	0.92	1.33	0.58	0.97	0.69	1.11	1.22	1.24	1.29	1.34	1.21	1.51
S	**S7t**	64 - 68	0,87	1,14	0,56	1,23	0,92	1,34	0,57	0,96	0,63	1,01	1,12	1,13	1,08	1,13	1,11	1,38
	S7b	76 - 81	0,88	1,15	0,58	1,27	0,93	1,34	0,62	1,03	0,80	1,27	1,12	1,14	1,08	1,13	1,15	1,44
T	**T1**	9 - 13	0.86	1.12	0.56	1.22	0.94	1.36	0.58	0.97	0.81	1.29	1.42	1.44	1.30	1.36	1.46	1.82
	a/T	16 - 17,5	0.97	1.26	0.59	1.29	0.93	1.35	0.66	1.10	0.78	1.25	1.38	1.40	1.33	1.39	1.06	1.33
	c/T	59,5 - 60,5	0.99	1.29	0.60	1.32	1.04	1.51	0.76	1.27	0.79	1.26	1.38	1.40	1.22	1.27	1.07	1.34
V	**a/V**	32,25-33,5	0.92	1.20	0.52	1.14	0.95	1.38	0.63	1.06	0.82	1.31	1.44	1.46	1.42	1.48	1.14	1.43
	d/V	68-70	0.90	1.17	0.56	1.22	1.08	1.56	0.63	1.05	1.02	1.63	1.43	1.45	1.26	1.32	1.16	1.45
	b/V	75-77	0.95	1.23	0.56	1.22	1.02	1.48	0.70	1.17	0.77	1.24	1.36	1.38	1.32	1.37	1.10	1.38
	c/V	89,5-92,25	0.94	1.23	0.61	1.33	0.99	1.43	0.61	1.02	0.68	1.09	1.49	1.51	1.26	1.32	1.10	1.37
	V3	124 - 126,5	0.92	1.20	0.55	1.20	0.98	1.41	0.61	1.01	0.84	1.34	1.47	1.49	1.14	1.19	1.17	1.46

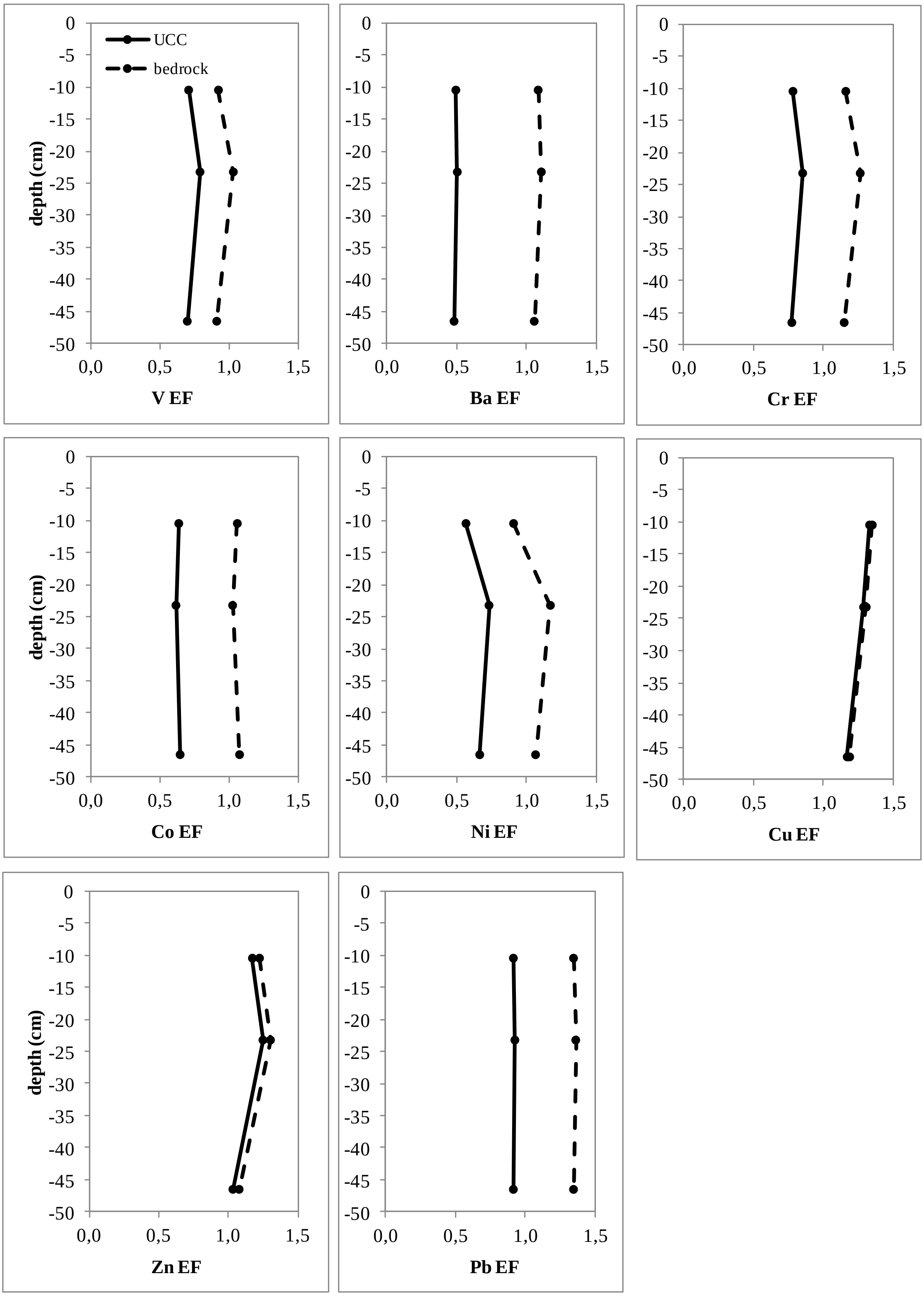

Figure 63. Enrichment factors for trace elements in the bulk fraction of the core F_1.

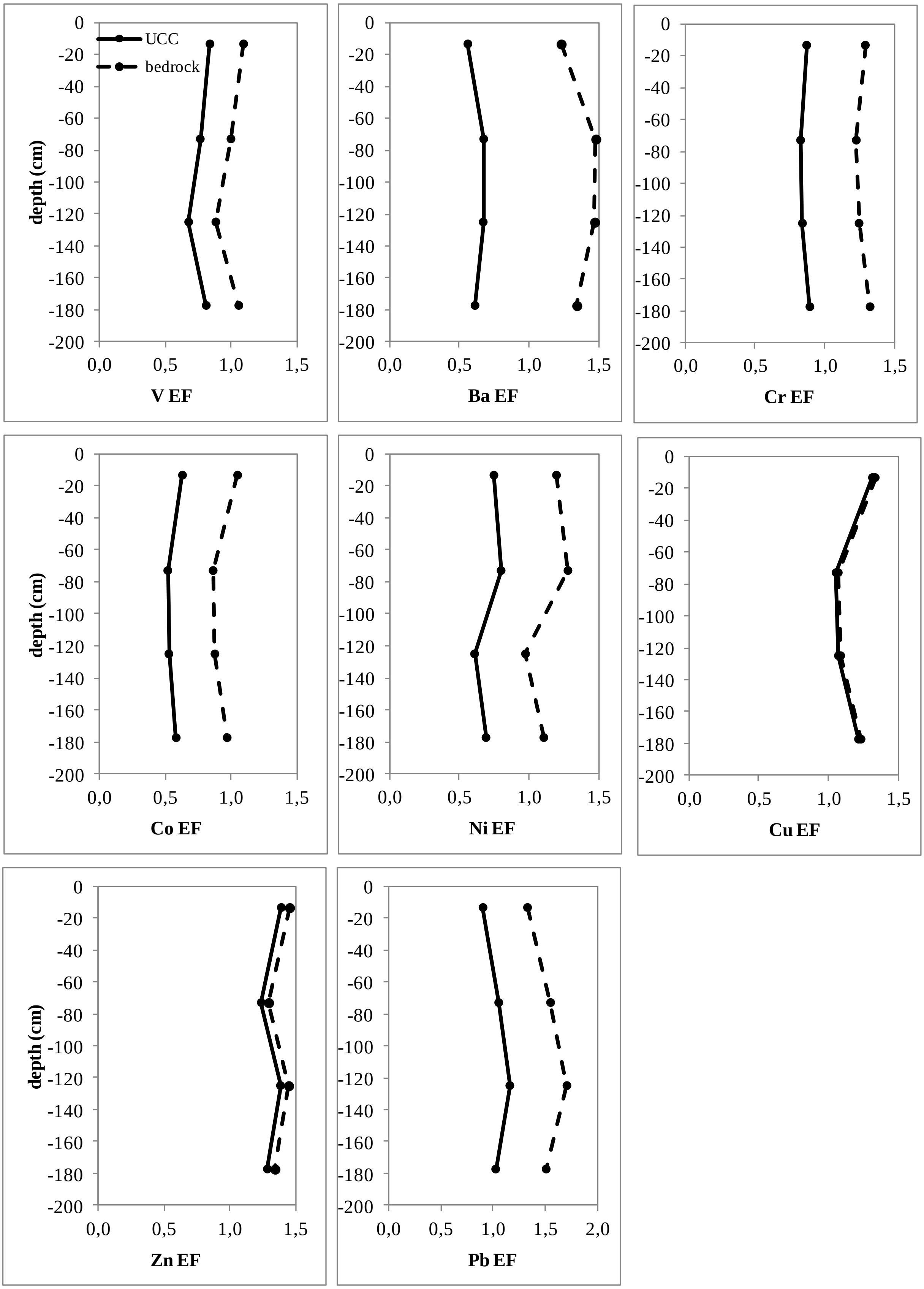

Figure 64. Enrichment factors for trace elements in the bulk fraction of the core R.

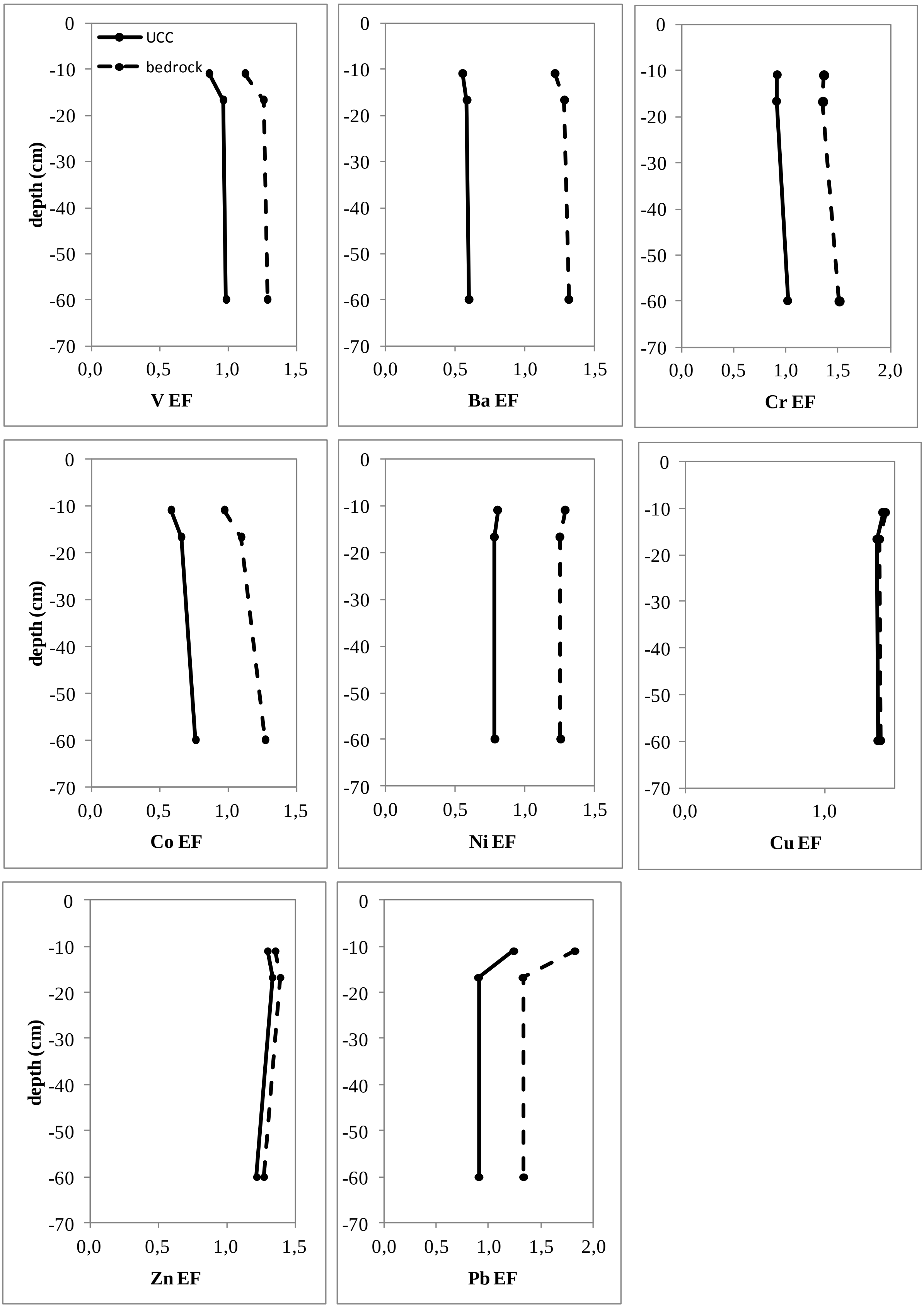

Figure 65. Enrichment factors for trace elements in the bulk fraction of the core T.

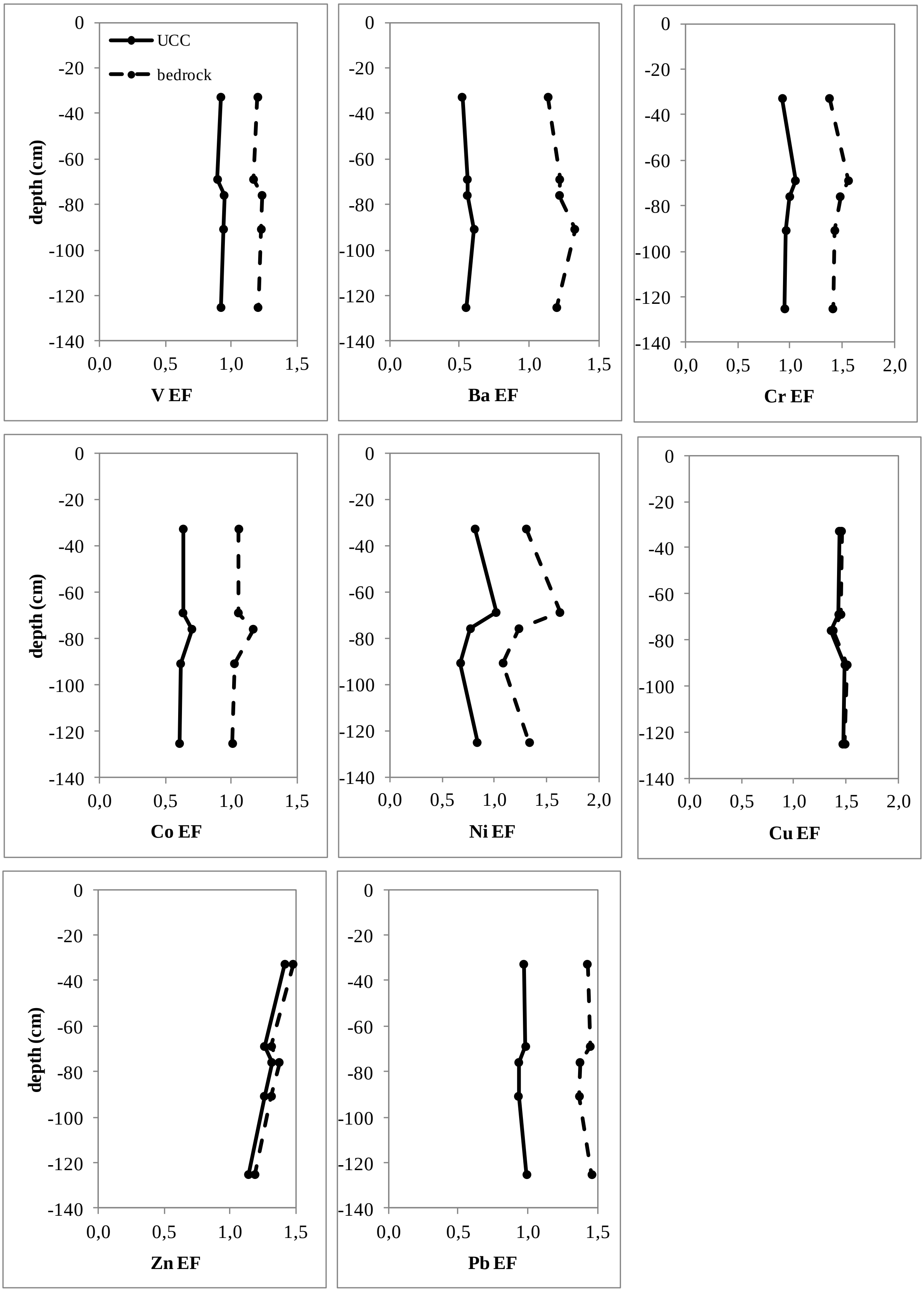

Figure 66. Enrichment factors for trace elements in the bulk fraction of the core V.

Clay fraction

In the clay fraction, EFs increase for almost all trace elements (figg. 67-70, tab. 9).

In the core $\underline{F_1}$, only Pb (both the $EF_{(bedrock)}$ and the $EF_{(UCC)}$) and As (the $EF_{(UCC)}$) show EF >2. Ba, Cr and Pb continued to be slightly enriched in the black layer F_16 (-23.25 cm) while the other elements (Co, Ni, Cu and As) are depleted in the same sample.

In the core R, Cr, Cu, Zn, Pb and As (only the $EF_{(UCC)}$) show some EF values >2. Pb and Ba continued to be enriched in the two samples R9 and R12, together with V and Cr, while Co, Ni, Cu, Zn and As show the same trend and are enriched in the black layer a/R (- 13.50 cm).

As concern the core T, only EF values of Pb and As are >2. All trace elements became enriched downwards and reach the maximum values in the black layer c/T.

The core V ehibits the same situation for Pb and As. The sample d/V (-69 cm) is enriched in V, Cr, Co, Ni, Cu and As, while the sample b/V (-79 cm) in Zn and Pb.

Table 9. Enrichment factors $EF_{(UCC)}$ (against the Upper Continental Crust values) and $EF_{(bedrock)}$ (against the local bedrock values) in the lacustrine clays.

Core	Sample	V		Ba		Cr		Co		Ni		Cu		Zn		Pb		As	
		$EF_{(UCC)}$	$EF_{(bedrock)}$	$EF_{(UCC)}$	$EF_{(bedrock)}$	$EF_{(UCC)}$	$EF_{(bedrock)}$	$EF_{(UCC)}$	$EF_{(bedrock)}$	$EF_{(UCC)}$	$EF_{(bedrock)}$	$EF_{(UCC)}$	$EF_{(bedrock)}$	$EF_{(UCC)}$	$EF_{(bedrock)}$	$EF_{(UCC)}$	$EF_{(bedrock)}$	$EF_{(UCC)}$	$EF_{(bedrock)}$
A	A1	1,05	1,36	0,54	1,19	1,13	1,68	0,74	1,23	1,01	1,62	1,78	1,80	1,56	1,63	1,81	2,67	3,70	1,26
B	B1t	1,03	1,34	0,56	1,23	1,07	1,59	0,82	1,37	0,95	1,53	1,68	1,70	1,38	1,44	1,61	2,36	4,37	1,49
F	F4	1,22	1,59	0,82	1,80	1,18	1,75	1,13	1,89	1,33	1,80	1,67	1,70	1,65	1,72	1,84	2,70	5,23	1,78
F1	F13	1.12	1.46	0.59	1.29	1.10	1.60	0.73	1.22	0.95	1.51	1.66	1.69	1.87	1.96	2.06	2.57	5.55	1.77
	F16	1.11	1.45	0.62	1.37	1.16	1.69	0.71	1.18	0.91	1.46	1.61	1.63	1.70	1.78	2.08	2.60	4.29	1.37
	F112	1.12	1.46	0.62	1.36	1.15	1.66	0.86	1.44	1.00	1.60	1.76	1.78	1.44	1.51	1.98	2.48	3.90	1.25
I	I2	1,08	1,40	0,58	1,26	1,04	1,53	0,65	1,08	0,83	1,33	1,76	1,79	1,55	1,62	2,53	3,72	3,21	1,09
	I12	0,88	1,14	0,47	1,04	0,86	1,28	0,73	1,22	0,77	1,23	1,36	1,38	1,03	1,08	1,19	1,74	3,53	1,20
L	4L	1,01	1,31	0,56	1,23	0,98	1,45	0,72	1,19	0,73	1,16	1,28	1,30	1,17	1,22	1,09	1,60	2,40	0,82
M	M2	1,06	1,38	0,75	1,64	1,02	1,52	0,67	1,11	0,91	1,46	1,60	1,63	1,32	1,38	1,60	2,36	4,60	1,57
R	a/R	1.19	1.55	0.66	1.45	1.19	1.72	0.82	1.37	1.12	1.80	2.31	2.34	2.55	2.66	2.08	2.60	5.49	1.75
	R9	1.33	1.74	0.77	1.69	1.38	2.00	0.78	1.29	1.00	1.60	1.76	1.79	1.86	1.94	2.23	2.78	4.69	1.50

Core	Sample	V		Ba		Cr		Co		Ni		Cu		Zn		Pb		As	
		$EF_{(UCC)}$	$EF_{(bedrock)}$	$EF_{(UCC)}$	$EF_{(bedrock)}$	$EF_{(UCC)}$	$EF_{(bedrock)}$	$EF_{(UCC)}$	$EF_{(bedrock)}$	$EF_{(UCC)}$	$EF_{(bedrock)}$	$EF_{(UCC)}$	$EF_{(bedrock)}$	$EF_{(UCC)}$	$EF_{(bedrock)}$	$EF_{(UCC)}$	$EF_{(bedrock)}$	$EF_{(UCC)}$	$EF_{(bedrock)}$
R	R12	1.33	1.74	0.76	1.67	1.40	2.03	0.79	1.32	1.02	1.63	2.15	2.18	2.02	2.10	2.26	2.83	4.77	1.52
	R18	1.12	1.47	0.68	1.50	1.19	1.73	0.67	1.12	0.86	1.38	1.52	1.54	1.61	1.68	1.57	1.96	2.54	0.81
S	S7t	1,08	1,40	0,63	1,39	1,07	1,58	0,70	1,16	0,79	1,27	1,39	1,42	1,28	1,33	1,22	1,79	2,62	0,89
	S7b	1,06	1,38	0,63	1,38	1,07	1,59	0,66	1,10	0,80	1,27	1,40	1,42	1,28	1,34	1,40	2,06	2,19	0,75
T	T1	1.04	1.36	0.59	1.29	1.11	1.61	0.67	1.11	0.81	1.29	1.42	1.44	1.40	1.46	1.59	1.98	3.31	1.06
	a/T	1.17	1.52	0.71	1.56	1.24	1.80	0.81	1.35	0.98	1.56	1.72	1.75	1.58	1.64	1.72	2.15	4.59	1.47
	c/T	1.29	1.68	0.74	1.63	1.25	1.81	0.92	1.53	0.98	1.57	1.73	1.76	1.71	1.78	1.83	2.29	5.77	1.84
V	a/V	1.07	1.40	0.58	1.28	1.04	1.51	0.68	1.13	0.82	1.31	1.44	1.46	1.32	1.37	2.07	2.59	3.84	1.23
	d/V	1.23	1.61	0.66	1.45	1.30	1.88	0.90	1.49	1.02	1.63	1.79	1.82	1.64	1.71	1.74	2.17	5.97	1.91
	b/V	1.20	1.57	0.67	1.47	1.23	1.78	0.85	1.42	0.97	1.55	1.70	1.73	1.92	2.00	2.15	2.69	5.10	1.63
	c/V	1.06	1.38	0.65	1.43	1.08	1.56	0.75	1.24	0.85	1.36	1.49	1.51	1.37	1.43	1.36	1.70	4.98	1.59
	V3	1.05	1.37	0.59	1.30	1.06	1.54	0.69	1.16	0.84	1.34	1.47	1.49	1.56	1.62	1.82	2.27	4.42	1.41

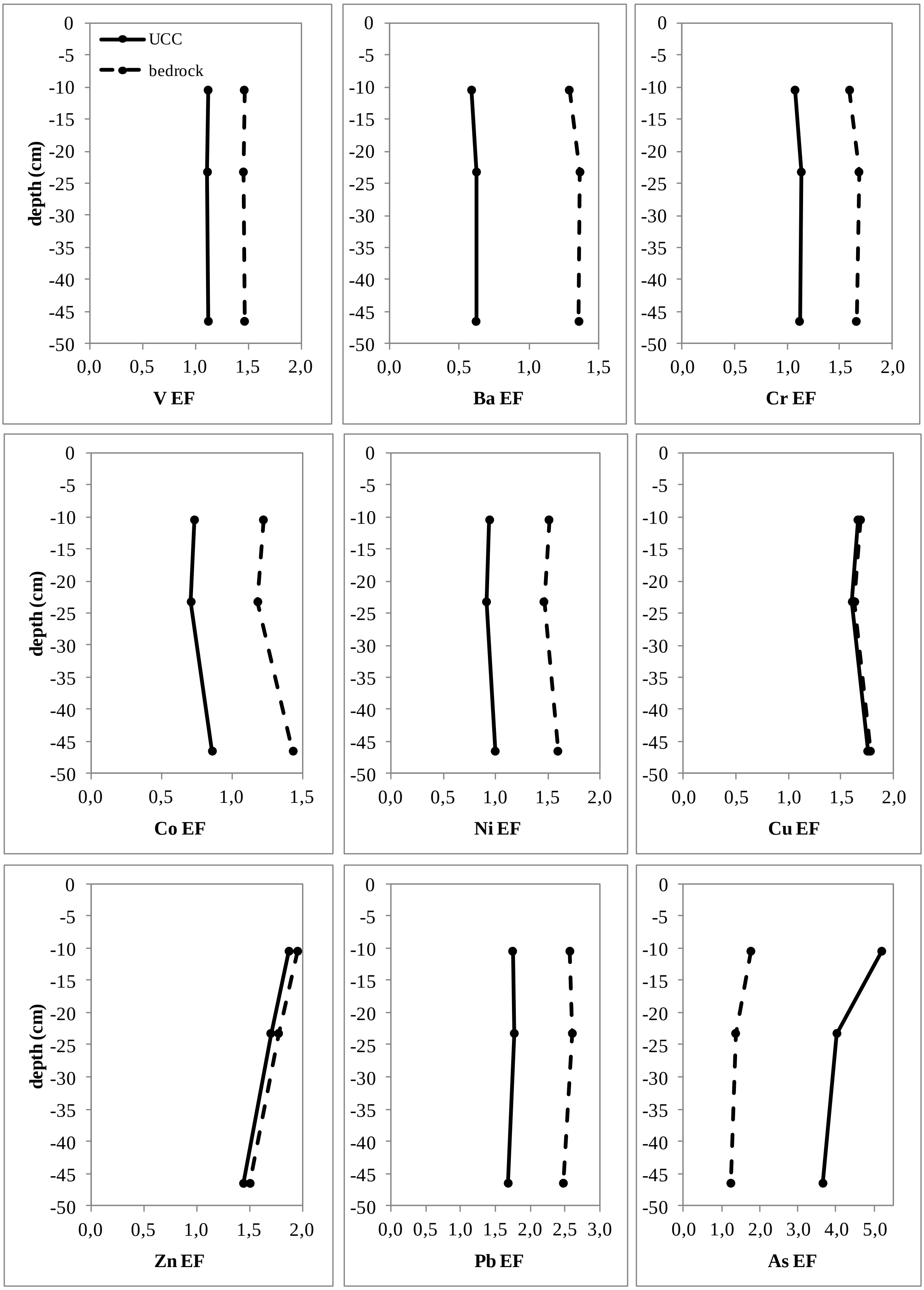

Figure 67. Enrichment factors for trace elements in the clay fraction of the core F_1.

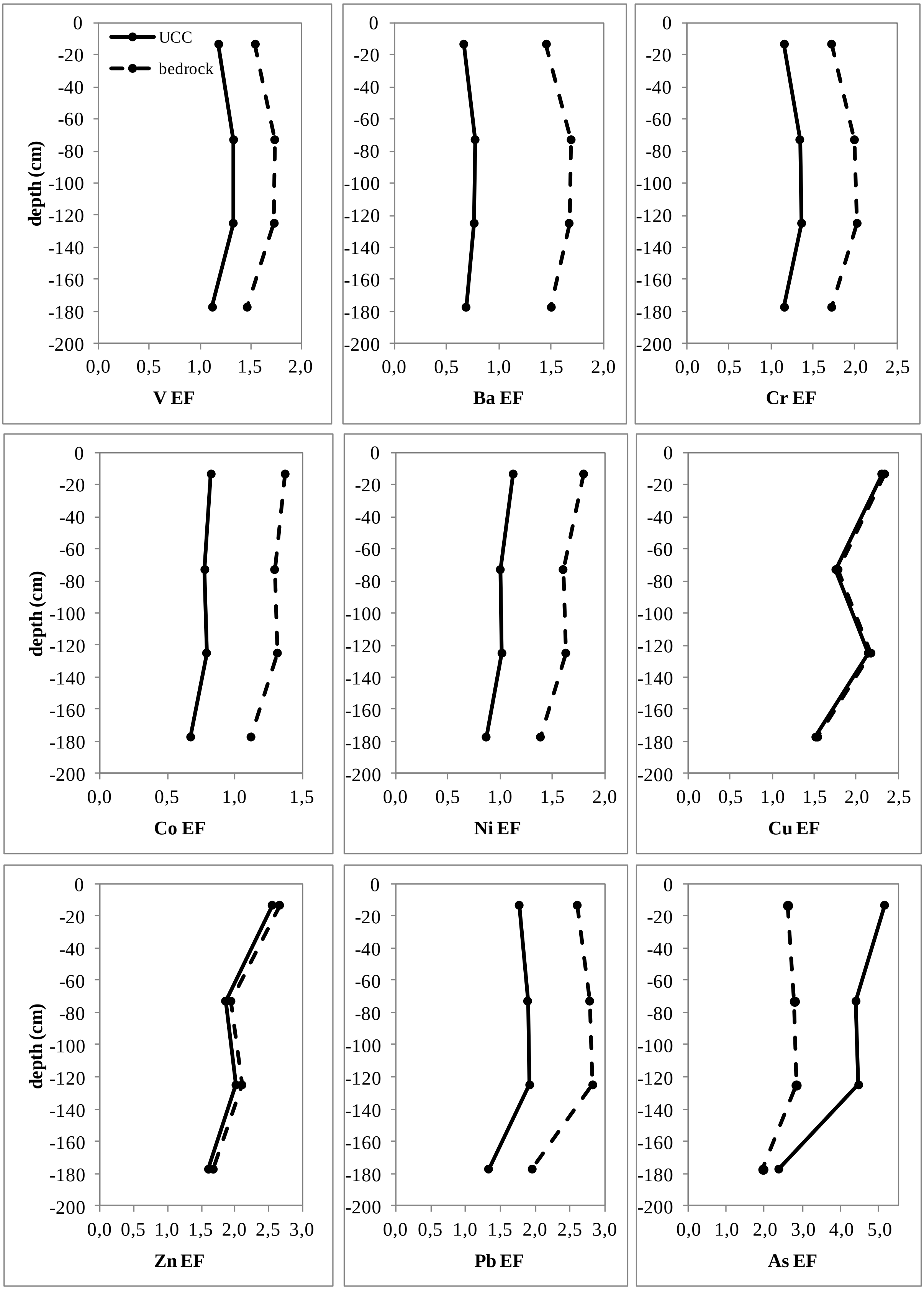

Figure 68. Enrichment factors for trace elements in the clay fraction of the core R.

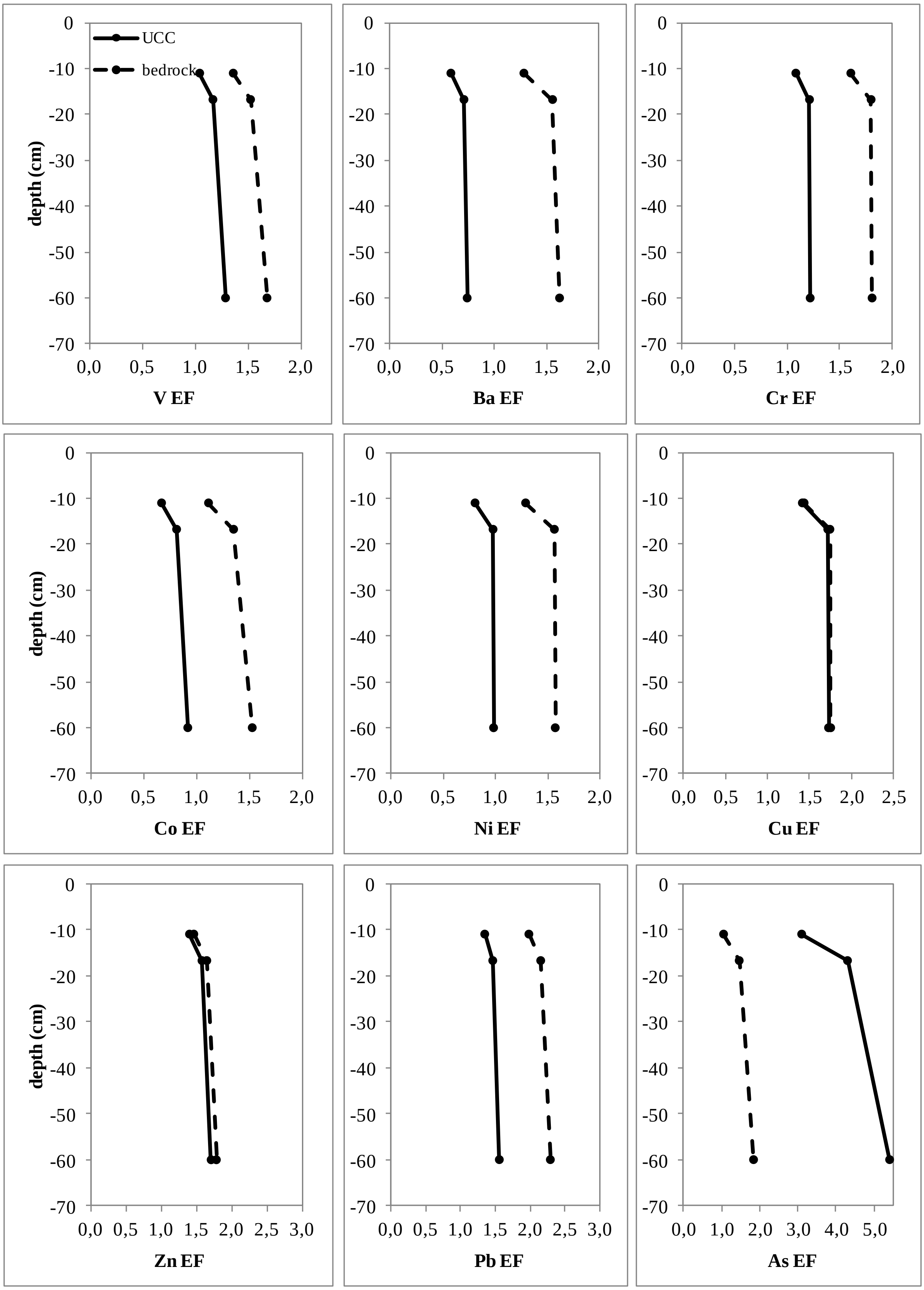

Figure 69. Enrichment factors for trace elements in the clay fraction of the core T.

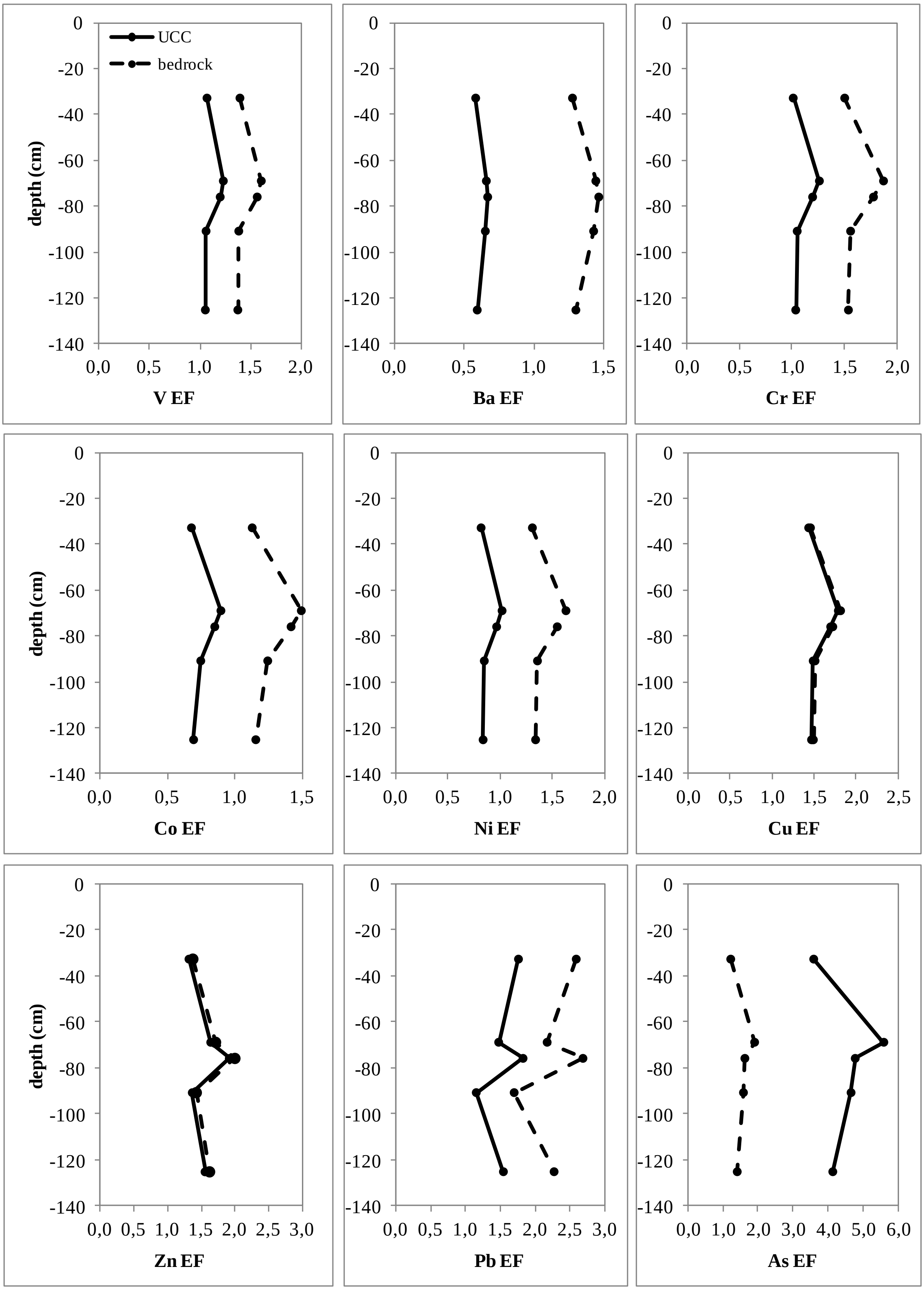

Figure 70. Enrichment factors for trace elements in the clay fraction of the core V.

4.5.2 The areal distribution of the enrichment factors

In order to evaluate possible basinwards enrichments of the trace elements, the longitudinal profiles of the $EF_{(bedrock)}$ for both bulk and clay fraction are calculated.

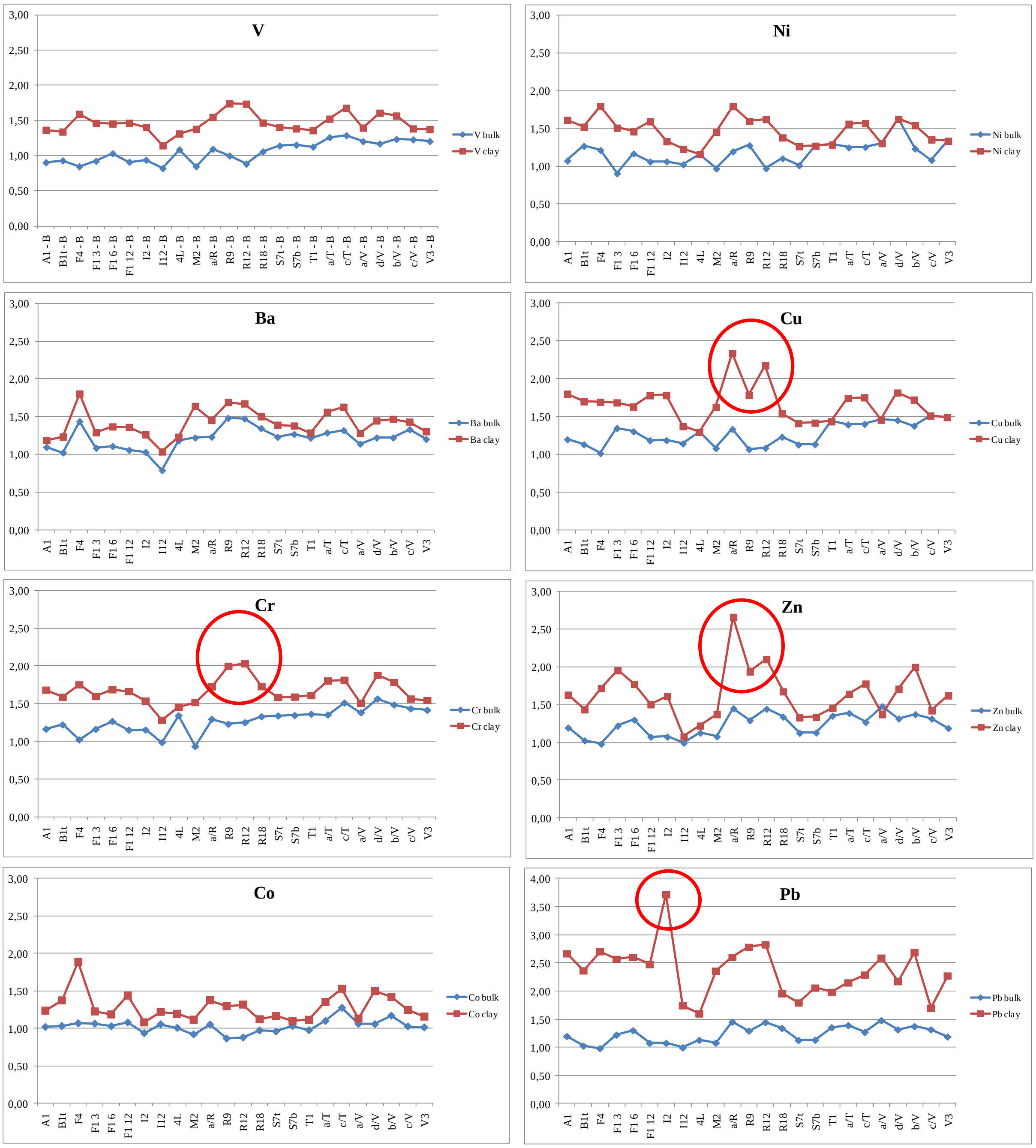

Figure 71. Comparison between the EF in the bulk and in the clay fraction. The red circles highlight the EF values ≥ 2.

The $EF_{(bedrock)}$ of the bulk and clay fractions have comparable values in the most of investigated cores (fig. 72). In detail, the $EF_{(bedrock)}$ values of the bulk are <2 and, as expected, they are constantly lower than that of the $EF_{(bedrock)}$ of the clay fraction. This last one, in fact, represents the more reactive fraction of a sample, and naturally concentrates the trace elements due to uptake processes of clay minerals and Fe-Mn oxi/hydroxides (Mameli et al., 2007; Sinisi et al., 2012; Mongelli et al., 2014). In addition: V, Ni, Ba and Co show EF values always <2; Pb shows 2<EF<3 in quite always the analyzed samples; Cu, Cr and Zn show EF values > 2 in the core R, in which Pb exhibits higher values as well (red circles).

References

- Abrahim & Parker, (2008). *Assessment of heavy metal enrichment factors and the degree of contamination in marine sediments from Tamaki Estuary, Auckland, New Zealand*. Environ Monit Assess, 136:227–238 DOI 10.1007/s10661-007-9678-2.

- Audry et al., 2004. *Fifty-year sedimentary record of heavy metal pollution (Cd, Zn, Cu, Pb) in the Lot River reservoirs (France)*. Environmental Pollution 132, 413–426.

- Boe¨s et al., 2011. *Evaluation of conservative lithogenic elements (Ti, Zr, Al, and Rb) to study anthropogenic element enrichments in lake sediments*. J Paleolimnol, 46:75–87 DOI 10.1007/s10933-011-9515-z.

- Callender, 2003. *Heavy Metals in the Environment - Historical Trends*. In: Treatise on Geochemistry Editors-in-Chief: Heinrich D. Holland and Karl K. Turekian. ISBN: 978-0-08-043751-4.

- Christophoridis et al., 2009. *Occurrence and distribution of selected heavy metals in the surface sediments of Thermaikos Gulf, N. Greece. Assessment using pollution indicators*. Journal of Hazardous Materials 168, 1082–1091.

- Hakanson and Jansson, 1983. Principles of lake sedimentology. Springer-Verlag, Berlin Heidelberg. ISBN-13:978-3-642-69276-5, DOI: 10.1007/978-3-642-69274-1.

- Hernandez et al., 2003. *Heavy metal distribution in some French forest soils: evidence for atmospheric contamination*. 2003;312:195–219.

- IMAA-CNR, 2005. *Analisi di materiali argillosi per diffrazione di raggi X e microscopia a scansione. Teoria ed applicazioni*. Atti del VII corso di formazione dell'Associazione Italiana per lo Studio delle Argille.

- Jones and Bowser, 1978. *The mineralogy and related chemistry of lake sediments*. In: Lerman A. Lakes - Chemistry, geology and physics. New York, Springer-Verlag, chap. 7, pp. 179-235.

- Liaghati et al., 2003. *Heavy metal distribution and controlling factors within coastal plain sediments, Bells Creek catchment, southeast Qeensland, Australia*. Environment International 29, 935-948.

- Mameli et al., (2007) – *Geological, geochemical and mineralogical features of some bauxite deposits from Nurra (Western Sardinia, Italy): insights on conditions of formation and parental affinity*. Int. Jour. Earth Sci. (Geol. Rundsch), 96, 887-902.

- McLennan et al., 2006. *Composition, differentiation and evolution of continental crust: constrains from sedimentary rocks and heat flow*. In: Brown, M., Rushmer, T. (Eds.), Evolution and Differentiation of The Continental Crust. Cambridge University Press, Cambridge, pp. 92–134.

- Moore et al., 2009. *Assessment of heavy metal contamination in water and surface sediments of the Maharlu saline Lake, sw Iran*. Iranian Journal of Science & Technology, Transaction A, Vol. 33, No. A1. Printed in the Islamic Republic of Iran, Shiraz University.

- Mongelli et al., 2014. *Trace elements and REE fractionation in subsoils developed on sedimentary and volcanic rocks: case study of the Mt. Vulture area, southern Italy*. Int J Earth Sci (Geol Rundsch) DOI 10.1007/s00531-014-1003-z.

- N'guessan et al., 2008. *Trace elements in stream bed sediments from agricultural catchments (Gascogne region, S-W France): Where do they come from?* Sci Total Environ, vol. 407 (n°8). pp. 2939 - 2952. ISSN 0048-9697.

- Reimann, De Caritat, 2005. *Distinguishing between natural and anthropogenic sources for elements in the environment: regional geochemical surveys versus enrichment factors*. Science of the Total Environment 337, 91– 107.

- Sahoo et al., 2015. *Use of multy-proxy approaches to determine the origin and depositional processes in modern lacustrine sediments: Carajas Plateau, Southeastern Amazon, Brazil*. Applied Geochemistry 52, 130-146.

- Salminen et al. 2006. *Geochemical Atlas of Europe. Part 2. Interpretation of Geochemical Maps, Additional Tables, Figures, Maps, and Related Publications*. De Vos W. and Tarvainen T. (Chief-editors).

- Shephard et al., 1954. *Sedimentary Environments Differentiated by Coarse-Fraction Studies*. AAPG Bullettin, vol.38, issue 8, 1792 -1802.

- Sinha and Chatterjee, 2000. *Mineralogy of lacustrine sediments in the Schirmacher Range area, Eastern Antarctica*. Journal Geological Society of India. Vol. 56, pp. 39-45.

- Sinisi et al., 2012. *Different Mn-ores in a continental arc setting: geochemical and mineralogical evidence from Tertiary deposits of Sardinia (Italy)*. Ore geology Reviews, 47, 110-125.

- Woods, 2009. *Tracing the Distribution of Heavy Metals in Sediments of the Pearl River Estuary*. Durham theses, Durham University. Available at Durham E-Theses Online: http://etheses.dur.ac.uk/87/.

DISCUSSION

5. Discussion

5.1 The methodological approach to the environmental quality assessment of the fresh-water reservoir sediments.

In order to investigate the environmental contamination of a fresh-water reservoir and of its catchment, previous understudied, a new methodological approach was developed. It was based on the analysis of different solid matrices, never assessed before, which have been chosen to consider the following:

- the parent rocks outcropping in the Pertusillo catchment are essential to evaluate the geogenic contribution; due to their high uptake and adsorption capacities, the lithologies with a predominate siliciclastic pelitic fraction lead us to measure the highest content of minor and trace elements;
- the fluvio-lacustrine sediments are collected in the peri-lacual zone in order to both assess the chemical and mineralogical composition close to the detrital supply entry points of the reservoir and to better locate the core sampling points. The lack of works concerning the distribution of trace elements in the sediments of the water-level fluctuation zone, makes our approach original in the investigation of a very dynamic and complex system;
- the lake bottom-sediments act as sinks for contaminants and constitute the major environmental archive of possible pollutant input of the area derived from the different urban and industrial sources of pollution. The collection and the accurate stratigraphic description of a great number of cores across the whole reservoir allowed us to first reconstruct the depositional lacustrine environments and then provide a basis for selecting the levels for XRPD analyses. The samples with the highest peaks of interstratified clay minerals together with illite peaks opened at low

2ϑ, lead us to assess the maximum concentrations of trace elements both in the bulk and clay fraction (< 4μ) of the deep sediments, previously never investigated.

5.2 Facies interpretation and assessment of the depositional environment

According to the sedimentological analysis, the Pertusillo fresh-water reservoir can be divided in three depositional sub-environments: the proximal deltaic areas, the transitional areas and the distal lacustrine zone s.s..

The deltaic areas correspond to the depositional areas at the mouths of the longitudinal Agri (cores A, B, F), and transversal Rifreddo (core H) and Spetrizzone-Scazzero (core Q) rivers. The seasonal dramatic water-level fluctuations of the reservoir and the torrential regime of several tributaries, rule the very complex flow patterns, with a consequently annual changes in the position of the tributary mouths, their morphologies and their deltaic deposits.

The vertical and lateral facies changes at the mouth and delta of the Agri River is due to the water level seasonal fluctuations, which result in the alternation and intersecting of typical lacustrine muddy deposits in a low energy environment (facies A and F) with silty-sand and sand deposits (facies G, H, I, L, M, N).

In the deltaic areas, the finer sediment is quite homogeneous, lamination is always absent or disturbed (facies C), underlying massive mud flocculation in oxidizing conditions at the bottom, that favor bioturbation. The subaerial emersion is testified by erosional surfaces and pedogenic levels with abundant roots and frustules (facies B). Red and black spherules, indicate the migration of Fe and Mn along the sediment column during the water level fluctuations. The coarser fractions (facies G, H, I, L, M) have often erosional limits and include rounded fluvial granules in the core A and F and white angular clasts in the cores Q and R, where detrital fluvial material from the shores (core Q) and from the islet interrupts the lacustrine deposition.

In the transitional areas (cores F_1, L, I, M) the disturbed sediments are always associated with laminated sediments (facies D), and thin black laminae appear, testifying the progressive deepening of the area and the establishing of redox conditions. Erosional surfaces disappear in this area.

The distal lacustrine zone s.s. corresponds to the eastern sector of the reservoir (cores N, P, R, S, T and V). This sector is hardly affected by water level fluctuations. Sediments are dominantly muddy, the colour is greyish, that becomes completely black in centimeter-bedded beds (facies E), that increase basinward in thickness, quantity and color intensity. They show the highest total organic contents, so most likely they were deposited under anoxia conditions of the hypolimnion. At the bottom of core S a massive coarse-grained deposit was found, probably related to the erosion of the upstream islet.

The higher water level, the higher sediment thickness, the presence of darker beds perfectly preserved, the absence of sand fraction, lead us to identify this portion of the lake as the accumulation zone, whose sediments properties are replicable over the whole area.

5.3 Mineralogical composition of the deep lacustrine sediments

The lacustrine sediments act as sinks for fluvial material and are commonly used to study the erosion history of the watershed and to understand the processes (natural as much as anthropogenic) affecting the concentration and mobility of trace elements in water and sediments.

The mineralogical composition of analysed sediments reflects the compositional features of the parent rocks. Quartz represents the principal allogenic phase, derived from the silico-clastic rocks outcropping around the lake basin. Only in the blackish clay samples of the cores R, T and V, the characteristic diffraction peak of calcite is taller than quartz one, probably due to the precipitation of organic calcite. In the same way, the fixation of inorganic carbon in the photic zone of the lake by photosynthetic organisms results in the reduction of the p_{CO2} with a subsequent increasing of the solubility of calcite in surface waters (Jones, Bowser, 1978). Eutrophic hard water lake, like those of the Pertusillo reservoir, commonly exhibit covariance of calcite and organic carbon concentrations in their sediments. Dolomite is found only basinward of the Agri mouth, together with large amount of magnesium oxide, coming from the Campania-Lucania Platform Units outcropping on the right margin of the basin.

Similarly to quartz, the distribution of feldspars in the lacustrine sediments also reflect the mineralogical composition of litologies outcropping along the drainage basin. Higher amounts of feldspars are in the distal cores (i.e. R, S, T and V) near the silico-clastic deposits (Gorgoglione and Albidona Flysches). As concern clay minerals (illite and chlorite), they are the weathering product of the rocks in the lake dranaige basin. Illite shows its highest characteristic peak in the samples from core M, where feldspars and calcite also are more abundant. This is probably related to the outcrop of the Albidona Flysch, characterized by some calcareous intercalations, on the southern portion of the lake. Chlorite shows the tallest diffraction peaks in the diffraction patters of the Maglia arm samples. This mineral may derive from the weathering of mafic silicates-rich rocks, such as Lagonegro basin rocks (Scisti Silicei, Galestri), Ligurian deposits, Albidona Flysch. The distribution of clay minerals does not show an homogeneous variation in deeper sediments, except in the core R, the most coarser deep core, in which they clearly decreases.

The low contents of mixed-layered clay minerals may indicate a limited clay transformation at the sediment-water interface; this may be linked to the high accumulation rate of the Pertusillo reservoir (19,7 cm/yr in the deepest area of the reservoir) calculated on the basis of the data reported by CRA-ABP (2007). In general, the decreasing of the interstratified mineral peak width in the core S, T and V is observed. There probably the clastic contribution of the channelized fluvial processes is negligible.

5.4 Chemical distribution of elements of environmental interest in the Pertusillo system

Heavy metals and As are among the most common environmental pollutants stressing the biotic community. They are readily bioavailable and highly persistent; as metals do not undergo any metabolic change or degradation, they move up the trophic levels, undergoing processes of bioaccumulation and biomagnification critical for the health (Agency for Toxic Substances and Disease Registry, ATSDR). According to the International Agency for Reaserch on Cancer (IARC): As (IARC, 1980; 1987; 2012) and Cr (VI) (IARC 1987; 1990; 2012) is carcinogenic to humans (group 1); the other Cr forms are not classificable as to its carcinogenicity to humans (group 3) (IARC, 1987; 1990); Ni metallic and alloys (IARC, 1987; 1990), V pentoxide (IARC, 2006) and Co compounds (IARC, 1991; 2006), Pb are possibly carcinogenic to humans (group 2B) (IARC, 1980; 1987; 2012). Ba is not a heavy metal; however, it is taken into account because its main mineral, the barite, enters into the composition of the drilling mud used during the construction of the oil wells.

Barium (Ba)

In sedimentary rocks, Ba^{2+} usually substitutes K^{+} in K-feldspar and in phillosilicates, so its concentration is related to the abundance of the potassium minerals. Moreover, it may be absorbed by clay minerals and hydrous Fe and Mn oxides (Lima et al., 2016; Salminen R. et al. 2006).

In the present-day sediments, Ba ranges within the bedrock values (fig. 72); it is well correlated with potassium, as the scatterdiagrams related to the fluvio-lacustrine sediments (r^2=0.84), to the lacustrine bulk (r^2=0.78) and clay fraction (r^2=0.74) highlight.

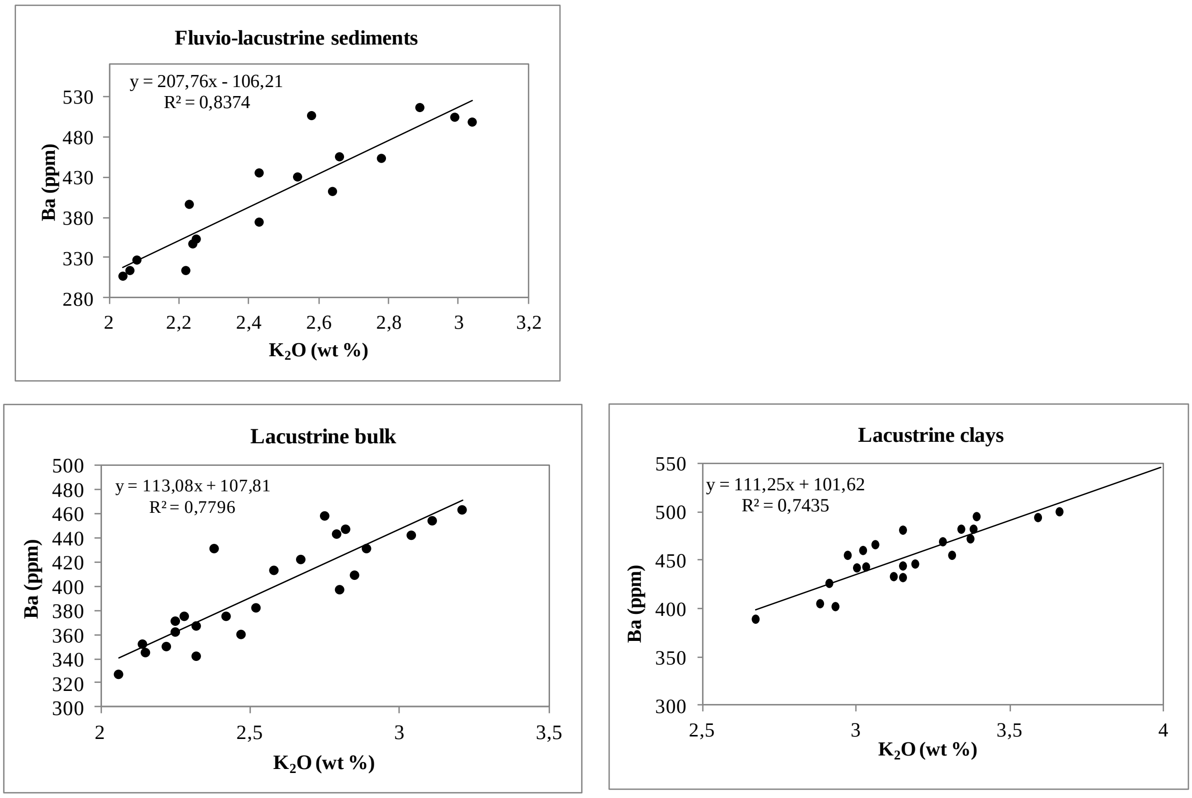

Figure 72. Scatterdiagrams K/Ba in the present-day sediments.

The barium maximum contents were found in the Vella catchment, both in a Quaternary sample and at Vella month and in the transitional area; the greatest potassium contents and the highest peaks of k-feldspar and illite in the different sediment types were also found.

So we can conclude that Ba mainly substitutes potassium in its minerals, k-feldspars and illite. Its EF always below 2 (fig. 71) confirm its geogenic origin.

Vanadium (V)

The fluvio-lacustrine median value (107 ppm) exceeds the same value of the other Lucanian stream sediments (26 ppm, Lima et al., 2016). In the present-day coarser fractions, vanadium is perfectly correlated with Fe_2O_3 (fluvio-lacustrine sediments: r^2=0.70; lacustrine bulk: r^2=0.94) and with Al_2O_3 (fluvio-lacustrine sediments: r^2=0.91; lacustrine bulk: r^2=0.92) (fig.

73). In the lacustrine clays, the vanadium values clearly increase, remaining below the bedrock range (fig. 55); the positive correlation with aluminium is still visible (r^2=0.73) (fig. 73). So, Fe-Al silicates, such as chorite and micas, host significant concentrations of vanadium; in the finest fraction it seems to be adsorbed by clay minerals as its positive correlations with Al_2O_3 shows.

The EF of both bulk and clay fraction are always below 2 (fig. 72), displaying a geogenic origin.

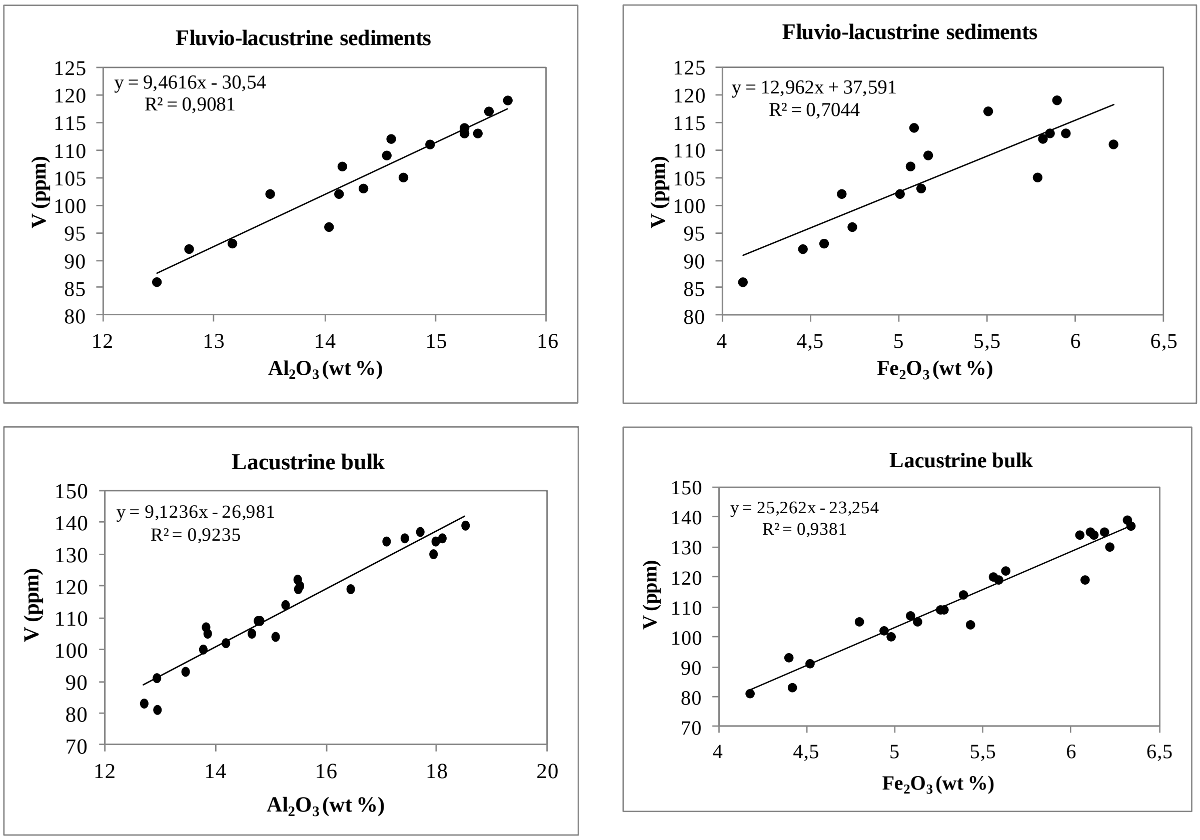

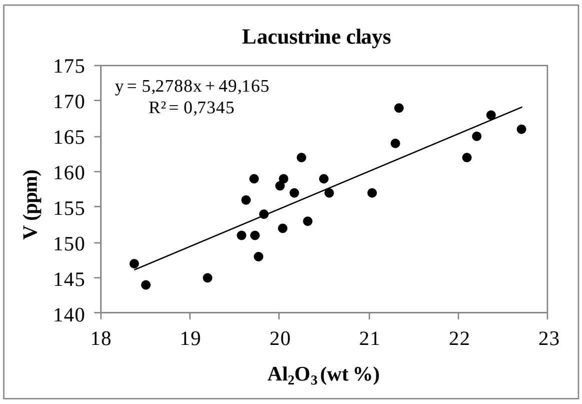

Figure 73. Scatterdiagrams Al/V and Fe/V in the presen-day sediments.

Chromium (Cr)

The fluvio-lacustrine median value (80 ppm ppm) is greater than the same value of the other Lucanian stream sediments (24,7 ppm, Lima et al., 2016).Only in the lacustrine bulk fraction, chromium shows an evident correlation with Fe_2O_3 (r^2=0.79) and Al_2O_3 (r^2=0.80). Excluding the samples collected at the months of Agri and Vella, in which Mg mainly substitutes Ca in the carbonates, chromium exhibits a good positive correlation with Mg (r^2=0.78). Moreover, it shows a quite good correlation with vanadium (r^2=0.87), indicating the same behavior (fig. 74).

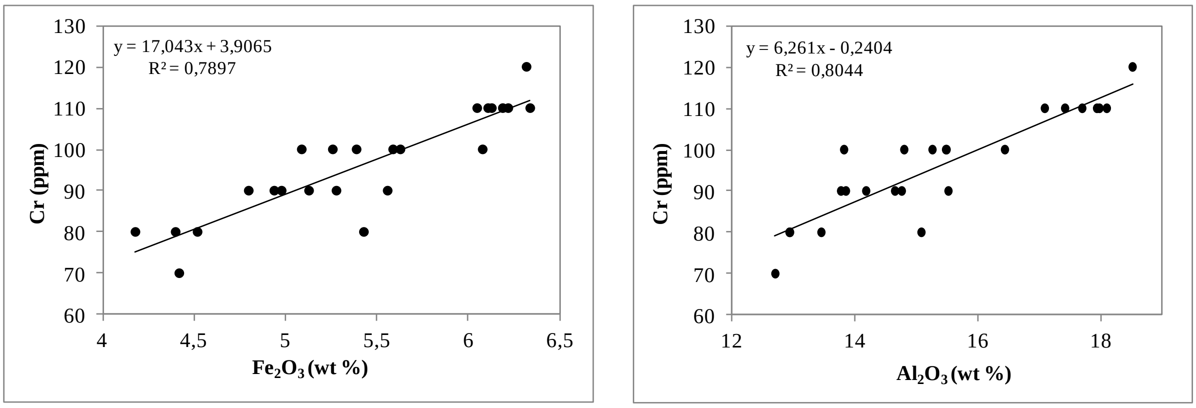

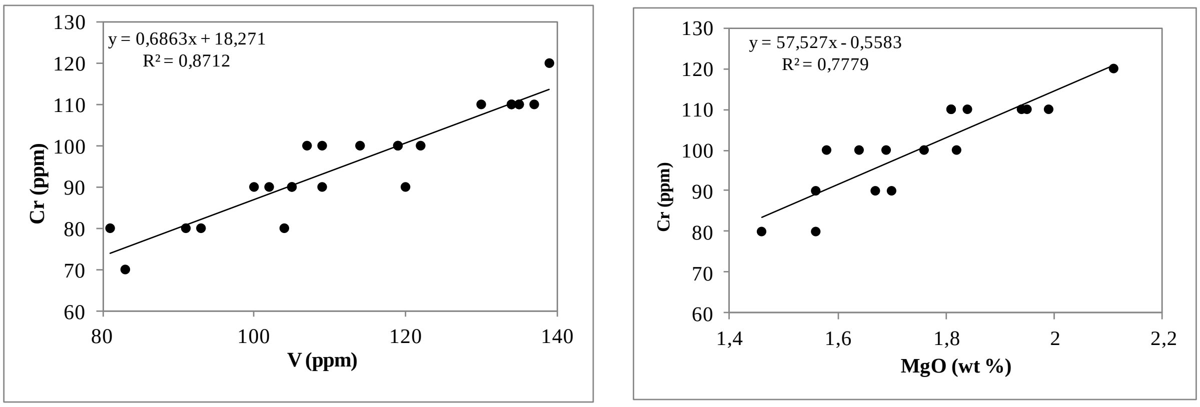

Figure 74. Scatterdiagrams of chromium in the lacustrine bulk fraction.

In the lacustrine clays it does not correlate with other elements due to the scarce variability in its dataset. So, chromium is undoubtedly linked to mafic minerals as demonstrated by its higher concentrations in the Galestri Formation; during the weathering, it maybe hosted in both Fe-Al-Mg silicates, such as chlorite.

EF values reach 2 in the clay fraction of two samples from the core R (R9 = 2.00; R12 = 2.03) (tab. 9; figg. 69, 71); for these samples an anthropogenic contribution can not be excluded.

Cobalt (Co)

In the lacustrine sediments, both in the bulk and clay fraction, cobalt does not show any correlation with other elements; however its concentrations are very low (down to 20 ppm) and always range within the bedrock values.

In the bedrock samples, cobalt reaches the highest values in the Galestri Formation (fig. 57), which also show the highest iron values (fig. 46). A slight positive correlation with Fe (r^2=0.63) was also found in the fluvio-lacustrine samples (fig. 75), whose median (13 ppm) is comparable to that of the Lucanian stream sediments (11,6 ppm, Lima et al., 2016). So, Co is maybe hosted by mafic minerals, as confirmed by the outliers, found in the cores collected at the confluences of Agri and Maglia, whose catchments display the Galestri outcrops, enriched of Fe and Mn oxides (Carbone, 2015) .

The EF values, always below 2 (fig. 72), lead us to conclude that cobalt display a geogenic origin.

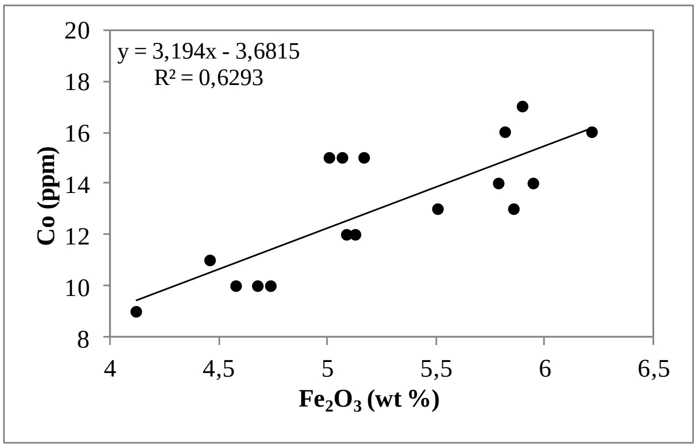

Figure 75. Scatterdiagrams of Co in the fluvio-lacustrine samples.

Nickel (Ni)

The Ni fluvio-lacustrine median value (40 ppm) exceeds the same value of the other Lucanian stream sediments (30,8 ppm, Lima et al., 2016). Nickel does not correlate with other elements due to the scarce variability in the dataset. Like Co, it shows the maximum values in the Galestri Formation; in the present-day sediments its trend appears similar to cobalt, which has the same chemical behavior, as their similar trend in the clay fraction highlights (fig. 76). Like Co, nickel is concentrated in mafic minerals, as confirmed by the higher values at the Maglia mouth.

Nickel always exhibits EF values lower than 2 (fig. 72), displaying its geogenic origin.

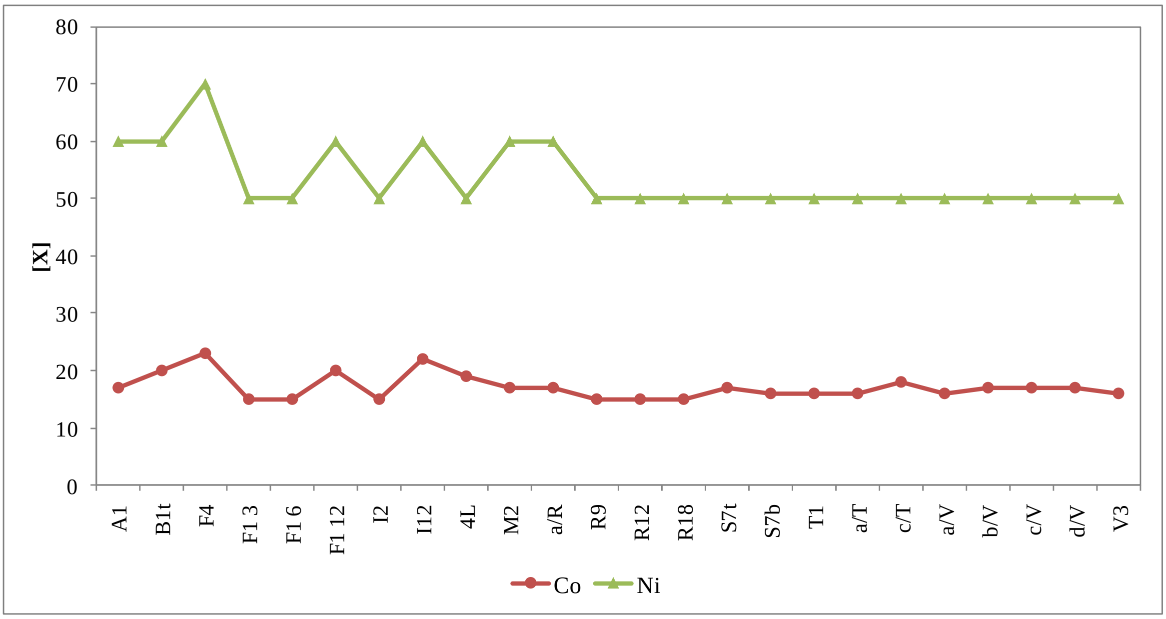

Figure 76. Comparison between the trend of Ni and Co in the lacustrine clays.

Copper (Cu)

Like Co and Ni, copper does not correlate with other elements as well due to the scarce variability in the dataset. The fluvio-lacustrine median value (40 ppm) is greater than that of the other Lucanian stream sediments (27,7 ppm), among which the Agri sediments show high enough (39-67 ppm) (Lima et al., 2016). It shows the maximum value in rocks containing mafic minerals (Galestri and Crete Nere) and in the present-day sediments at the Maglia month (fig. 59); so, it seems to derive from the weathering of mafic silicates.

The EF values are always below 2, except in the clay fraction of two samples from the core R (a/R = 2.34; R12 = 2.18) (tab. 9; figg. 69, 72); we can't exclude that these samples contain an anthropogenic contribution.

Zinc (Zn)

The median value of zinc in the local bedrock (110 ppm) exceeds the international reference values (UCC = 71 ppm) (tab. 7).

In the fluvio-lacustrine sediments, Zn median value (110 ppm) are higher than the other stream sediments collected in the Basilicata Region (Lima et al., 2016), that highlights the significant zinc concentrations in the High Agri Valley. Two outliers (190 and 170 ppm) were found in the Scazzero Stream, close to the Montemurro waste water treatment plant and in the core R (220 ppm), collected even more basinwards of the Scazzero month (fig. 60). Two samples of the core R show EF > 2 (a/R = 2.66; R12 = 2.10) (tab. 9; figg. 69, 72), leading us to conclude that there is an anthropogenic source of Zn in the Scazzero catchment.

In the other clay samples, the median concentration value increases (140 ppm) but the analytical method applied does not quantify Zn concentration below 10 ppm and consequently any possible correlation can't be highlighted.

Lead (Pb)

Lead median value greatly differs from the lithoid rocks (16.5 ppm) and the Quaternary incoherent deposits (31 ppm). The maximum value (79 ppm) was found in an exposed outcrop of the Albidona Flysch, containing mafic rocks (i.e., pillow-lavas) in the vicinity of the study area; the other two outliers (60 and 64 ppm), related to two outcrops of the Quaternary deposits, are possibly derived from the weathering of the Albidona Flysch with these features.

In the fluvio-lacustrine samples three abnormal values are found at the mouths of Agri, Rifreddo, and Vella streams, which drain outcrops of the Albidona Flysch, including the same mafic rocks. Excluding the outliers, instead, the median value of the fluvio-lacustrine sediments (23 ppm) is similar to the median (22 ppm) of the Italian stream sediments (Lima et al., 2016).

In the lake system, the Pb concentrations seems to be more regular and homogeneous; the bulk fraction shows the lowest Pb concentrations, with an only quite low anomalous value (35 ppm). Here, Pb appears to be slightly correlated with K (r^2=0.61), which commonly substitutes in k-feldspar and mica (fig. 77).

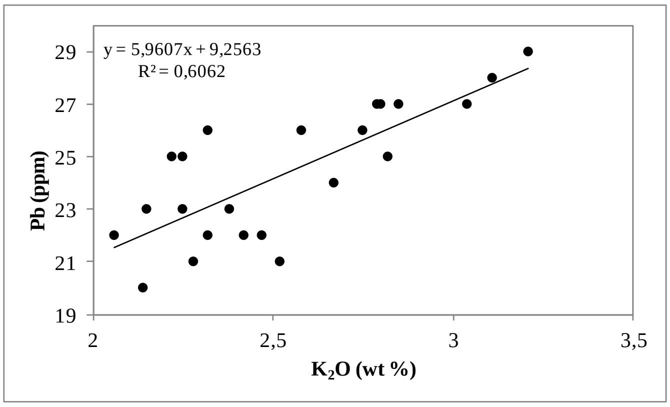

Figure 77. Correlation K/Pb in the bulk lacustrine fraction.

In the clay fraction, Pb values clearly increase without any apparent correlation with the other major and trace elements and with the organic matter; a single outlier (69 ppm) was found in the Maglia arm.

Pb shows 2<EF<3 in almost all the analyzed samples (fig. 72). Due to its great mobility in the natural waters (fig. 78), it may be mobilized and transported from the outcropping rocks into the lake, where may be adsorbed by the reactive phases (Fe-Mn oxides, clays).

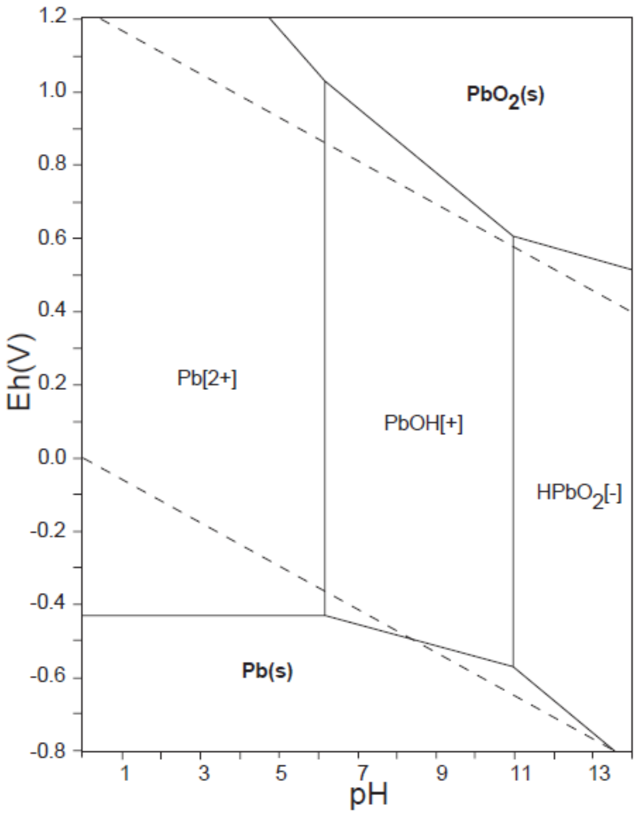

Figure 78. Eh-pH diagrams of the system Pb-O-H (National Institute of Advanced Industrial Science and Technology, 2005)

However, EF>>2 in the sample I2 and the higher values in the core R may be due to anthropogenic contributions.

Arsenic (As)

The arsenic concentrations in the local bedrock (7.2 ppm) are significantly greater then the

UCC (1.6 ppm) (tab. 7), so the EF_{UCC} exhibit the highest values (until 5.97) with respect to $EF_{bedrock.}$ On the other hand, among the Meso-Cenozoic rocks, 15 out of 23 samples show As contents under the detection limits. In the incoherent Quaternary deposits, As values increase and their median value doubles.

In the coarser fractions (fluvio-lacustrine sediments and lacustrine bulk), the As contents are quite always under the detection limit (fig. 62).

In the lacustrine clays, the As values slightly increase due to its affinity with the fine fraction, remaining still under 10 ppm.

So, the As contents in the lake system are low; it concentrates in the finest fraction as confirmed by the higher concentration in the Quaternary deposits and in the lacustrine clays.

Summarizing, in the bulk fraction, the very strong positive correlations between Fe, Al, V and Cr suggest that Fe-Al silicates (chlorite and micas) host significant concentrations of V and Cr, while Ba and Pb usually substitute K in K-feldaspars (Lima et al., 2016; Salminen et al. 2006; Gay and Roy, 1968; Heier, 1962) and illite (Brigatti et al., 2006; Rieder et al., 1998), as is well-documented.

In the clay fraction the previous correlations are no longer so clear; this is maybe due to the lack of clays with a high cation-exchange capacities (chlorite and illite) together with low total organic carbon percentages (tab. 10). However the positive correlations between Al and V and between K and Ba are still evident.

Table 10. Values of cation exchange capacity for different materials (IMAA-CNR, 2005).

Material	Cation exchange capacity (meq/100g)
Kaolinite	3 - 15
Halloysite	5 - 50
Illite	10 - 40
Chlorite	10 - 40
Montmorillonite	60 - 150
Vermiculite	100 - 150
Organic matter	130 - 500

Co, Ni, Cu, Zn and As do not correlate with other elements due to the scarse variability in the dataset. However their concentrations are included within the bedrock ranges, as the box and whiskers plots (figg. 57-62) still highlighted. The higher EF values for lead may be due to its mobilization and transport from the lead-enriched outcropping formations into the lake where may be adsorbed by the reactive phases (Fe-Mn oxides, clays, organic matter).

The EF>>2 in the sample I2 may be due to anthropogenic contributions; in particular the core I was collected in the Maglia arm, in whose catchment different anthropogenic activities are located: intensive agricultural activities, a landfill, a local airfield and a waste water treatment plant (fig. 79).

In addition, the figure 72 highlights that Cu, Cr and Zn show EF values > 2 in the core R, in which Pb exhibits higher values as well. The core R was collected basinwards of the Spetrizzone-Scazzero months, in whose catchment a waste water treatment plant and several dumpings are present; moreover, the core R was located closest to the State Road 598 (fig. 80).

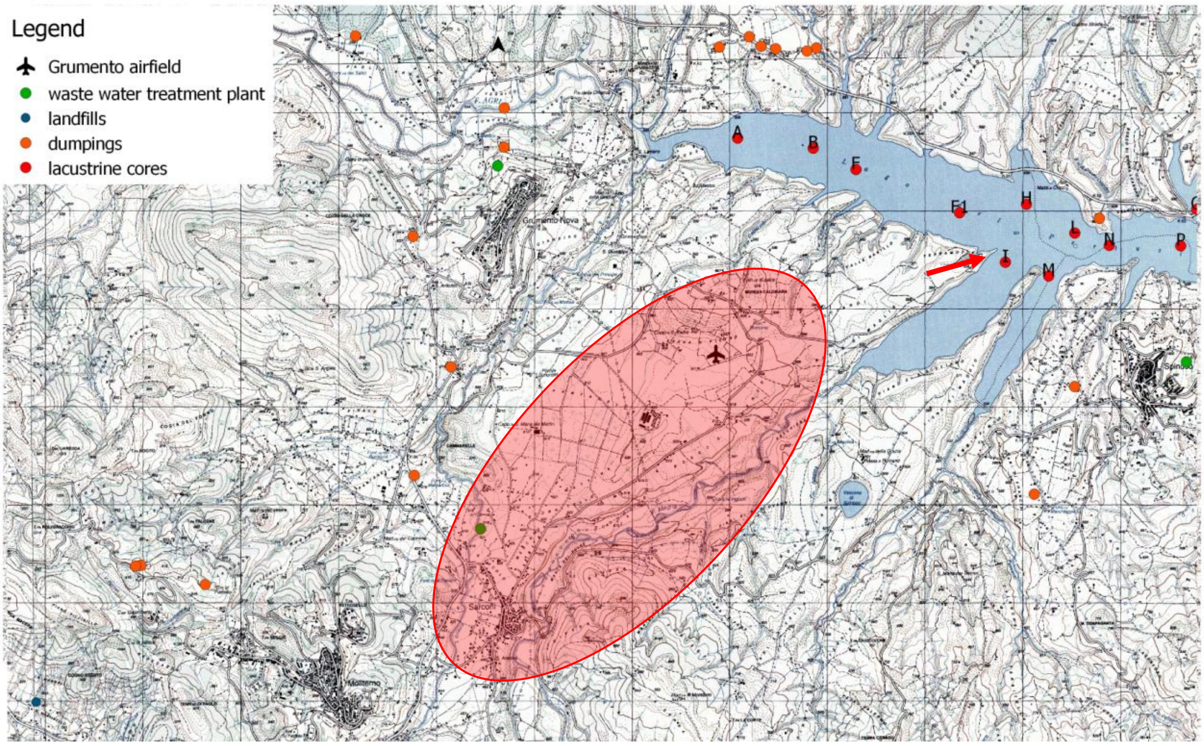

Figure 79. Anthropogenic activities in the Maglia catchment (the landfill of "Fontana d'Eboli" is located outside of this map) .

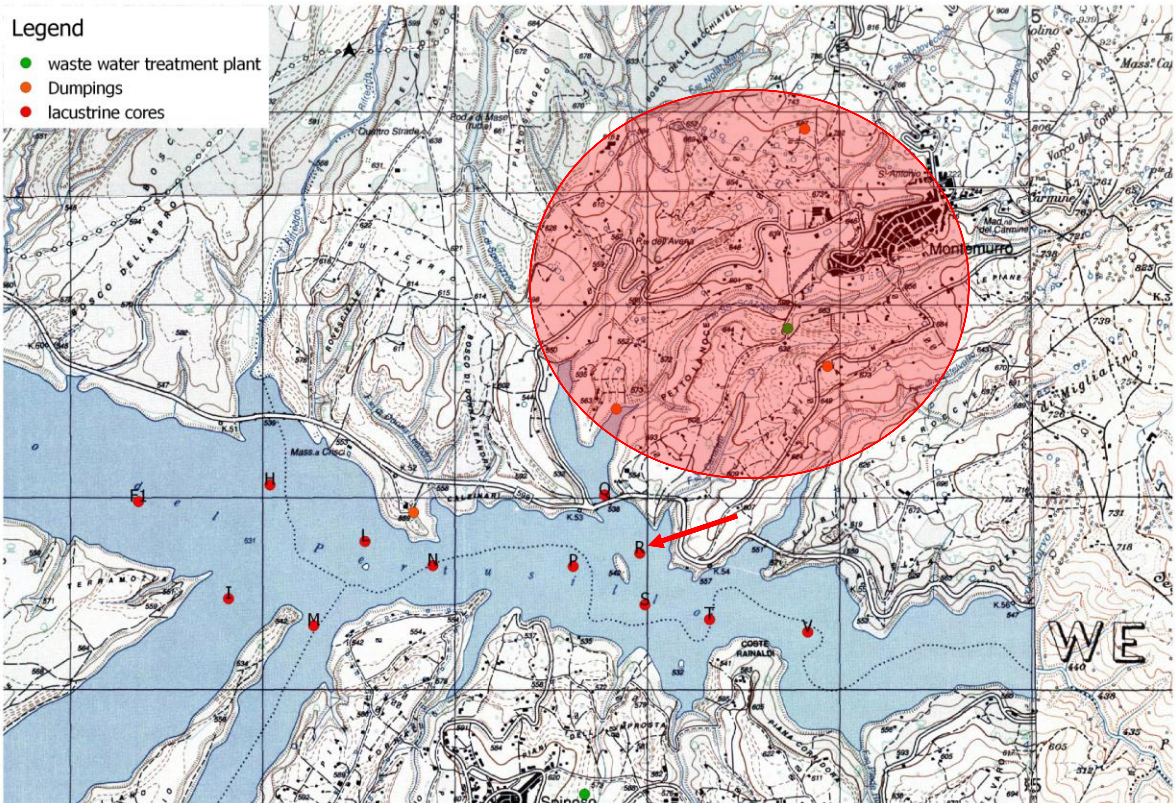

Figure 80. Anthropogenic activities in the Scazzero-Spetrizzone catchments.

5.5 Comparison of the lacustrine sediment values with the regulatory levels

The table 11 shows, if existent, regulatory limit values; since no national legislation on stream sediments exists, the reference chemical levels proposed by (ex) APAT for some metals and the Ministerial Decree 152/06 were taken into consideration as a national reference values. The lower and the upper threshold values for sediments laid down by Canadian jurisdiction (Canadian Sediment Quality Guidelines for the Protection of Aquatic Life, 2002), are used as the international benchmarks for comparison.

Comparison outlines that:

- barium is never considered by the national and international guidelines;
- the bulk fraction of the lacustrine sediments is always below the national and international guidelines, except for Cu and Cr with respect to the Canadian lower

threshold values (ISQG);

- the clay fraction is always within the Canadian range and, except for V, below the national threshold values; however the $EF_{(bedrock)}$ values of vanadium, constantly < 2, prove its geogenic origin.

Table 11. Comparison between the Pertusillo sediment values (both in the bulk and in the clay fraction) and the national and international guidelines.

	Pertusillo sediments		Italian guidelines			Canadian guidelines	
Element	Bulk fraction Median value (this study) (ppm)	Clay fraction Median value (this study) (ppm)	RLC (ISPRA, 2009) (ppm)	L.D. 152/06 Part IV, Title IV Col. A (ppm)	L.D. 152/06 Part IV, Title IV Col. B (ppm)	Canadian ISQG (Interim Sediment Quality Guidelines) (ppm)	Canadian PEL (Probable Effect Level) (ppm)
Arsenic	-	8	16	20	50	7.24	41.6
Barium	389.5	455	-	-	-	-	-
Cobalt	14	16	17	20	250	-	-
Chromium	100	125	157	150	800	52.3	160
Nickel	40	50	62	120	150	-	-
Lead	25	42	52	100	1000		
Copper	40	50	55	120	600	18.7	108
Vanadium	111.5	157	134	90	250	-	-
Zinc	110	140	146	150	1500	124	271

References

- Agency for Toxic Substances and Disease Registry. *Toxicological profiles*.

- Ball et al., 1998. *An assessment of availability of pollutant constituents on road surfaces*. The Science of the Total Environment, 209, 243-254.

- Blaser et al., 2000. *Critical examination of trace elements enrichments and depletions in soils: As, Cr, Cu, Ni, Pb and Zn in Swiss forest soils*. Science of the Total Environment, Vol. 249, Issues 1-3, pagg. 257-280.
- Brigatti et al., 2006. *Structures and mineralogy of clay minerals*. Pp. 19-87 in: Handbook of Clay Science. Developments in Clay Science, Vol. 1 (F. Bergaya, B.K.G. Theng and G. Lagaly, editors). Elsevier, Amsterdam.

- Canadian Council of Ministers of the Environment, 2001. *Canadian Environmental Quality Guidelines*.

- Carbone, 2015. *Note Illustrative della Carta Geologica d'Italia alla scala 1:50.000 – Foglio 489 Marsico Nuovo*. Con i contributi di F. Lentini, A. Di Stefano, S.I. Giano, e la collaborazione di M. Romeo, M. Chiocchini. Coordinamento Scientifico Editoriale S. Carbone. 124 pp. ISPRA/Regione Basilicata, SystemCart, Roma (pdf di stampa). file:///C:/Users/asus3/Documents/dottorato/Pertusillo/articoli/geologia%20e%20geomorfologia/489_Marsico_Nuovo.pdf.

- Da Deppo 2011. *Raccolta e trattamento delle acque di prima pioggia. IX giornata sul drenaggio urbano sostenibile*. Università di Brescia.

- Decreto legislativo 3 aprile 2006, n. 152. Norme in materia ambientale.

- De Vivo et al., 2004. *Geochimica ambientale*. *Metalli potenzialmente tossici*. Liguore Editore.

- Escobar et al., 2012. *Isotope record of anthropogenic lead pollution in lake sediments of Florida, USA*. J Paleolimnol DOI 10.1007/s10933-012-9671-9.

- Gay and Roy, 1968. *The mineralogy of potassium-barium feldspar series III: subsolidus relationships*. Mineralogical Magazine, 36, 914-932.
- Heier, 1962. *Trace elements in feldspars--a review*. Norsk Geol. Tiddsskr., 42(2): 415-454 (Feldspar Volume).

- International Agency for Research on Cancer (IARC), 1980. *IARC Monographs on the Evaluation of Carcinogenic Risks of Chemicals to Humans. Sorne Metals and Metallic Cornpounds*. Vol. 23. http://monographs.iarc.fr/ENG/Monographs/vol1-42/mono23.pdf.

- International Agency for Research on Cancer (IARC), 1987. *IARC Monographs on the Evaluation of Carcinogenic Risks to Humans. Overall Evaluations of Carcinogenicity: An Updating of IARC Monographs Volumes 1 to 42*. Sup. 7. http://monographs.iarc.fr/ENG/Monographs/suppl7/Suppl7.pdf.

- International Agency for Research on Cancer (IARC), 1990. *IARC Monographs on the Evaluation of Carcinogenic Risks to Humans. Chromium, Nickel and Welding*. Vol. 49. http://monographs.iarc.fr/ENG/Monographs/vol49/mono49.pdf.

- International Agency for Research on Cancer (IARC), 1991. *IARC Monographs on the Evaluation of Carcinogenic Risks to Humans. Chlorinated Drinking- water; Chlorination By-products; Some Other Halogenated Compounds; Cobalt and Cobalt Compounds*. Vol. 52. http://monographs.iarc.fr/ENG/Monographs/vol52/mono52.pdf.

- International Agency for Research on Cancer (IARC), 2006. *IARC Monographs on the Evaluation of Carcinogenic Risks to Humans. Cobalt in Hard Metals and Cobalt Sulfate, Gallium Arsenide, Indium Phosphide and Vanadium Pentoxide*. Vol. 86. http://monographs.iarc.fr/ENG/Monographs/vol86/mono86.pdf.

- International Agency for Research on Cancer (IARC), 2012. *IARC Monographs on the Evaluation of Carcinogenic Risks to Humans. arsenic, metals, fibres, and dusts*. Vol. 100C. http://monographs.iarc.fr/ENG/Monographs/vol100C/mono100C.pdf.

- IMAA-CNR, 2005. *Analisi di materiali argillosi per diffrazione di raggi X e microscopia a scansione. Teoria ed applicazioni*. Atti del VII corso di formazione dell'Associazione Italiana per lo Studio delle Argille.

- ISPRA, 2009. Proposta per la valutazione dello stato qualitativo dei sedimenti fluviali nel sito di interesse nazionale Fiumi Saline ed Alento.

- Jones and Bowser, 1978. *The mineralogy and related chemistry of lake sediments*. In: Lerman A. Lakes - Chemistry, geology and physics. New York, Springer-Verlag, chap. 7, pp. 179-235.

- Lima et al., 2016. *Atlante geochimico-ambientale dei sedimenti fluviali della Basilicata*. Aracneeditrice int.le S.r.l. ISBN 978-88-548-9078-7.

- Mc Lennan et al. 2006. *Composition, differentiation, and evolution of continental crust: constrains from sedimentary rocksand heat floor*. In: Brown & Rushmer (Eds), Evolution and Differentiation of the continental crust.

- Mongelli et al., 2014. *Trace elements and REE fractionation in subsoils developed on sedimentary and volcanic rocks: case study of the Mt. Vulture area, southern Italy*. Int J Earth Sci (Geol Rundsch) DOI 10.1007/s00531-014-1003-z.

- Oskierski et al., 2009. *Geogenic and anthropogenic lead isotope signatures in the urban environment of Natal (NE-Brazil).* Environ Geol (2009) 58:1811–1817, DOI 10.1007/s00254-008-1679-0.

- Papiri and Todeschini, 2004. *Qualita' e controllo delle acque di dilavamento di infrastrutture viarie*. Università degli Studi di Pavia.

- Reimann, De Caritat, 2005. *Distinguishing between natural and anthropogenic sources for elements in the environment: regional geochemical surveys versus enrichment factors*. Science of the Total Environment 337, 91– 107.

- Rieder et al., 1998. *Nomenclature of the Micas*. Clays and Clay Minerals 46, 586–595.

- Salminen et al., 2006. *Geochemical Atlas of Europe. Part 2. Interpretation of Geochemical Maps, Additional Tables, Figures, Maps, and Related Publications*. De Vos W. and Tarvainen T. (Chief-editors).

- Sinisi et al., 2012. *Different Mn-ores in a continental arc setting: geochemical and mineralogical evidence from Tertiary deposits of Sardinia (Italy)*. Ore geology Reviews, 47, 110-125.

- Sutherland, 2000. *Bed sediment-associated trace metals in an urban stream, Oahu, Hawaii*. Environmental Geology 39, 611-37.

CONCLUSIONS

Conclusions

The present work represents the first systematic and comprehensive study of Pietra del Pertusillo fresh-water reservoir, an artificial lake built about 50 years ago in the High Agri Valley (Basilicata Region, Italy). Its lacustrine sediments were studied with a multi-proxy analysis to understand the processes (natural as much as anthropogenic) affecting the concentration and mobility of the following trace elements: vanadium (V), barium (Ba), chromium (Cr), cobalt (Co), nickel (Ni), copper (Cu), zinc (Zn), lead (Pb) and arsenic (As).
The results of the study are summarized below.

1. <u>Proposal of a methodological approach to the environmental quality assessment of the fresh-water reservoir sediments.</u>
   In order to investigate the environmental contamination of a fresh-water reservoir and of its catchment, a new methodological approach was developed, on the basis of the analysis of different solid rock and sediment types: the <u>parent rocks</u> with a predominate siliciclastic pelitic fraction for evaluating the geogenic contribution of the trace elements; the <u>fluvio-lacustrine sediments</u> at the confluences of the active tributaries for assessing the chemical and mineralogical composition close to the detrital supply entry points of the reservoir; the <u>lake bottom-sediments</u>, allowing us to first reconstruct the depositional lacustrine environments and then, on the basis of XRPD analyses, to assess the maximum concentrations of trace elements both in the bulk and clay fraction (< 4μ).

2. Understanding the sedimentological and minero-chemical processes, occurring in the reservoir sediments.

   Eleven sedimentary facies have been identified; according to the facies analysis, the Pertusillo fresh-water reservoir can be divided in three depositional sub-environments: the delta areas, strongly affected by dramatic water-level fluctuations; the transitional areas, showing transitional facies, and the lacustrine zone s.s., which probably corresponds to the accumulating zone, constantly submerged and hardly affected by water level fluctuations.

   The sedimentation within the Pietra del Pertusillo fresh-water reservoir is essentially clastic, except for minor amount of organic calcite, and reflects the mineralogical composition of litologies outcropping along the drainage basin; according to the XRPD analyses, quartz (Qz), calcite (C), feldspar (Feld.), muscovite/illite (M/Ill.), chlorite (Ch) and minor amount of mixed-layered clay minerals are the main identified mineralogical phases; dolomite (D) was found only at the confluence of the Agri River. The low contents of mixed-layered clay minerals may indicate a limited clay transformation at the sediment-water interface probably due to the high accumulation rate of the Pertusillo reservoir (19,7 cm/yr in the deepest area of the reservoir).

3. Environmental quality assessment of the lacustrine sediments.

   The trace elements in the core sediments (V, Ba, Cr, Co, Ni, Cu Zn, Pb and As) mostly derived from the weathering and erosion of the surrounding source rocks, among which the mafic components and the Quaternary deposits may have played an important role. The EF values frequently below 2, confirm the geogenic origin of the trace elements.

   The anthropogenic contribution is spatially limited to two single spots: the core R for Cu, Cr and Zn and Pb and the core I for Pb.

All the elements are below the upper threshold values for Canadian sediments guidelines and except for V, below the national threshold values; however the $EF_{(bedrock)}$ values of vanadium, constantly below 2, prove its geogenic origin.

ACNOWLEDGMENTS

Acknowledgments

- First of all, I would like to thank my research institution, Fondazione Eni Enrico Mattei (FEEM) and in particular my Coordinator, Mr. Cristiano Re, for having immediately belived in my research project. Without his fully support in economical and logistics issues, this project would never had been developed.

- The high quality and professional skills of the debates I have had with my academic working group have made the completion of this project possible. I would like to thank sincerely:
  - my tutor, Dr. Michele Paternoster for improving my knowledge, for his patience, optimism and support mostly in particularly complex circumstances of my research;
  - the full professor Giacomo Prosser I really consider my scientific mentor; his constant availability, encouraging presence and scientific leadership have been essential during my PhD;
  - the full professor Albina Colella for her willingness to share her sedimentological knowledge with me; I also thank her for the accurate revisions of the sedimentological work and for the frank conversations;
  - the associate professor Giovanni Mongelli for his directness, guidance and inspiration in the minero-geochemical work; his strong experience allowed me to reach quickly and directly my PhD goals;
  - the dr Rosa Sinisi for her accurate and qualified guidance in many laboratory operations and analyses;
  - the associate professor Mario Bentivenga especially helpful in the fieldwork; I also thank him for the confidence and trust in me;

- The technical assistance of many people have contributed in the successful completion of this project. In particular I wish to thank:
    - the laboratory technicians: Dr. Antonio Romano, for his fundamental logistic support; Vincenzo Tolla, for his precious and patient help in the core splitting; Fausto Langerame for his availability and professional support in the TOC analysis;
    - the chief of the research, Prof. Marco Cantonati, and the technical assistant, dott. Nicola Angeli, of the Limnology and Algology Section of Muse-Sciences Museum of Trento for their complete willingness to share the great experience on the lacustrine sediment coring.

- I am very grateful to all my colleagues of the Fondazione Eni Enrico Mattei in Viggiano; they are a continuous professional stimulation as well as my second family; in particular I wish to thank:
    - the colleagues of my workgroup "Energy and Environment", Dario Colucci, Tiziana Perri and Francesca Scannone for their presence in my fieldwork, their support and help in delicate laboratory operations, their scientific confrontation and continuous support;
    - the colleagues Francesco Calabrese and Ernesto Ferrara for providing the stratigraphy of the cores and the other stratigraphical maps, for taking photos and editing videos of the core drilling and splitting;
    - the colleagues Caterina Verrone and Matteo Bernecoli for their qualified help in the graphics of my works.

- Last but not least I owe a special thanks to my family for its precious support and great patience: to my parents who have supported and endured me during these years; my husband who has always been by my side as a trusted advisor and my children whose presence gave me another gear.

APPENDICES